

GRADUATE SCHOOL LECTURES 2014
P A R T I

**OPTICAL PROPERTIES
OF
NANOSTRUCTURED MATTER**

**THE MODEL
OF
METAL NANOPARTICLES**

UWE KREIBIG
ALMUTH HILGER,
HEINZ HÖVEL,
MICHAEL QUINTEN

I. Physikalisches Institut IA
der R W T H Aachen / BRD

kreibig@physik.rwth-aachen.de



nanotechnologie

technologie

Nano

Nanotechnologie

Innovation aus dem Nanokosmos



bmb+f

Bundesministerium für
Bildung, Wissenschaft,
Forschung und Technologie

PART I :

NANOS AND ALL AROUND MIE'S THEORY

- (1) Introductory Remarks
- (2) Several Nanoparticle Samples
- (3) Example: The Nanoparticle Source LUCAS
- (4) Plasmons
- (5) Extended and Localized Surface Plasmon Polaritons (S P P)
- (6) The Nano as Optical Dipole
- (7) The Theory of Gustav Mie
- (8) Inverse Mie Theory
- (9) Relaxation of the S P P Decay
- (10) Linear Optical Material Functions (D F)

PART II :

NANOOPTICS BEYOND MIE'S THEORY

- (11) Reality Beyond Mie's Theory
- (12) Example 1 : Maxwell's Boundary Conditions
- (13) Example 2: Realistic Optical Dielectric Functions
- (14) Example 4: Optical Properties of Schmid Clusters and Nanoparticles
- (15) Example 5: Photosensitive Glass : Size Effects of the DF
- (16) Example 6: Interband Transition Edge of Noble Metal Nanos
- (17) Example 7: Heterogeneous Nanos
- (18) Surfaces and Interfaces of Nanos
- (19) Charge Transfer at Nano Interfaces
- (20) Electronic Interactions in Nano-Interfaces (Silver Nanos in Fullerite)
- (21) Experiments on 2nm Silver-Nanos
- (22) Nanos on Substrates
- (23) Chemical Interface Reactions
- (24) Many-Particle Systems
(The Generalized Mie Theory (GMT))

LITERATURE (SOME BOOKS AND REVIEWS) :

Uwe Kreibig, Michael Vollmer :

OPTICAL PROPERTIES OF METAL CLUSTERS

Springer Series in Material Science 25, Springer, Berlin 1995

Uwe Kreibig

OPTICS OF NANOSIZED METALS

Handbook of Optical Properties

Ed. R.E. Hummel, P. Wißmann, CRC Press, Boca Raton 1997

Uwe Kreibig, Michael Gartz, Almuth Hilger, Heinz Hövel

OPTICAL INVESTIGATIONS OF SURFACES AND INTERFACES
OF METAL CLUSTERS

Advances in Metal and Semiconductor Clusters, Vol. 4, Ed. M. Duncan

Uwe Kreibig, Helmut Bönнемann, Josef Hormes

NANOSTRUCTURED METAL CLUSTERS AND COLLOIDS

Handbook of Surfaces and Interfaces of Materials

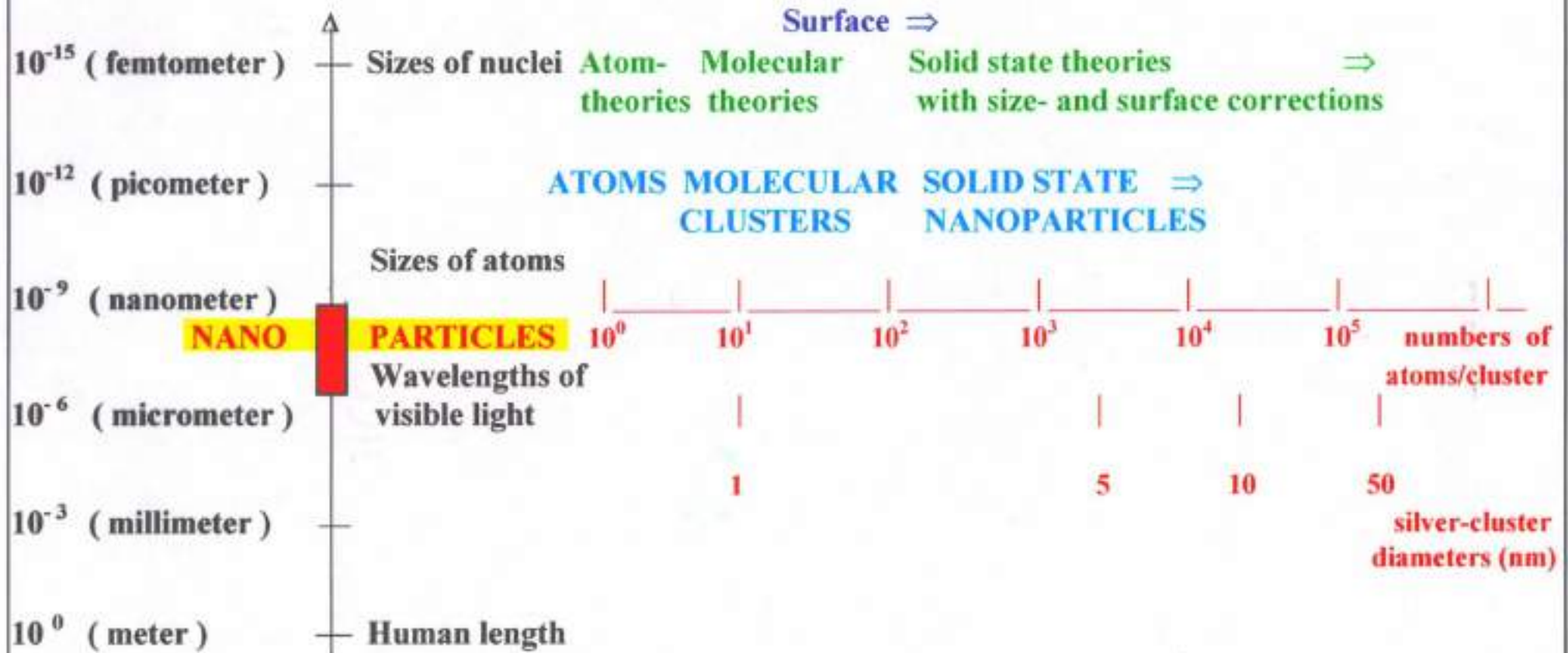
Vol. 3: Nanostructured Materials, Micelles and Colloids

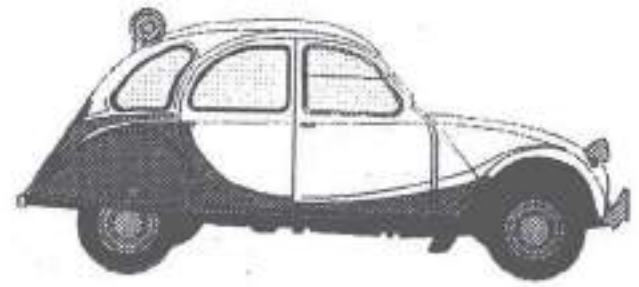
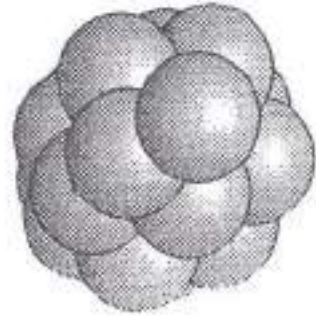
Ed. H. S. Nalwa, Academic Press, 2001

(1) Introductory Remarks

LENGTH - SCALE

NANOPARTICLE - PROPERTIES





NANO - MATERIAL SCIENCE :

SIZE RANGES OF NANOPARTICLES

(1) "LARGE" NANOPARTICLES: Solid state particles

MIE -THEORY : Geometric scaling down of the theoretical background of the bulk solid state (Maxwell electrodynamics) and of bulk optical material properties (complex dielectric function $\epsilon(\omega)$).
Size limits : $\infty > 2 R > 10^1$ nm

(2) "MINUTE" NANOPARTICLES

MIE - THEORY : Lower validity limit at the transition region from the solid state to the molecule.
Molecule: quantum theoretical molecule background (" Vlasta Koutecky : "every atom counts")
Optical properties : atomic polarizability $p(\omega, \dots)$
Size limits : $2 R > 1.5$ nm

(3) INTERMEDIATE RANGE : Size dependences of geometric and electronic structures and of optical properties (size dependent complex dielectric function $\epsilon(\omega, R, \text{surrounding} \dots)$).
Size interval : 10^1 nm $< 2 R < 1.5$ nm

This is the most challenging region for "novel physics" in applications.
Failures of the classical theory of Mie:
Corrections, supplements and extensions required or available to obtain quantitatively correct results.

In the Intermediate range the role of the particle surface / interface is prevailing and with diminished size is finally dominating physical and chemical behavior.

Beginnings of the Nanoplasmonics Technology

First archeological hints of Coloration by Plasmon Polaritons in Metallic Nanoparticles :

- (1) **OBJECT:** Clay Slab with Cuneiform Letters :
Receipt to produce opaque red
Cu-Nanoparticle Glasses ("Hematinon")
(The British Museum)

EXCAVATION: Nimrod (Assyria)

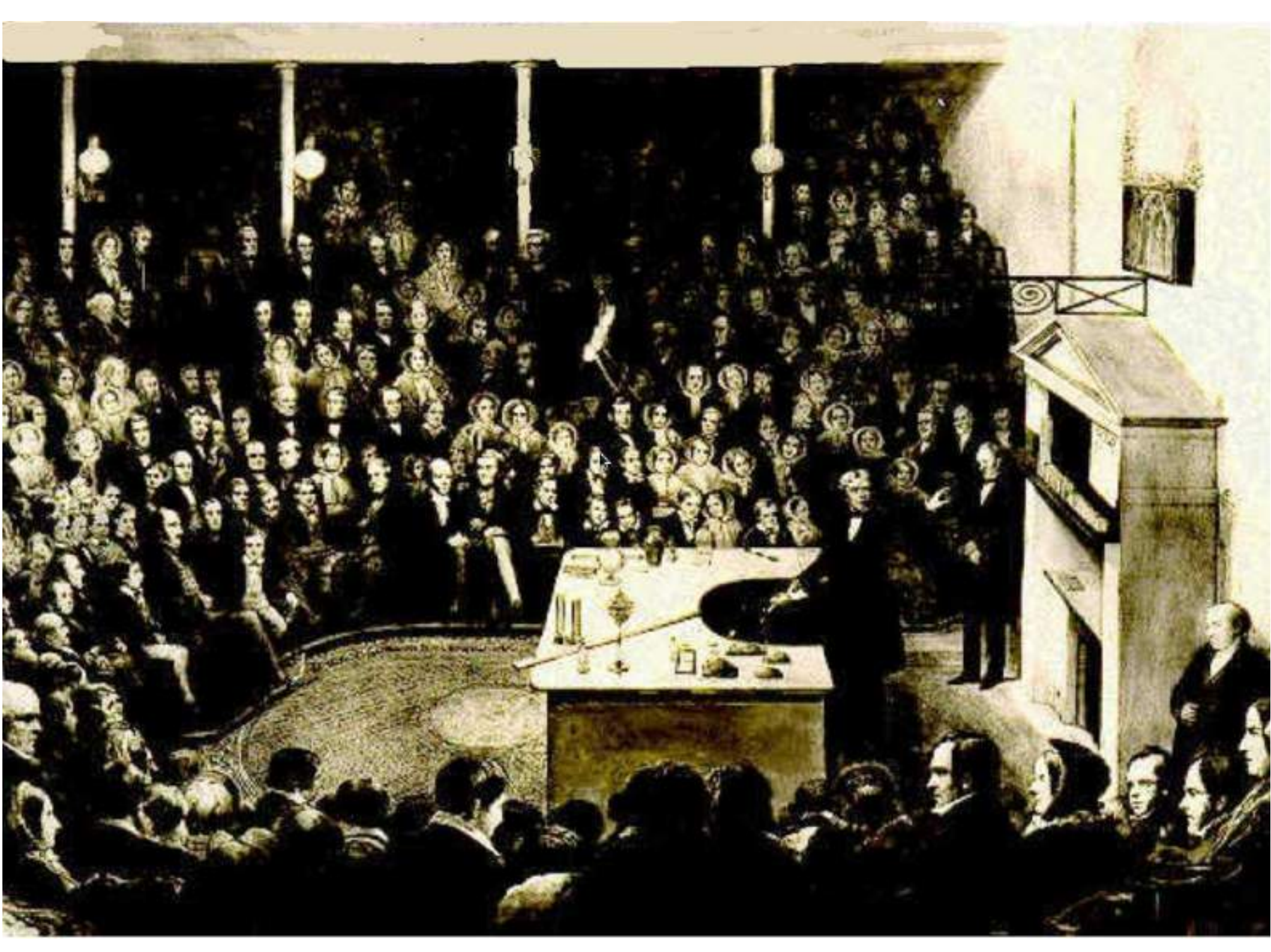
TIME : Bronze Age (13. Century a.C.)

- (2) **OBJECT:** Relief Head in opaque red Glass
(The Brooklyn Museum)

EXCAVATION : Egypt

TIME : 19. Dynasty (12. century a.C.)







Richard Zsigmondy Nobelpreis Chemie 1925
(*1. April 1865 Wien +23. September 1929 Göttingen)

KOLLOIDCHEMIE

EIN LEHRBUCH

VON

RICHARD ZSIGMONDY

PROFESSOR AN DER UNIVERSITÄT GÖTTINGEN
DIREKTOR DES INSTITUTS FÜR ANORGANISCHE CHEMIE
DR. ING. H. C., DR. MED. H. C.

FÜNFTE, VERMEHRTE
UND VOLLSTÄNDIG UMGEARBEITETE AUFLAGE

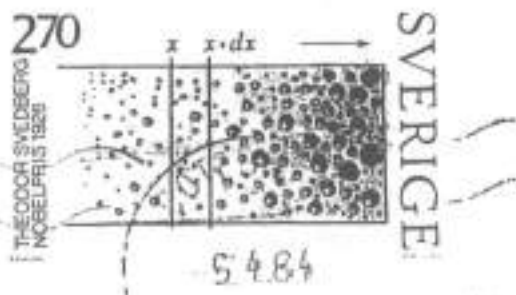
I. ALLGEMEINER TEIL
MIT 7 TAFELN UND 34 FIGUREN IM TEXT



LEIPZIG
VERLAG VON OTTO SPAMER
1925



Theodor Svedberg (1884) · 1926
Schweden



DIE METHODEN ZUR HERSTELLUNG KOLLOIDER LÖSUNGEN ANORGANISCHER STOFFE

EIN HAND- UND HILFSBUCH FÜR DIE
CHEMIE UND INDUSTRIE DER KOLLOIDE

VON

DR. THE SVEDBERG

PRIVATDOZENT AN DER UNIVERSITÄT UPSALA

MIT 60 ABBILDUNGEN, ZAHLREICHEN TABELLEN UND 3 TAFELN



DRESDEN 1909 :: VERLAG VON THEODOR STEINKOPFF

(2) Several Nanoparticle Samples

Examples of Nanoparticles in Nature, Technology and Life-Sciences

Interstellar space dust

Geo-Colloids (minerals, hydrosols, aerosols, volcanic dust, Diesel exhaust)

Nanocrystalline solid materials

Cerodur heat resistant glass

Emulsions (e.g. milk)

Liquid crystals

Island films (thin films)

Sol-Gel systems (Sinter-materials, Ormocers)

Nanoceramics ("Super-ceramics")

Fullerenes, Carbon nanotubes

Solar absorbers

Electronic devices (Cermets, Varistors, Nano-transistors,
Single electron devices)

Digital data storage systems (Tapes, Magnetic, Optic systems,
Phase change, Read/write heads)

Pigment colors (minerals, glass, ceramics etc)

Inks for printing machines

Photonic crystals

Meta-materials

Analog, digital Photography

Quantum dots (e.g. quantum dot lasers)

Ferro-fluids (mechanical, medical applications etc.)

Heterogeneous catalysts

Nutrition fillers (e.g. TiO_2)

Desinfection in households (Ag-nanos)

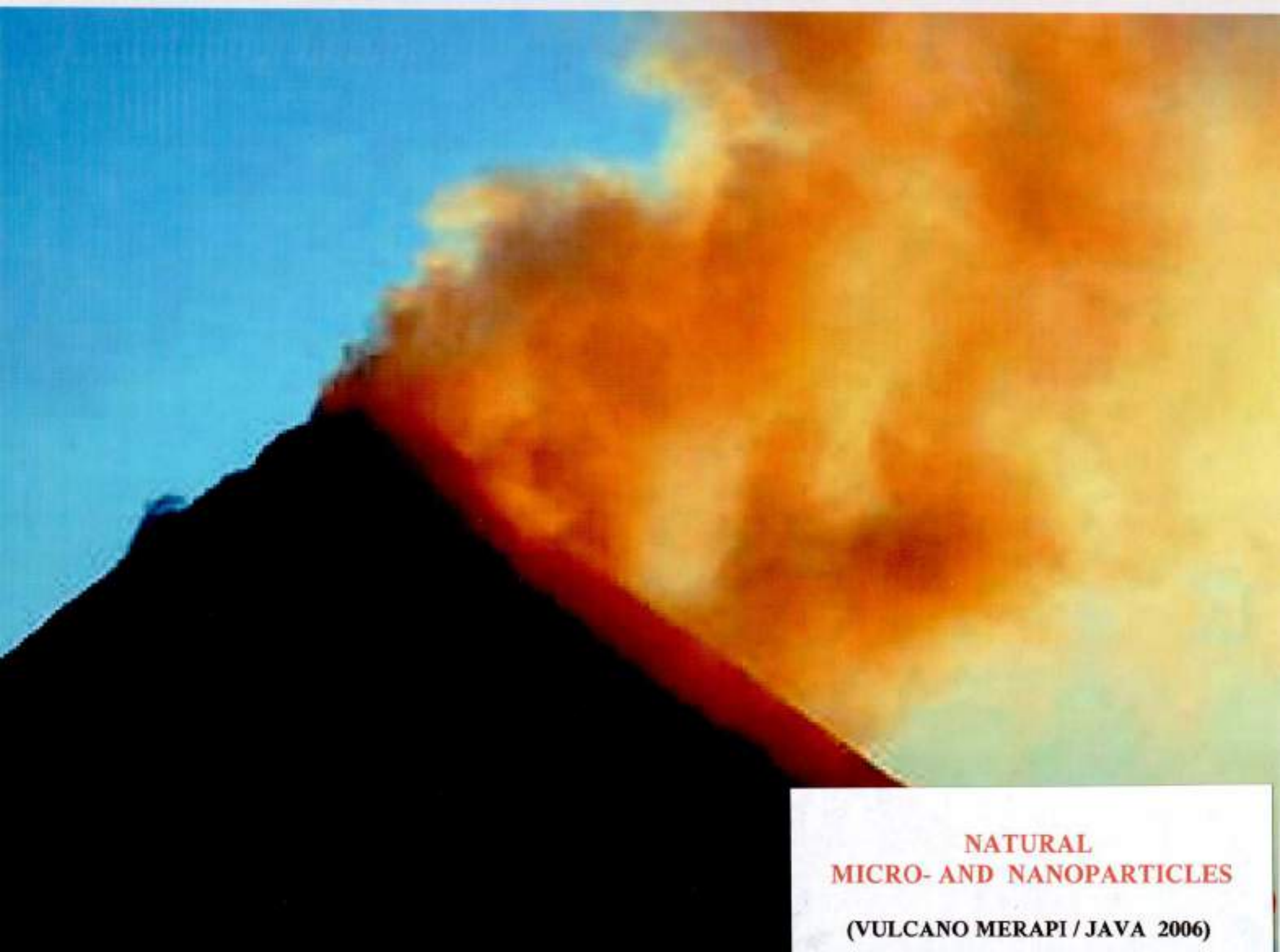
Cosmetics, sun-protecting creams, tooth cream, etc.

Sensors (Gas, molecule-specific, drugs etc.)

Medical drugs

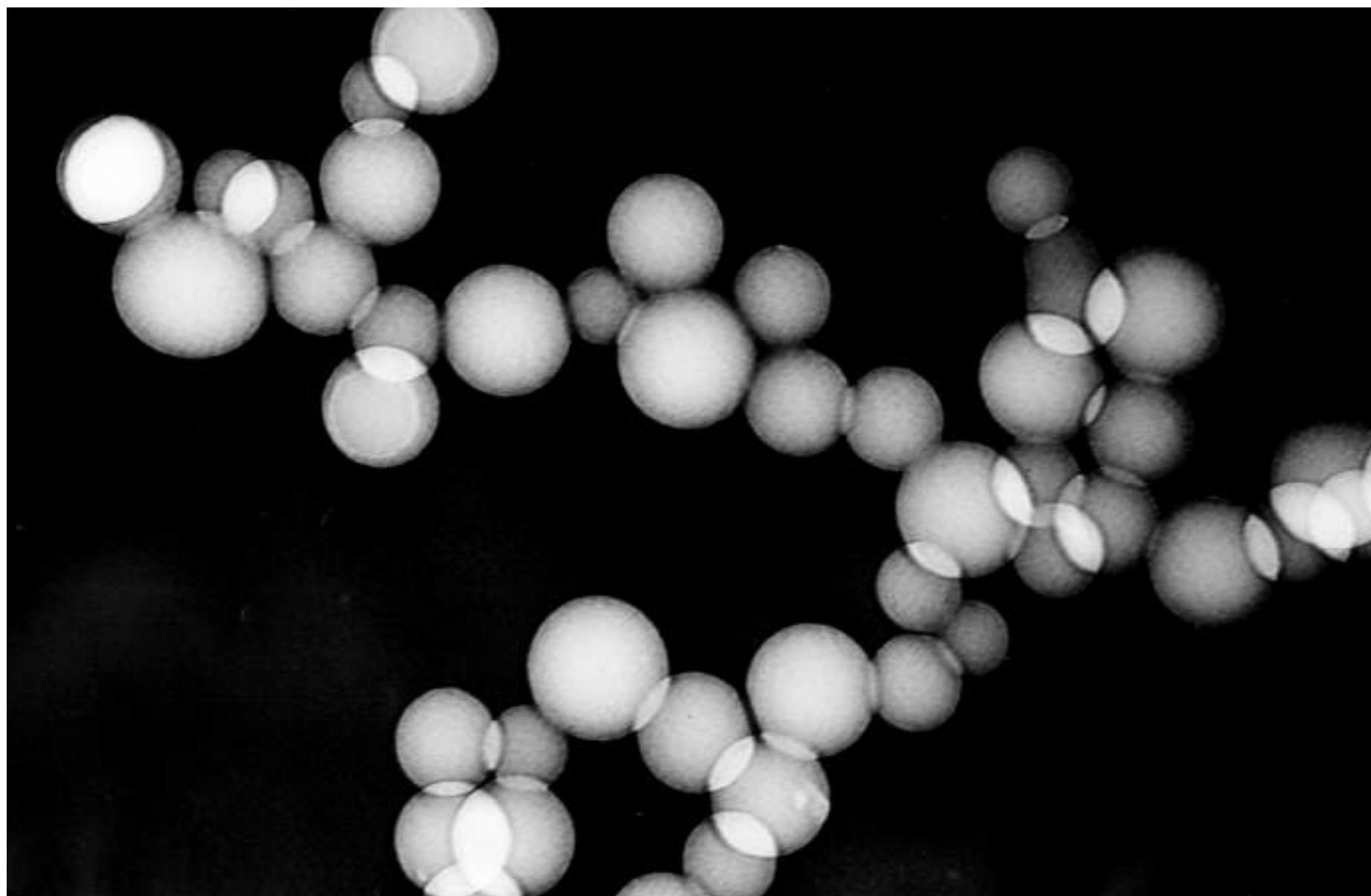
Scientific markers (Bio-fluorescence, radioactive markers)

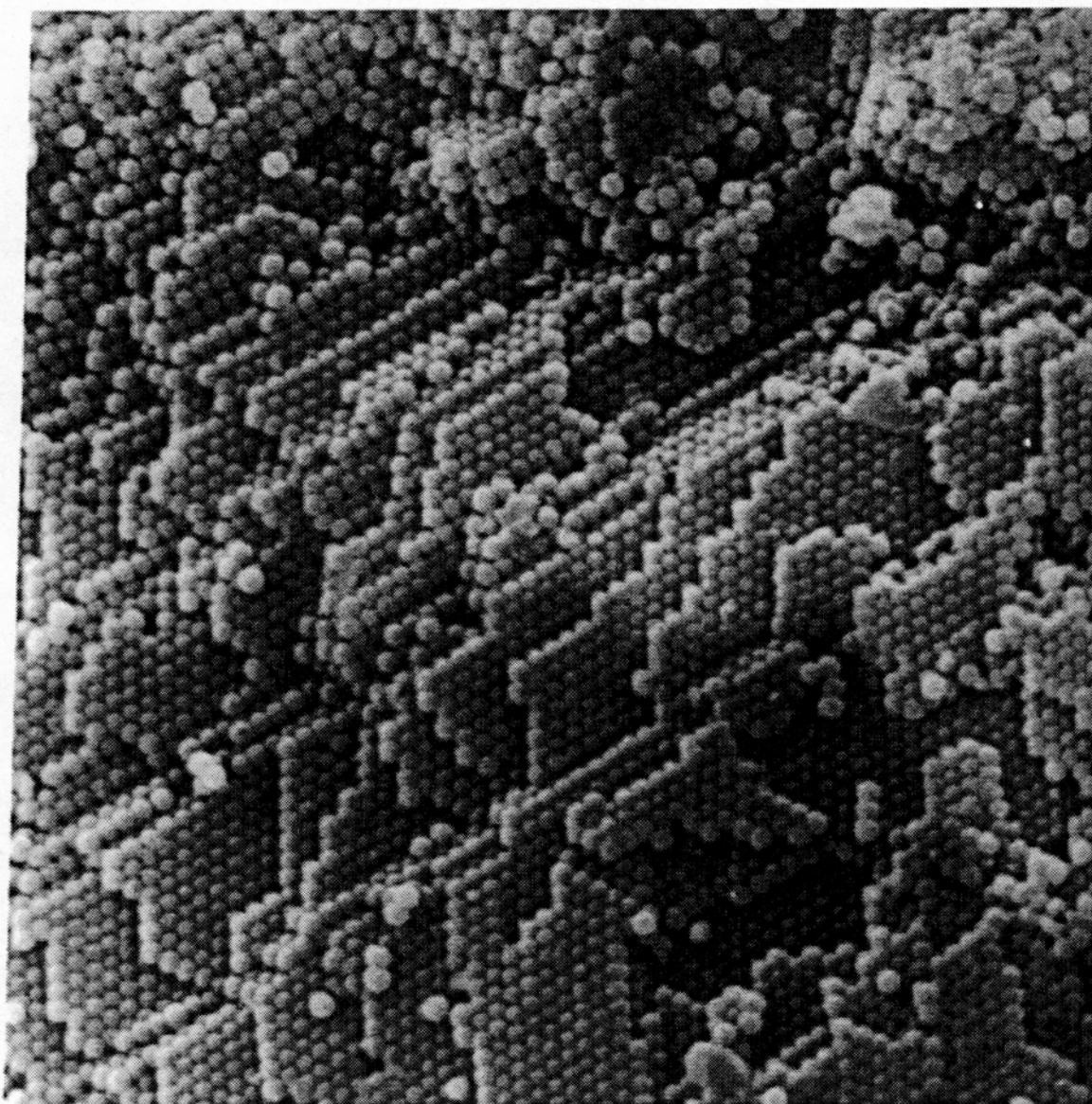
Organic and biologic systems (latex, proteins, viruses, magnetosomes,
organic/anorganic hybrid systems (DNA/Gold) etc.)



**NATURAL
MICRO- AND NANOPARTICLES**

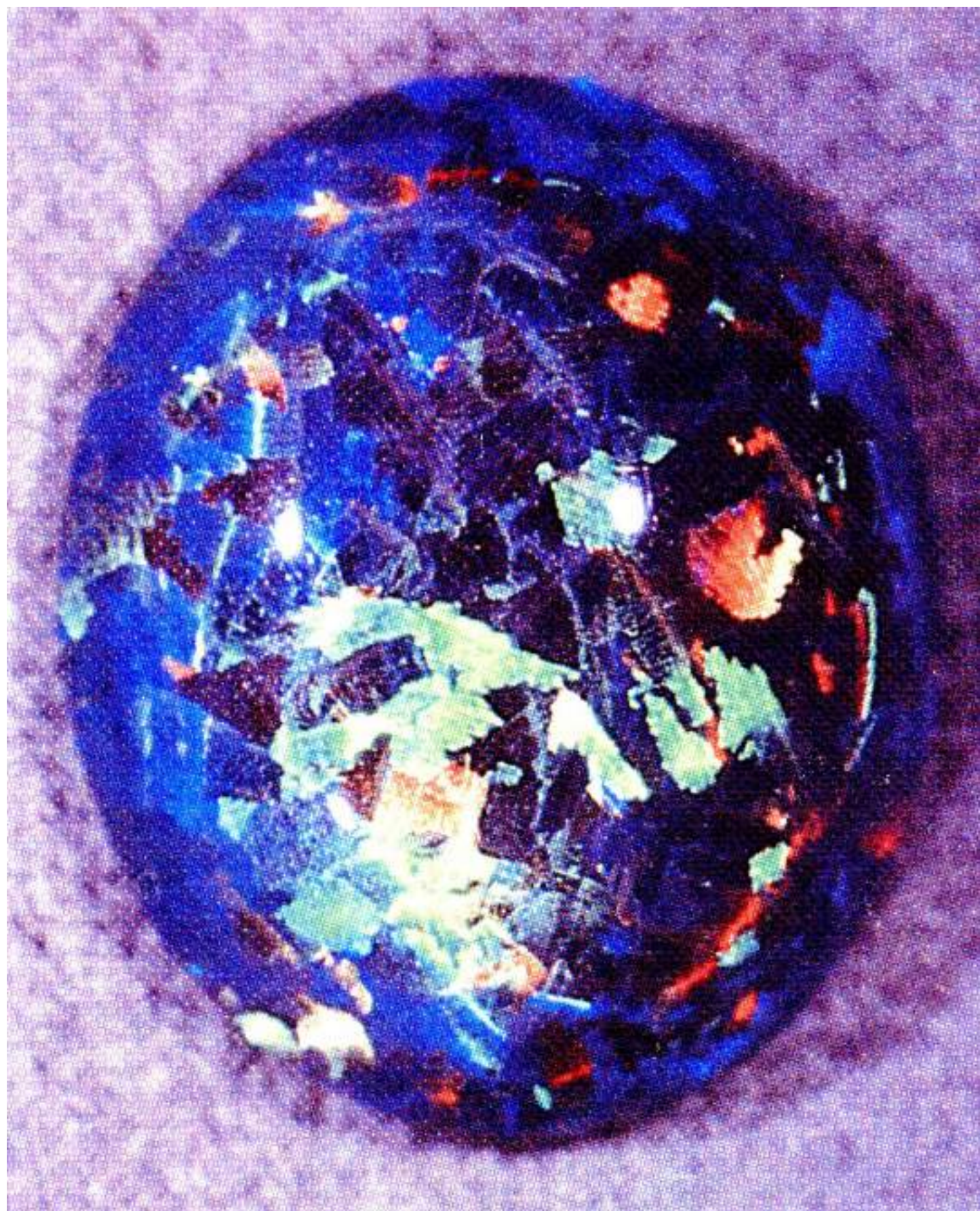
(VULCANO MERAPI / JAVA 2006)

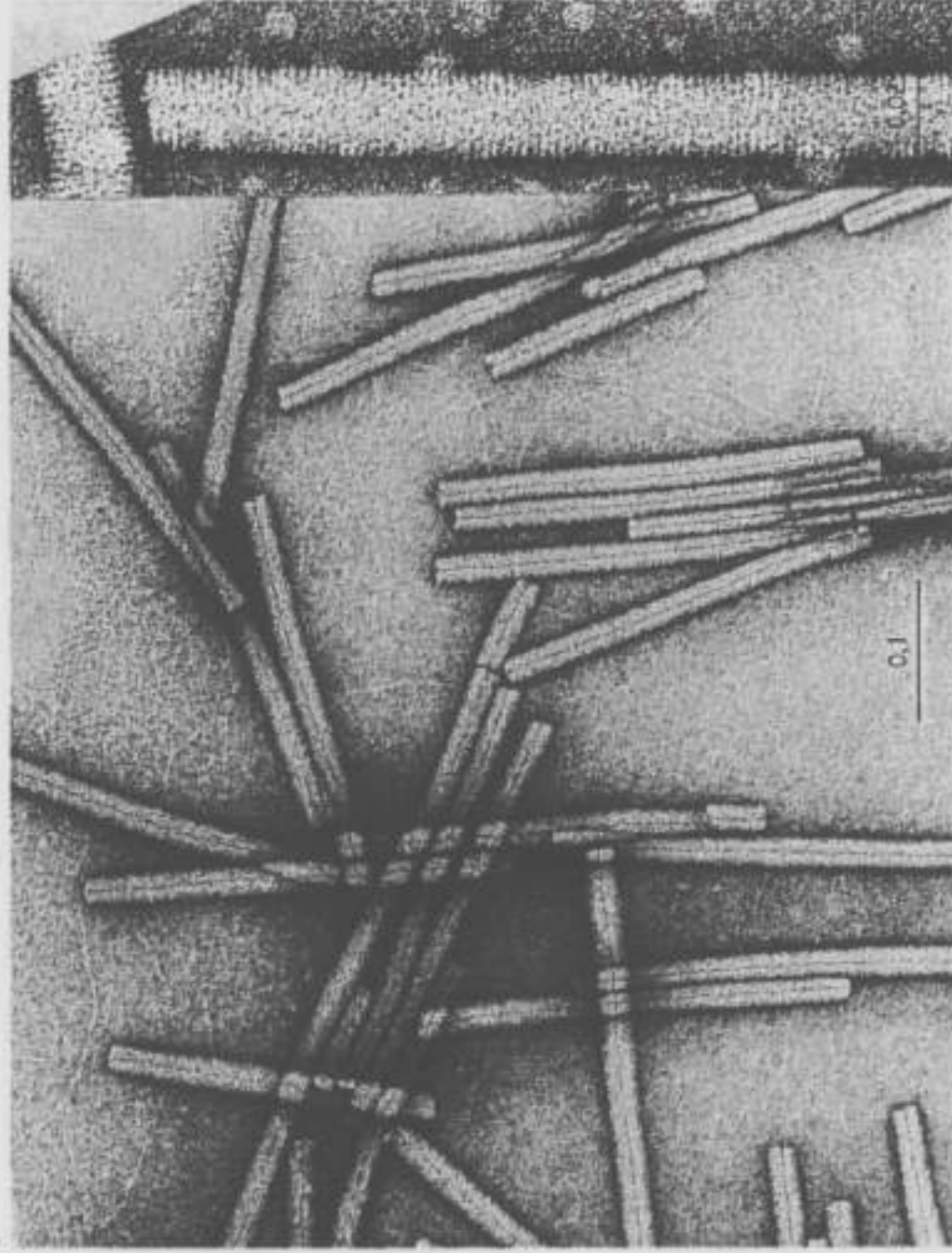


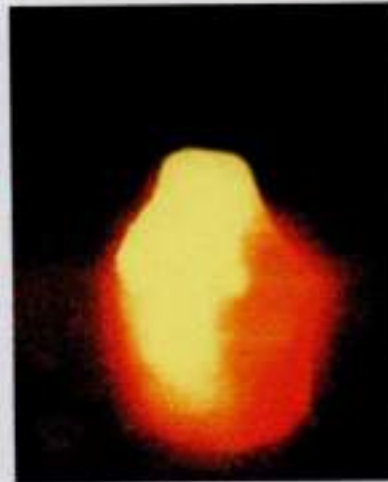
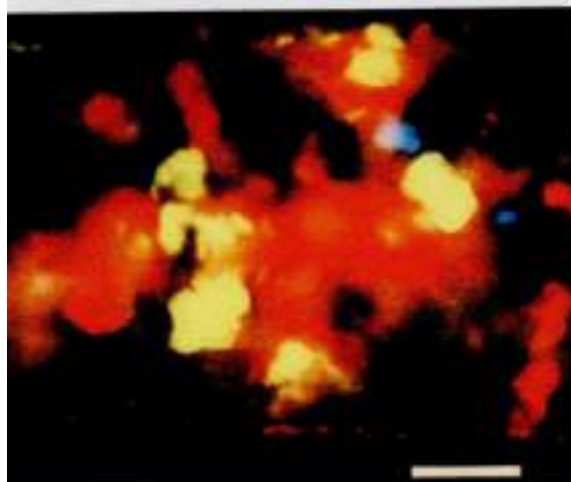


ELECTRON MICROGRAPH OF AN
OPAL – SURFACE

(Silicate spheres : ≈ 200 nm diameter)







TOBACCOMOSAIC-VIRUS-CRYSTALS

Tube diameter 4 mm

Length of the bar 0.5 mm

(U.Kreibitz, C. Wetter Z. Naturforschung 35 c, 750)



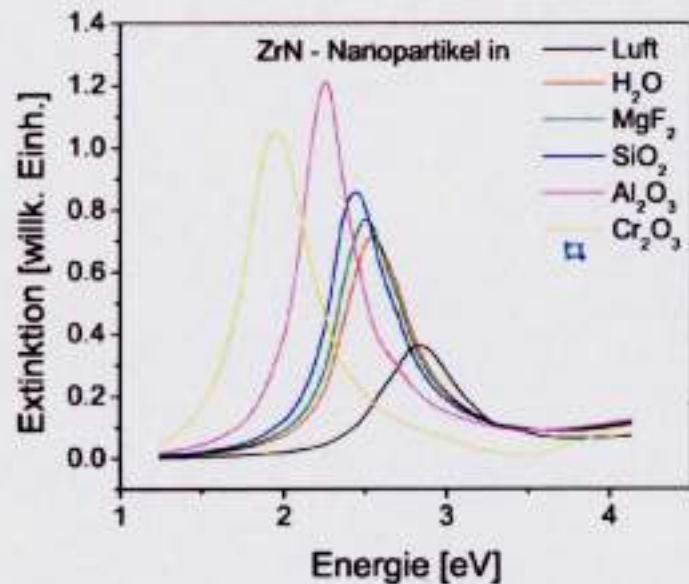
Sie wurden bei der Wied. err. ge-
stellt 9. 1901 hier vorges. d. den.

Mariendom Erfurt
Josephsfenster
um 1375



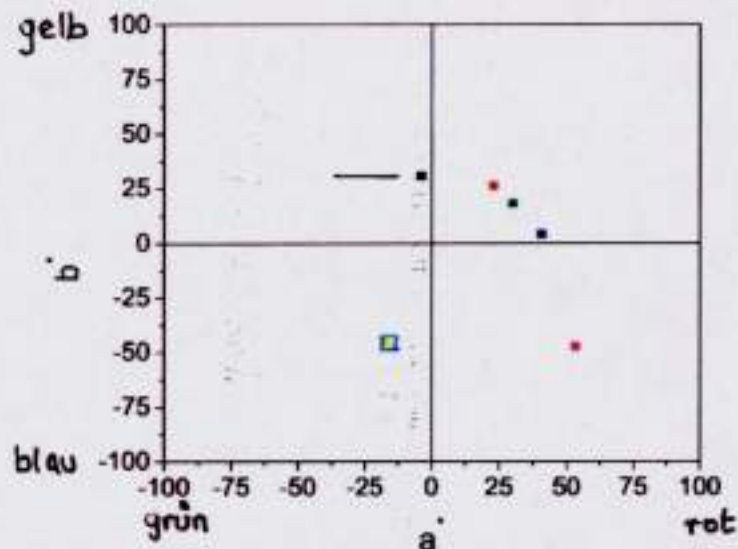
Rechnungen zu eingebetteten ZrN-Nanopartikeln⁵

MIE-Rechnungen⁶ zur Bestimmung der Extinktion:



mit Teilchendurchmesser $2R = 30$ nm
Teilchenkonzentr. $c = 7.09$ kg/m³
Schichtdicke $d = 10$ μ m

Mit den Daten erhält man folgende Farborte mit den Koordinaten a^* , b^* (L^* nicht dargestellt):



Reihenfolge der Einbettmaterialien nach steigendem ϵ : Luft, H₂O, MgF₂, SiO₂, Al₂O₃, Cr₂O₃.

⁵M. Quinten (MQMIE) : CIELAB - Farbmatrik-System

⁶U. Kreibitz, M. Vollmer : Optical Properties of Metal Clusters, Springer





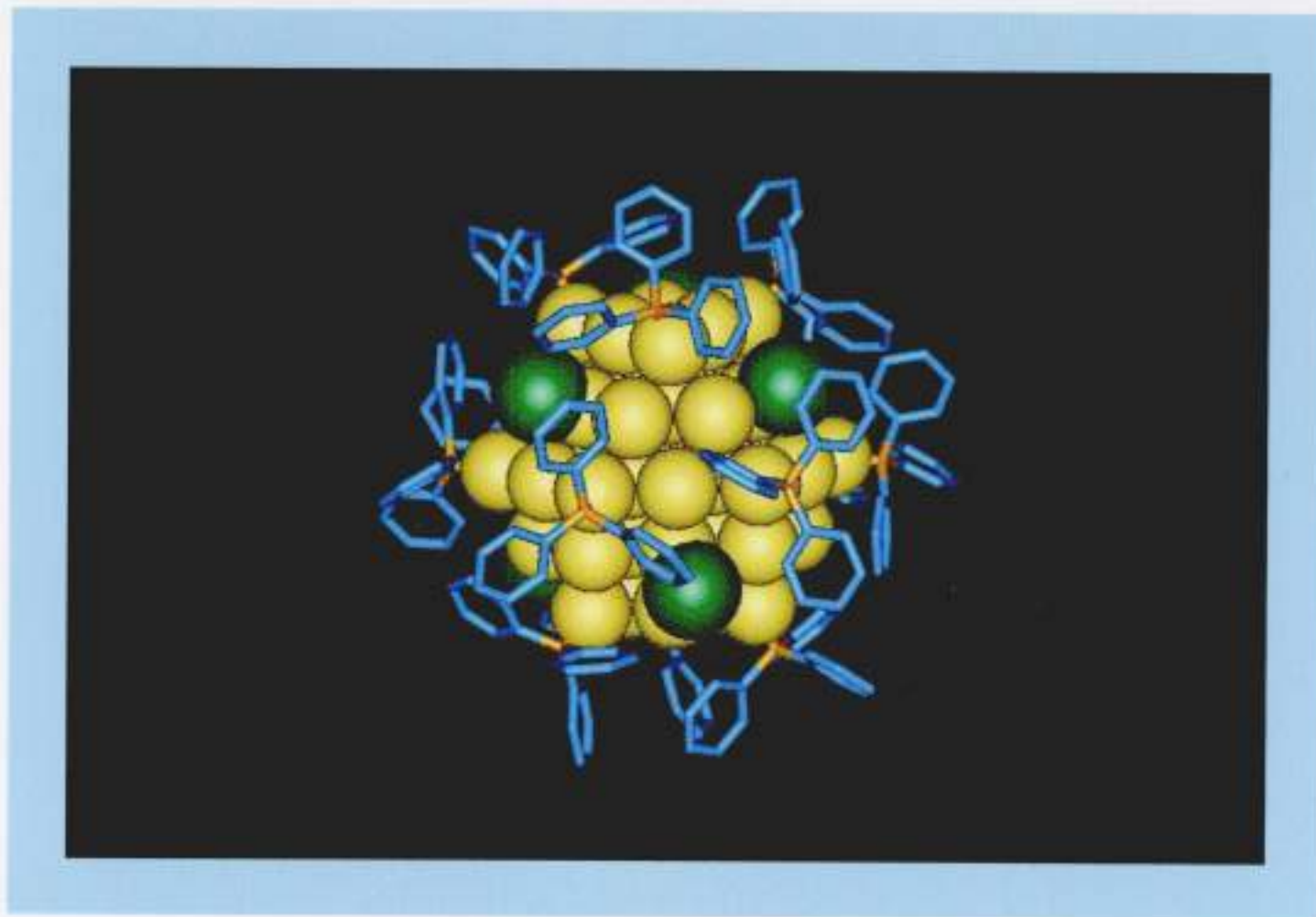
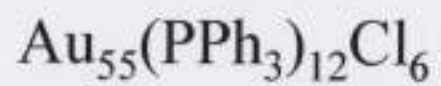
Transmitted Light ↑↑

LYKURGOS - GOBLET
(Roman, 4th century; $4 \cdot 10^{-3} \% \text{ Au}$, $3 \cdot 10^{-2} \% \text{ Ag, Mn}$)

↑↑ Backscattered Light



406 – August Böhm, Meistersdorf, um 1840



gelb: Au; grün: Cl; orange: P; blau: Phenyl

ANISOTROP GEORDNETES KOMPOSIT-MATERIAL AUS IM MAGNETFELD ORIENTIERTEN KOBALT-NANOPARTIKELN (Wollgarten, Dipl.arb.RWTH 1997)

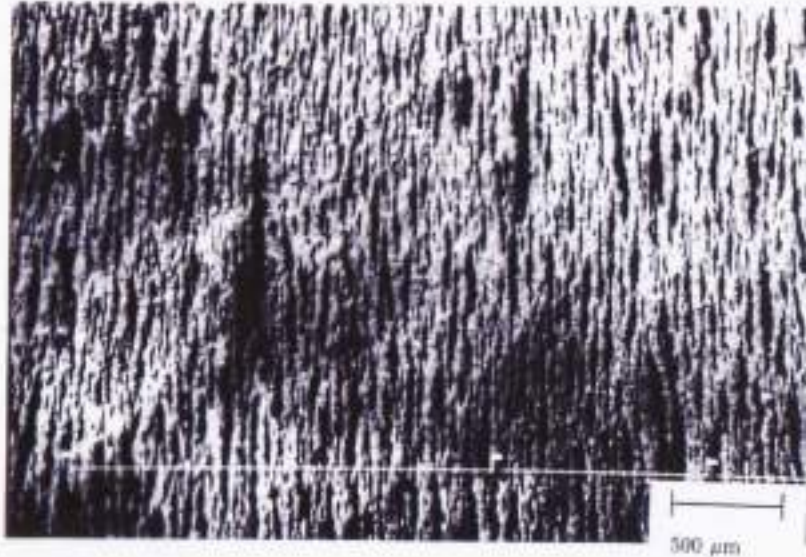


Abbildung 5.11: In einem Magnetfeld mit einer Feldstärke von 0.3 Tesla eingetrocknete Kobaltteilchen (Übersichtsaufnahme mit 35-facher Vergrößerung)

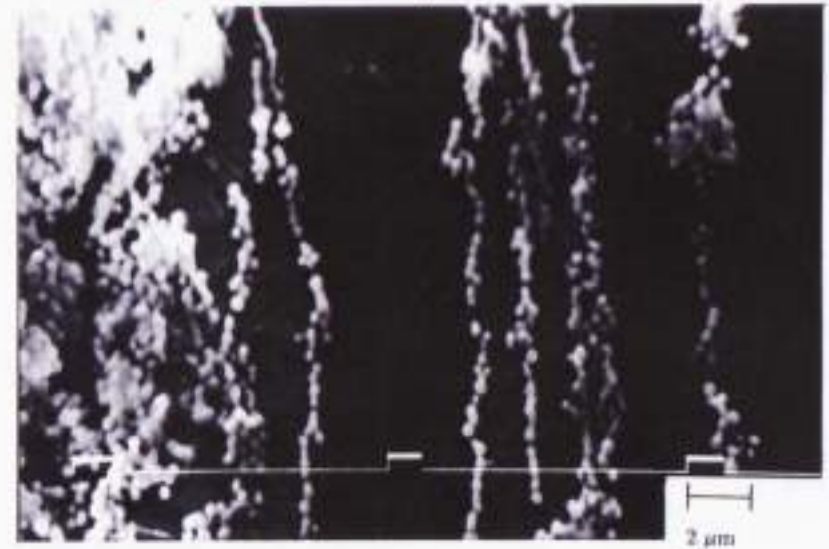


Abbildung 5.13: In einem Magnetfeld mit einer Feldstärke von 0.3 Tesla eingetrocknete Kobaltteilchen (REM-Aufnahme mit 5000-facher Vergrößerung)

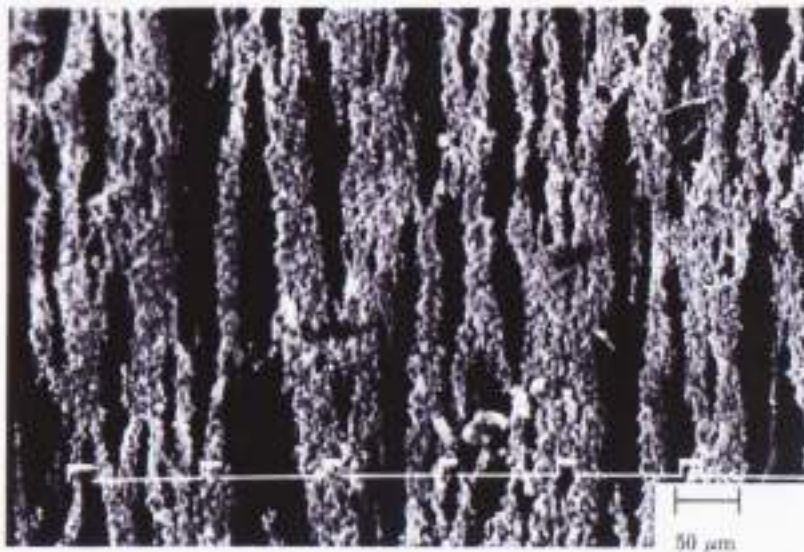


Abbildung 5.12: In einem Magnetfeld mit einer Feldstärke von 0.3 Tesla eingetrocknete Kobaltteilchen (REM-Aufnahme mit 700-facher Vergrößerung)

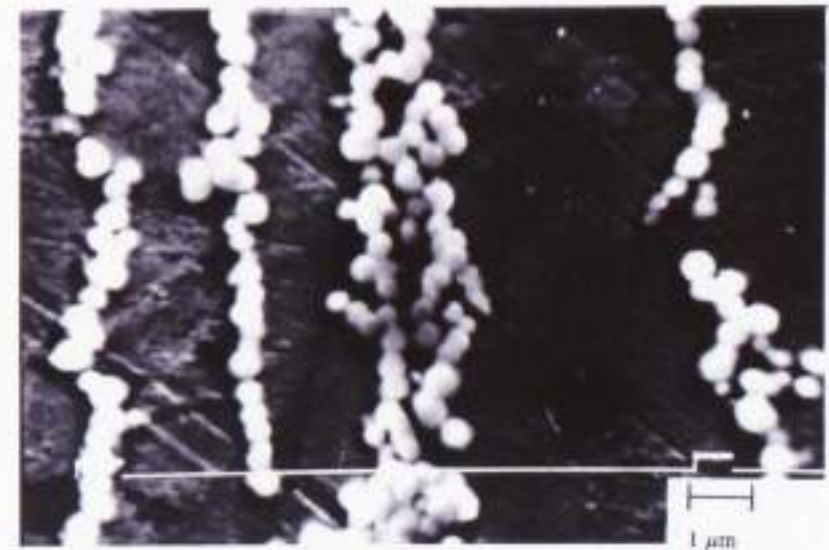
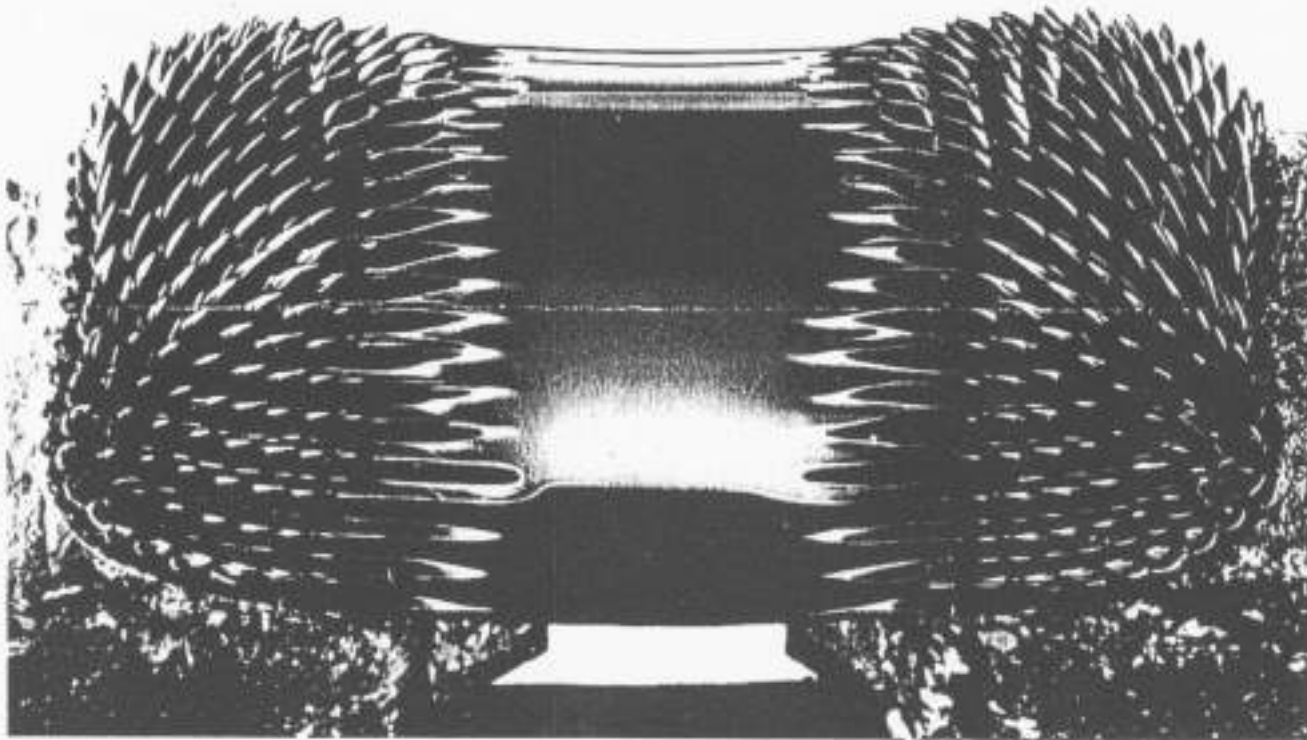


Abbildung 5.14: In einem Magnetfeld mit einer Feldstärke von 0.3 Tesla eingetrocknete Kobaltteilchen (REM-Aufnahme mit 10000-facher Vergrößerung)

Ferrofluid – Die Magnetische Flüssigkeit

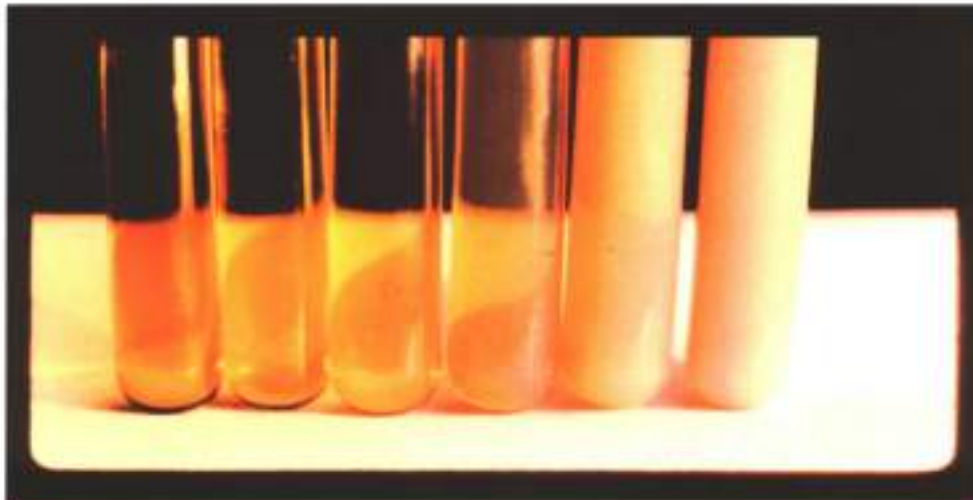


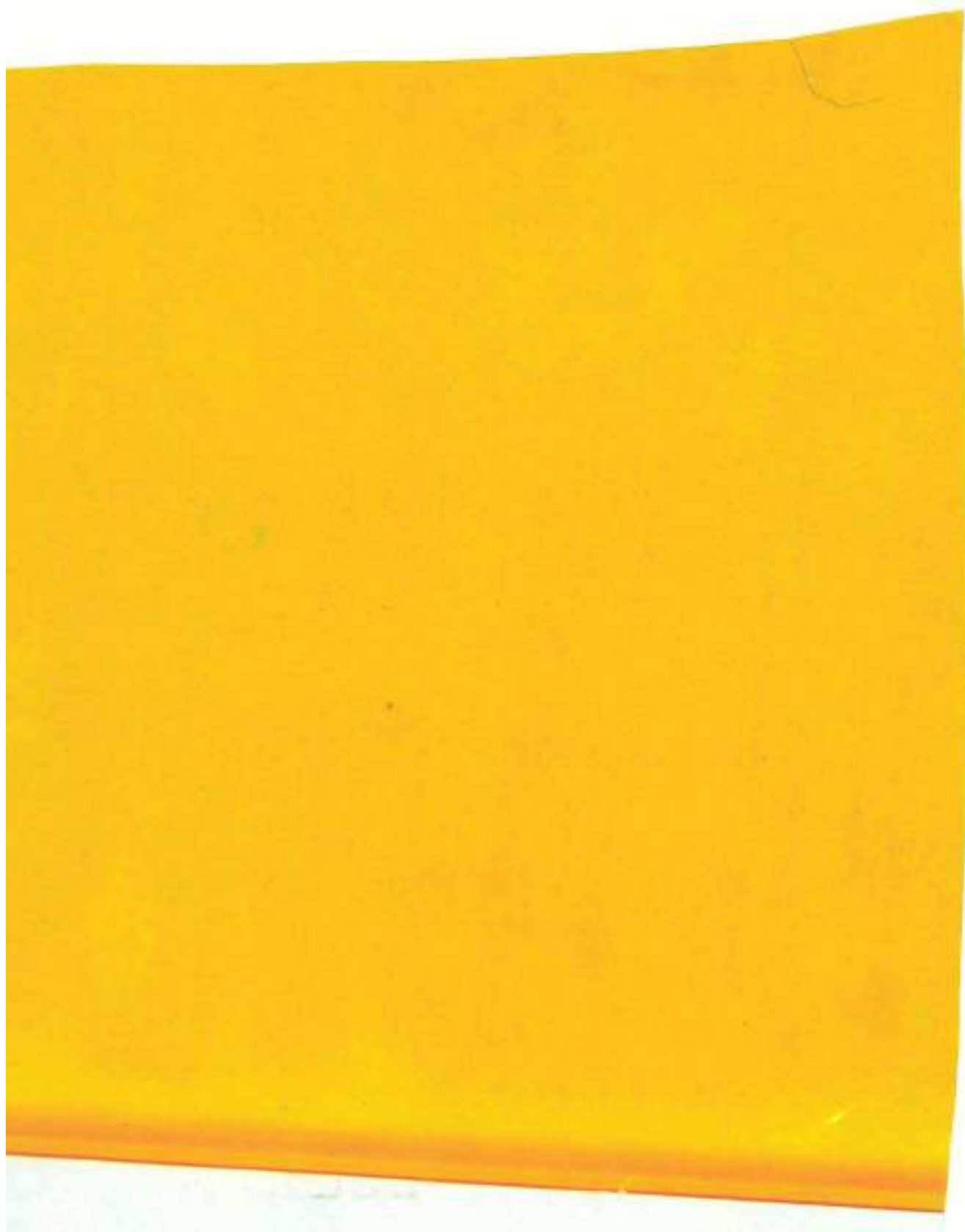
Ferrofluid-Probe mit dem eigenartigen struppigen Aussehen ist trotzdem eine Flüssigkeit. Hier auf einem Uhrglas über einem Magnet.

Ein Ferrofluid ist eine kolloidale Suspension magnetischer Teilchen in einer Trägerflüssigkeit. Die Flüssigkeit bleibt in flüssiger Phase, auch wenn sie geregelt, gesteuert oder kinetisch von einem Magnetfeld beeinflusst wird.



ZSIGMONDY-Ag- COLLOIDS: Mean sizes increasing from 6 to 60 nm
Top: Transmitted light. Bottom: Scattered light





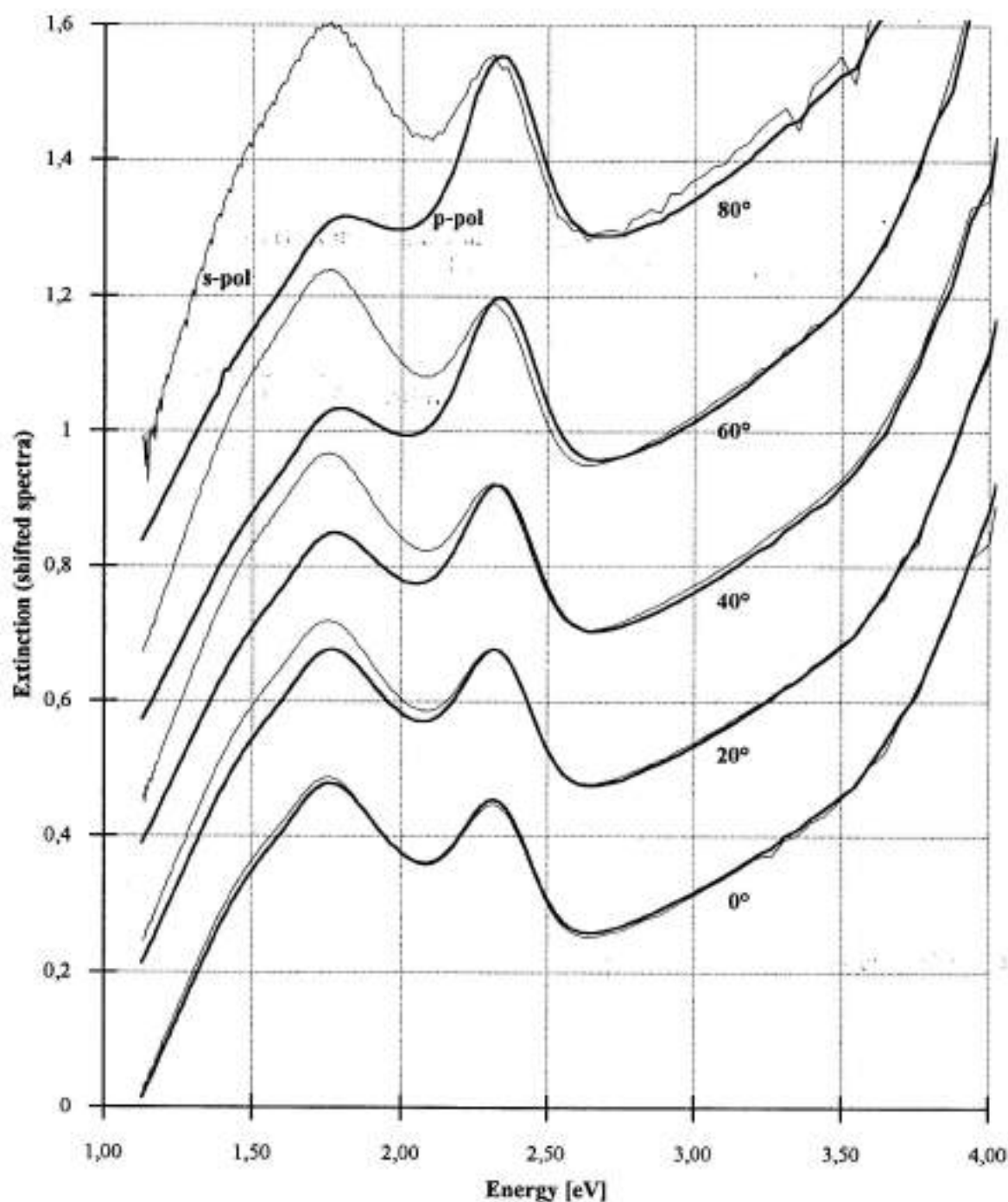
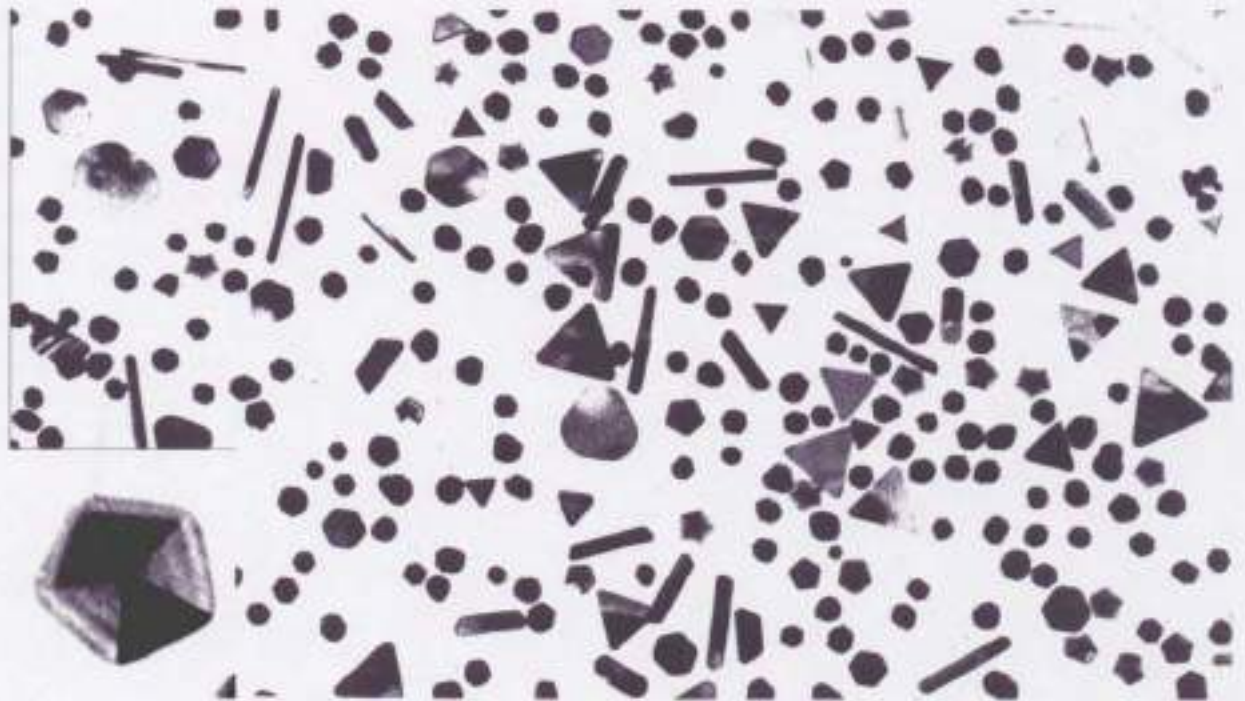


Abbildung 8.47: Au 13.7 : Extinktionsspektren bei verschiedenen Einfallswinkeln mit s- und p-polarisiertem Licht

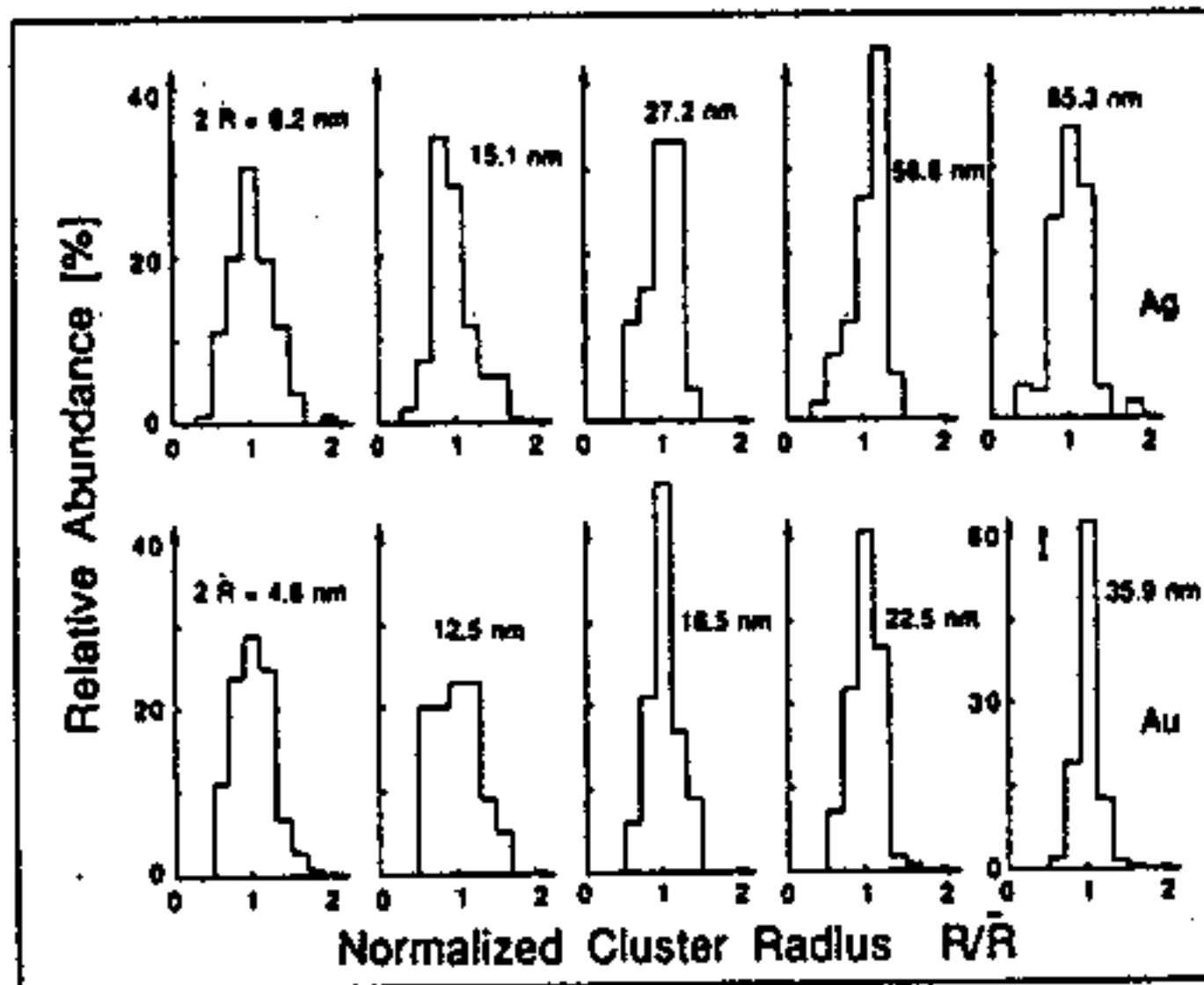
**Various Gold Nanostructures
produced by the
Zsigmondy aqueous colloid method**



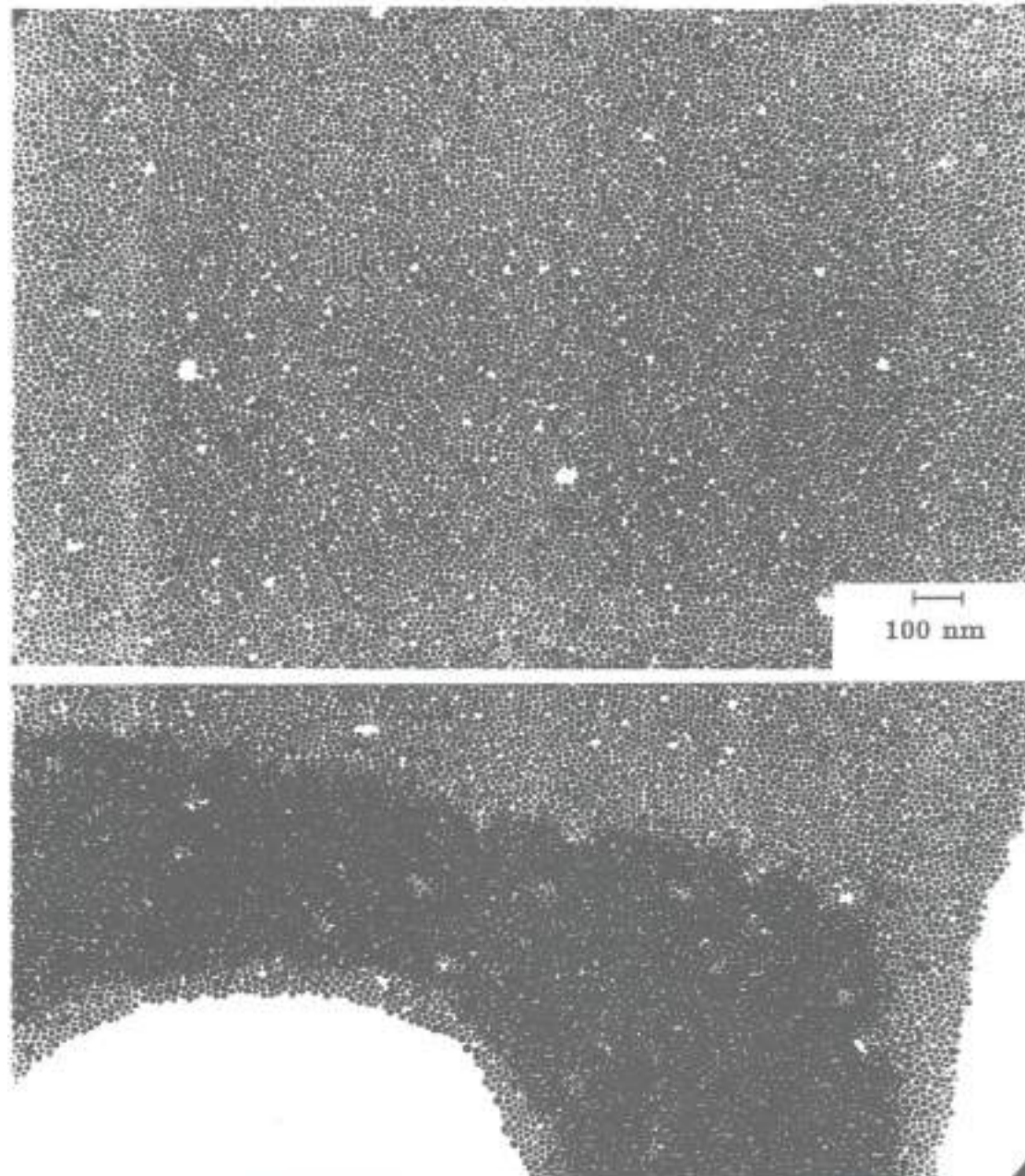
Picture: Mean nanoparticle size 36 nm
Longest nanowires 200 nm

Inset: Pentagonal twin particle with diameter 40 nm

(U. Kreibig, thesis, Universität des Saarlandes 1971)



WEAK SELF-ASSEMBLY OF LIGAND-STABILIZED AU-CLUSTERS
(Kreibig, Schmid)



PRODUCTION METHODS OF CLUSTER-MATTER

Condensation of atoms

Dispersion of bulk

**Supersaturation
in vapor
Deposition on substrate
Embedding in matrix**

**Supersaturation
in liquids**

**Supersaturation
in matrix**

**Mechanical
dispersion**

**Electrical
dispersion**

Physical Methods(UHV)

Thermal evaporation
Adiabatic expansion
Sputtering + seeding gas
Laser ablation+seeding

Chemical Methods

Colloidal Systems
Chemical reduction
Photolysis, radiolysis
Sol-gel

Physical or Chemical Methods

Diffusion in solid matrix
Diffusion into matrix
Phase separation
Co-evaporation (matrix
isolation)

Physical Methods

Milling
Porous matrix
Ultrasound
Spraying

Physical Methods

arc discharge
exploding wire
(laser ablation)

(3) Example : The Nanoparticle Source LUCAS

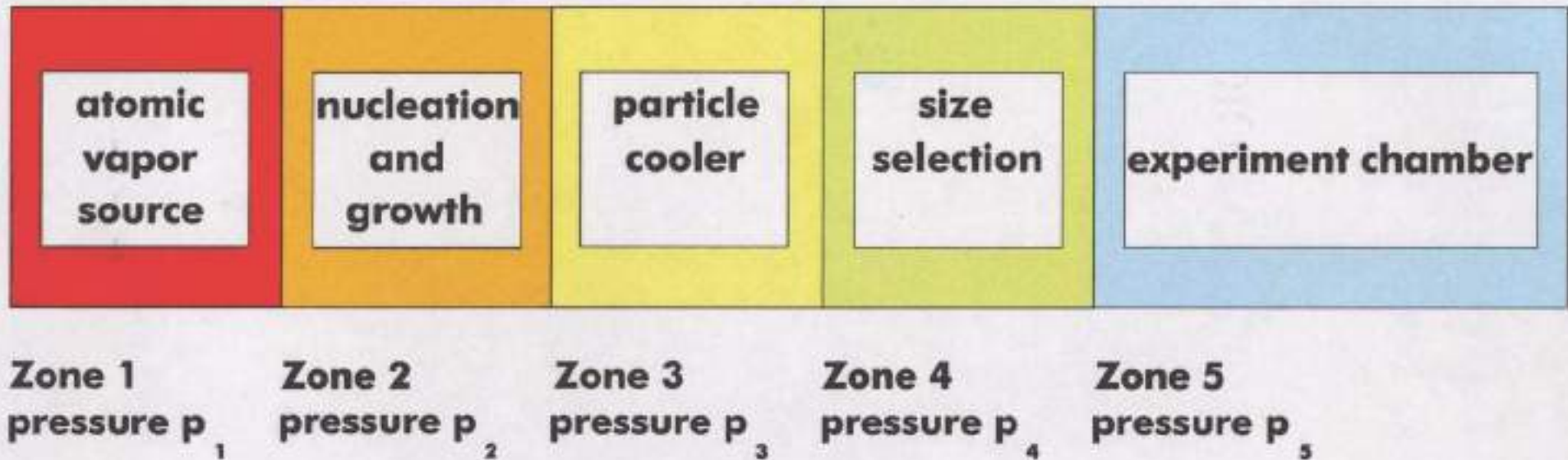
Cluster - Source and Preparation-Chamber :

LUCAS

Laser Universal Cluster Ablation Source

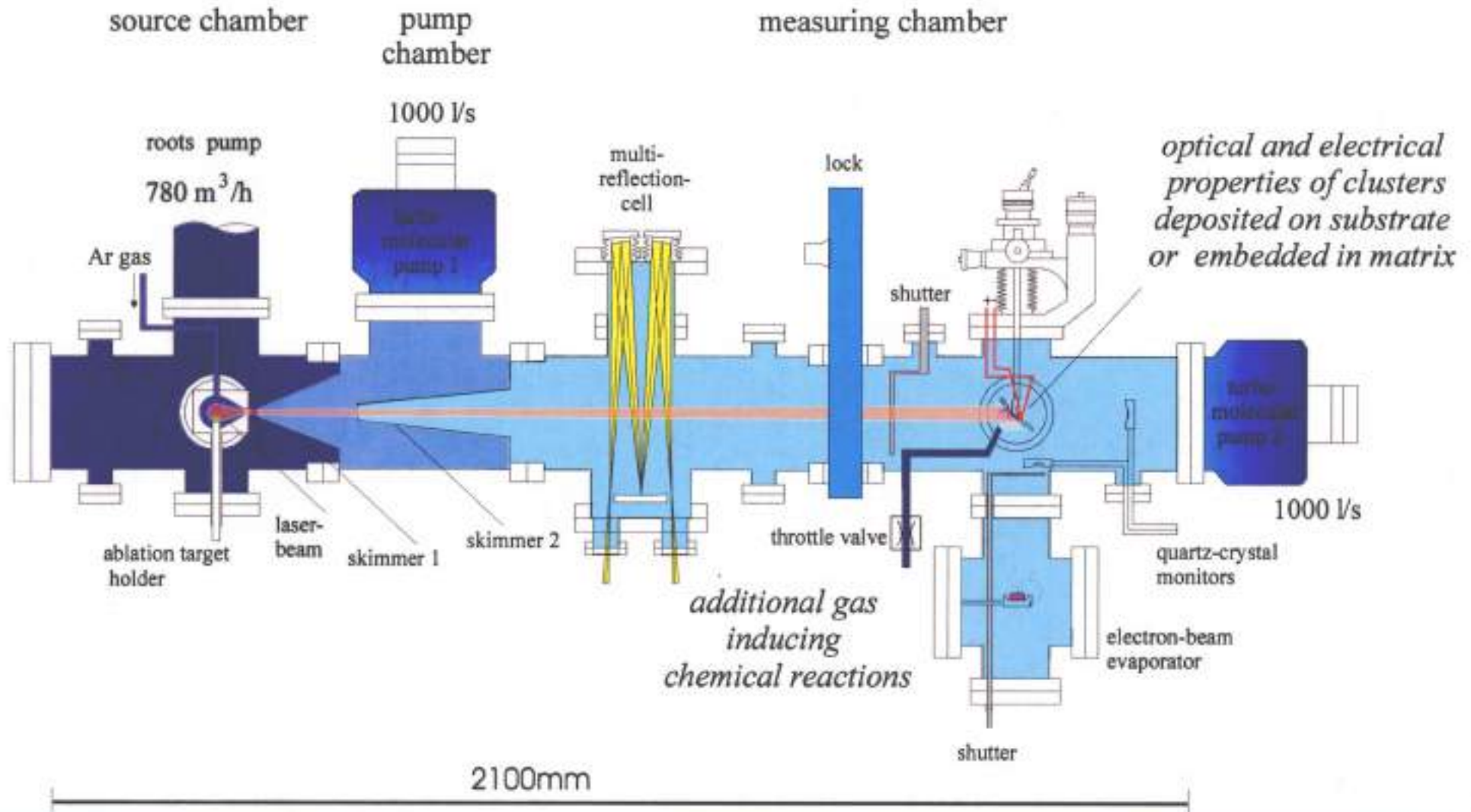
Michael Gartz 1998
Alexander Reinholdt 2005

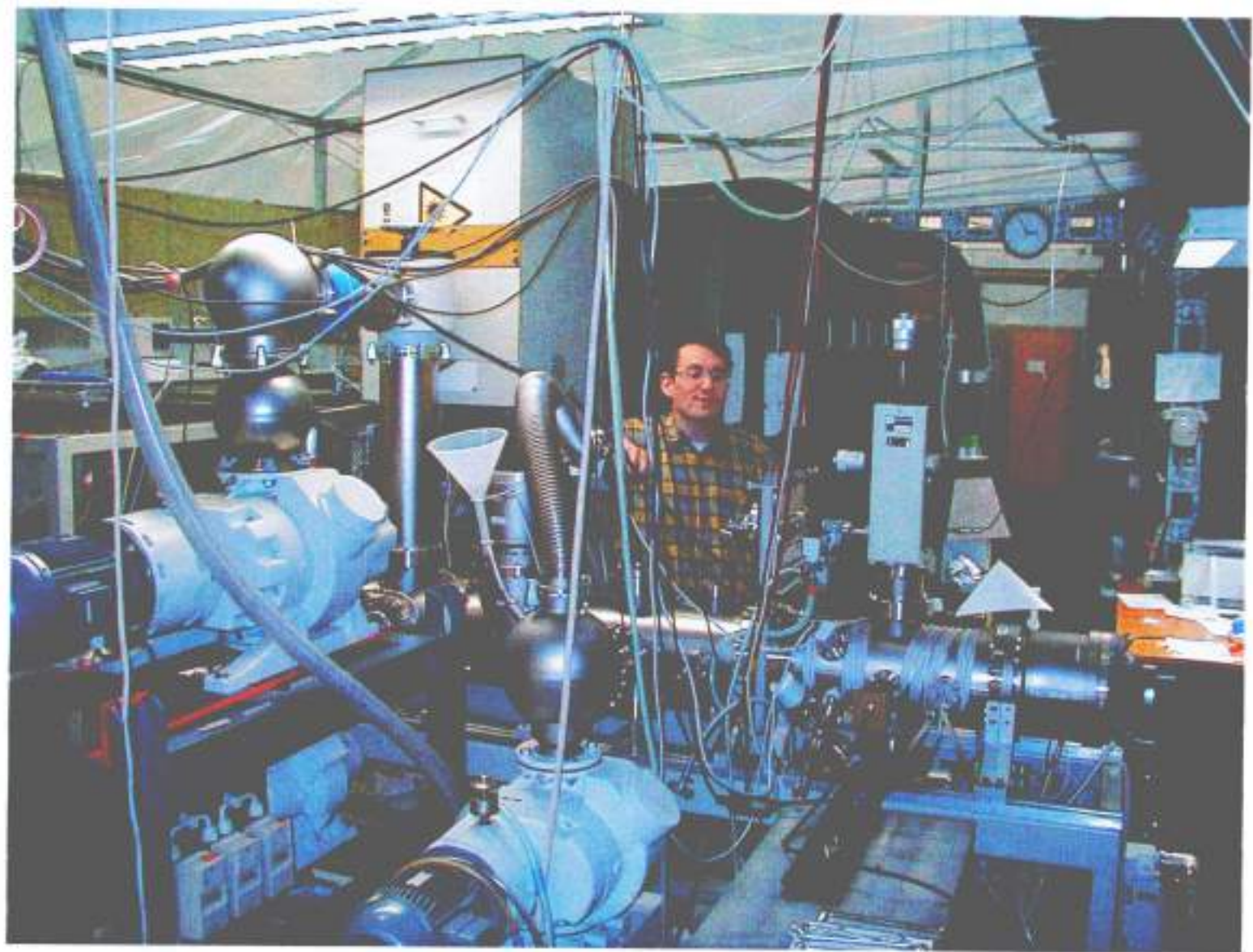
SCHEMATIC CONSTRUCTION OF A NANOPARTICLE SOURCE



LUCAS

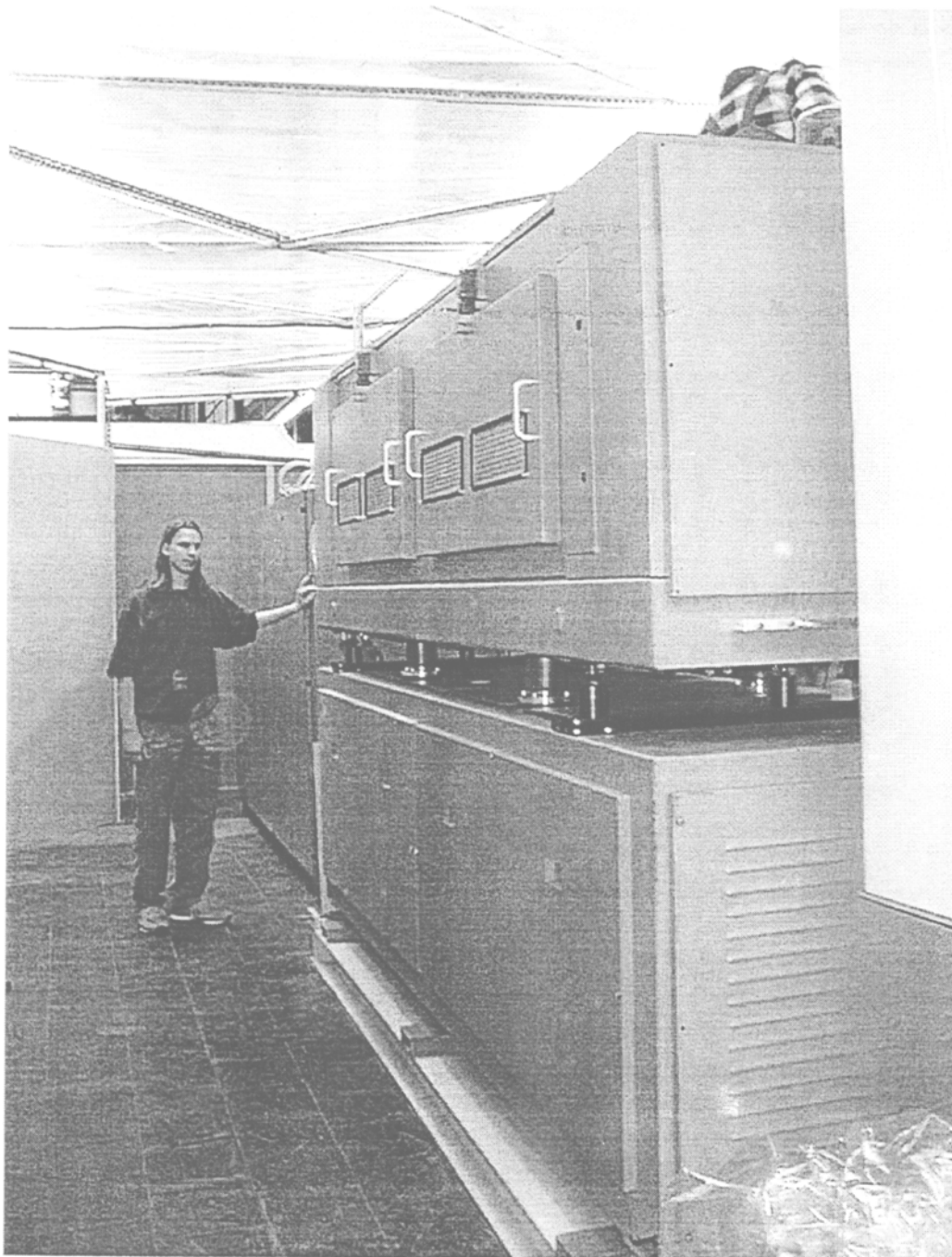
Laser Universal Cluster Ablation Source





THE R-S 2500 CO₂ - LASER

(SPONSORED BY THE FRAUNHOFER-INSTITUT FÜR LASERTECHNIK)



(4) Plasmons

Plasmons in Free-Electron Material (DRUDE Material) of Various Shapes in Quasistatic Approximation (Unretarded Dipole Mode)

Definition: Plasmons = Energy quantized resonance modes of collective, coherent motions of a free electron plasma. This motion is connected with a (negative) charge wave.

Depending on the sample shape and size, many different modes can be excited.

By electron relaxation processes their life-time is very short ($\approx 10^{-14}\text{s}$).

Plasmons are not included in electronic band structures (which describe single electron-hole excitations).

Localized versus propagating plasmons :

1) If the electrons are confined in a volume with dimensions smaller than the mean free path (MFP) of the single electron motion, then the plasmon is localized; the modes are oscillatory modes.

Examples are observed in nanoparticles of various shapes.

2) If the sample is large compared to the MFP the plasmon propagates as a plasma wave.

Examples are nanowires, thin films, bulk materials.

Surface versus bulk plasmons :

1) In surface plasmons, the el. excess charges are bound to the sample surface or sample/surrounding interface. Then, the wave is exponentially damped into the inner of the sample. The plasmon waves are commonly transverse.

2) In the extended bulk without surface, longitudinal volume plasmons (charge density waves) can be excited.

**(5) Free Surface Plasmons
and
Surface Plasmon Polaritons**

**A Comparison of
Electron Energy Loss Spectroscopy
and
Optical Spectroscopy**

(U. Kreibig, 1970)

Free plasmons versus plasmon polaritons

1) After some pulse-like excitation (e.g. by fast-electron collisions) the electron plasma can oscillate freely with its eigenfrequency.

2) If a plasmon is excited by incident electromagnetic fields, the collective, coherent electron motions are induced via the electrical charges.

The samples act as "nano-antenna" reemitting scattering fields which, again, interact with the field outside the sample. Hence, the total excitation state is a hybrid state of the light field and the mechanical motion of the material system of the electrons, coupled by the electronic charge.

Only if the sizes of the nanostructures R are extremely small to the light wavelength, $R \ll \lambda$, then the resonance frequencies equal the eigenfrequencies of the electron system. In larger samples, the external el.mag. field changes the resonance frequency drastically. The dispersion curves $\omega(\mathbf{K})_{\text{electron}}$ of propagating plasmon waves must coincide with the light line $\omega(\mathbf{K})_{\text{light}}$.

Example: The eigenfrequencies of nanoparticles with DRUDE electrons:

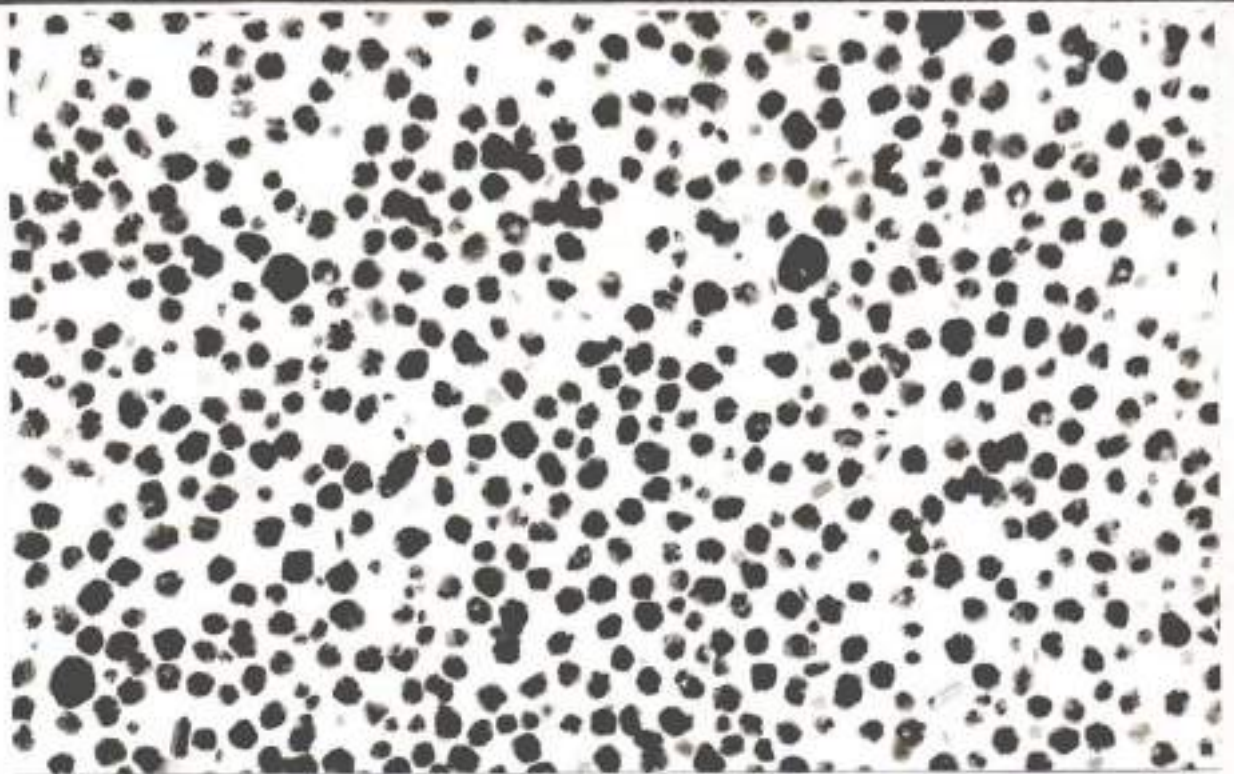
The internal field in the case of a spherical nano is (see above) :

$$E_{\text{interior}}(\omega) = E_0(\omega) [3 \epsilon_{\text{medium}} / (\epsilon(\omega) + 2 \epsilon_{\text{medium}})]$$

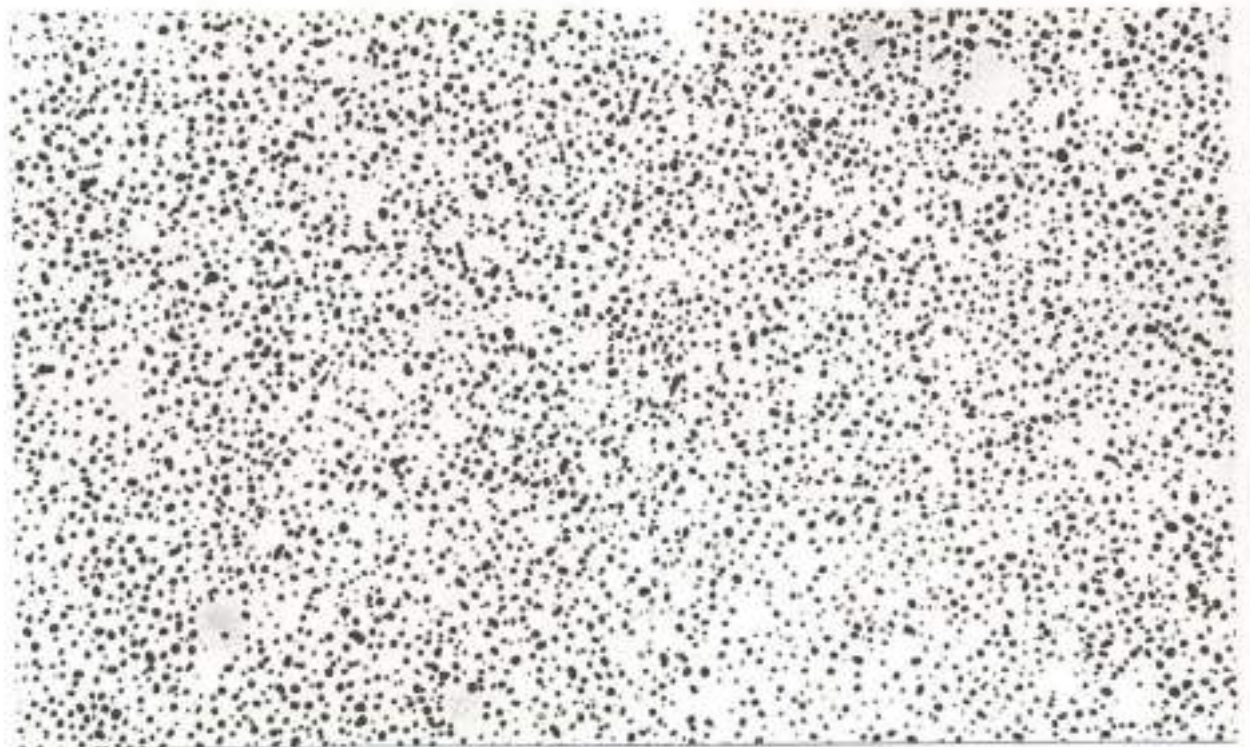
The resonance of E_{interior} is obtained at the minimum of the denominator:

$$[\epsilon_1(\omega_{\text{resonance}}) + 2 \epsilon_{\text{medium}}]^2 + [\epsilon_2(\omega_{\text{resonance}})]^2 = \text{minimum.}$$

Since $\epsilon_2(\omega) > 0$ always, $\epsilon_1(\omega_{\text{resonance}})$ must be negative, $\epsilon_1 < 0$.



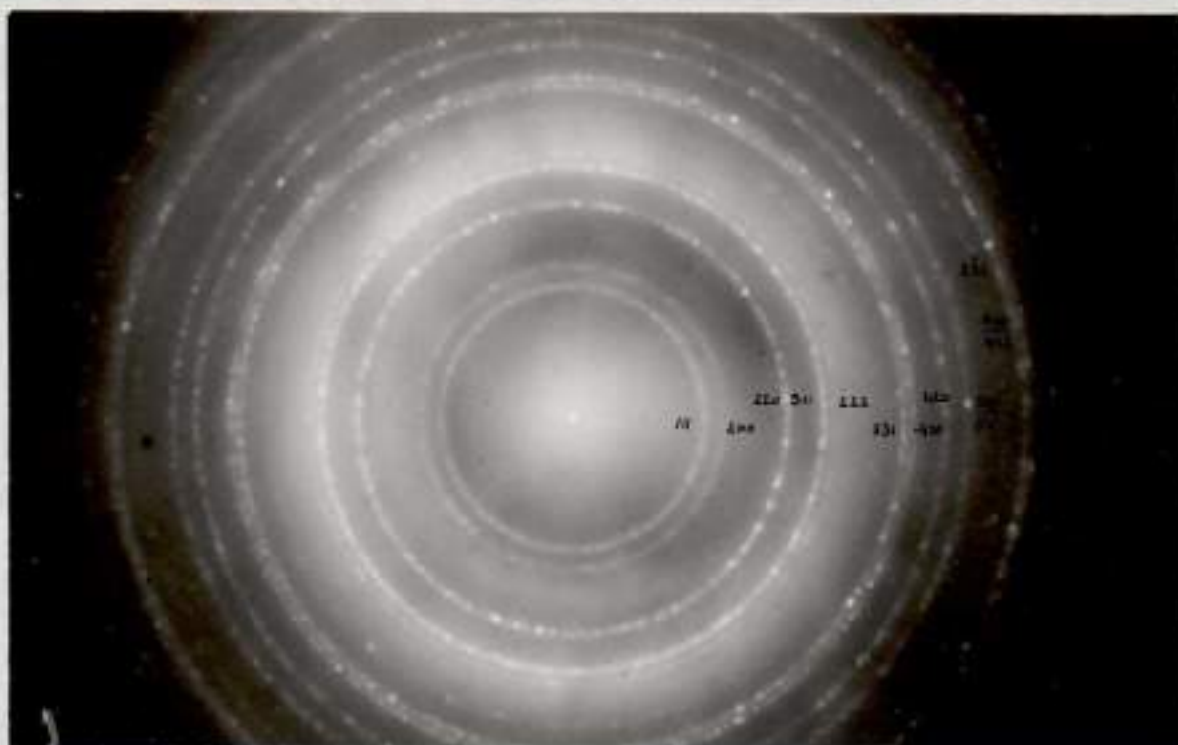
Silber $2R = 566 \text{ \AA}$ 100 kV



Gold $2R = 48 \text{ \AA}$ 100 kV

*Exp.
Physik I
Saarbr.*

Fig.10 Elektronenmikroskopische Aufnahmen
der Silberkristallit-Probe von Sol Nr.11
($2R = 566 \text{ \AA}$) und der Goldkristallit-
-Probe von Sol Nr.1 ($2R = 48 \text{ \AA}$)
Spannung: 100 kV



Silber $2R=204 \text{ \AA}$ 100 kV



Gold $2R=125 \text{ \AA}$ 100 kV

*Exp.
Physik I
Saarbr.*

Fig.13 Feinbereichsbeugung von Silber-
und Goldkristallit-Proben.
Silber: Sol Nr.5 ($2R = 204 \text{ \AA}$)
Gold: Sol Nr.2 ($2R = 125 \text{ \AA}$)
Spannung: 100 kV

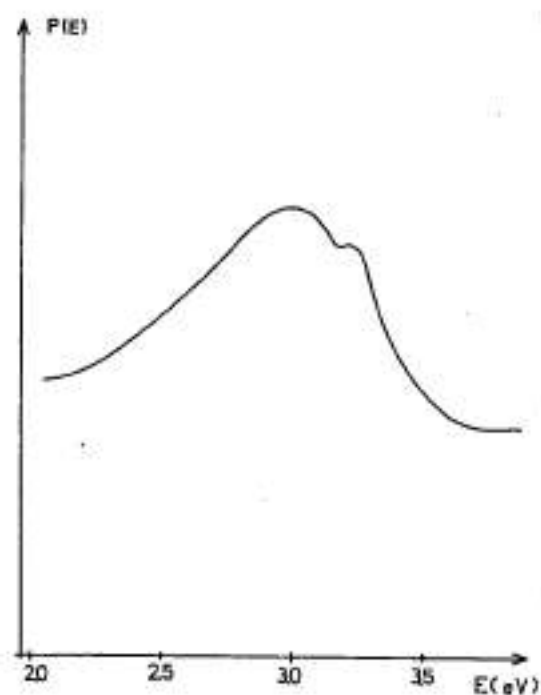


Fig. 3. Energy loss spectrum for silver particles with $2R = 322 \text{ \AA}$

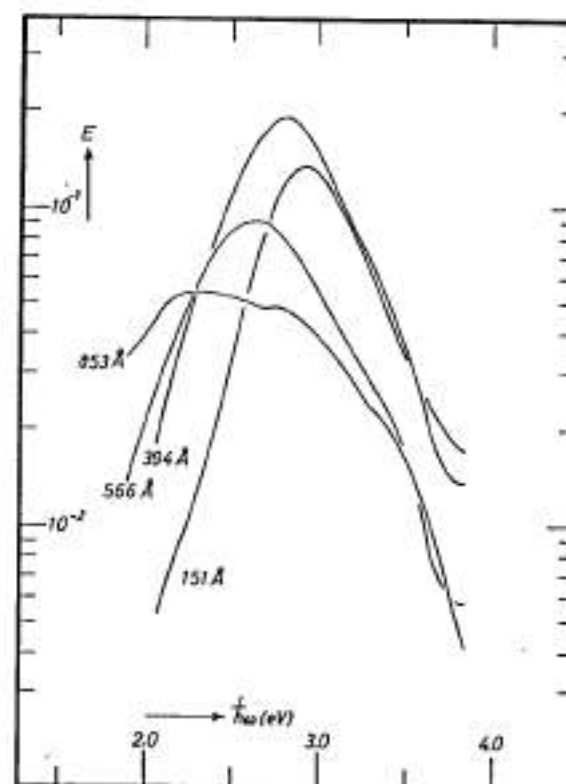


Fig. 7. Dependence of the measured extinction E of some of the silver colloids in solid layers on photon energy of the incident light. Parameter: mean particle diameter $2R$

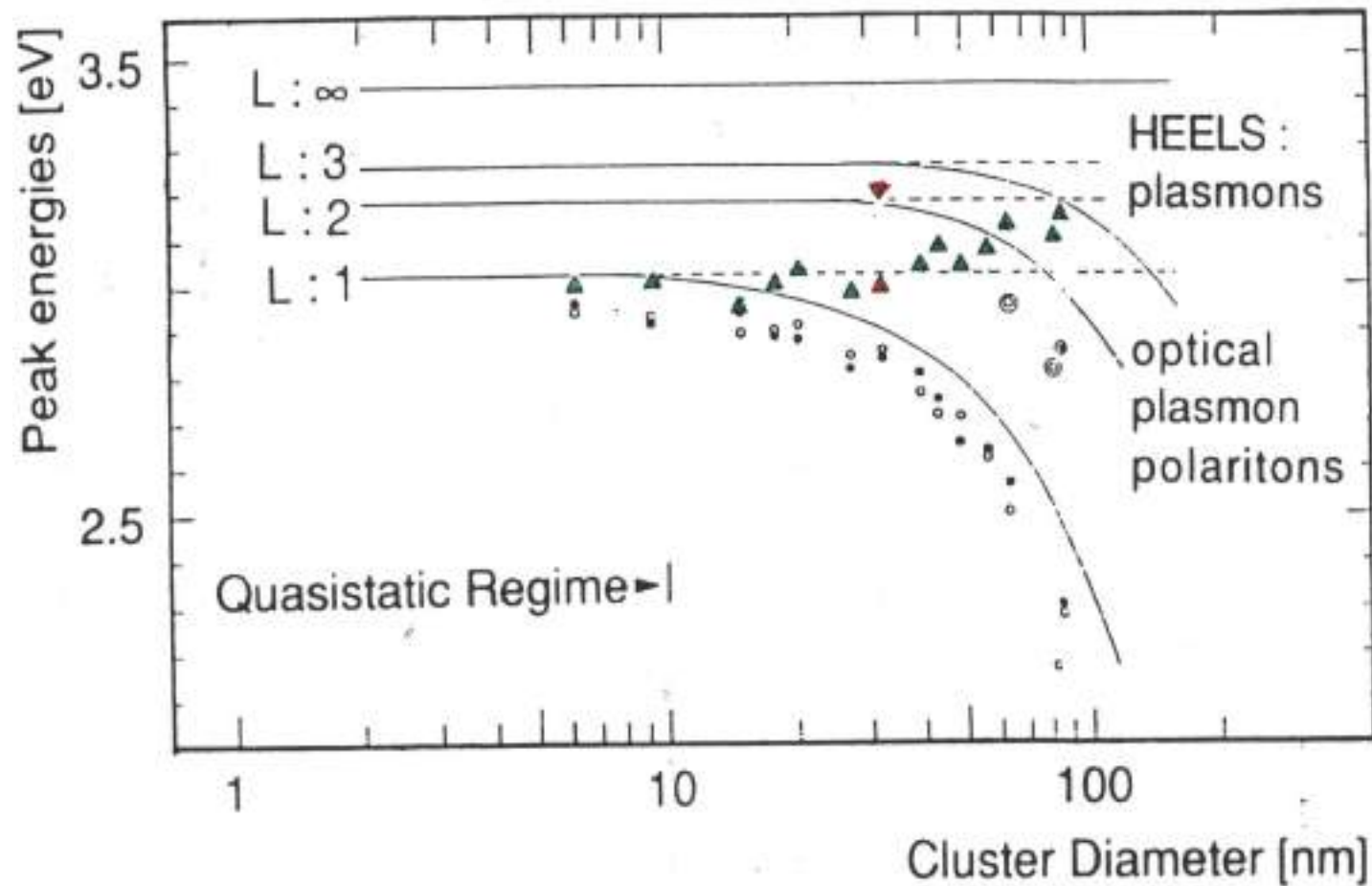


Fig. 2.24. Peak energies of free plasmons in Ag clusters, e.g. excited by electrons in High Energy Electron Loss Spectroscopy (HEELS) and of optically excited plasmon polaritons, of various multipole order L (after [2.75]). The resonance energies of the free plasmons are almost independent of cluster size (no dispersion) whereas excitation with light shows phase retardation effects. All symbols denote experiments, the solid lines (polaritons) and dashed lines (plasmons) refer to theory. Embedding matrix: solid gelatin.

(U. KREIBIG, P. ZACHARIAS, Z. PHYSIK 1970)

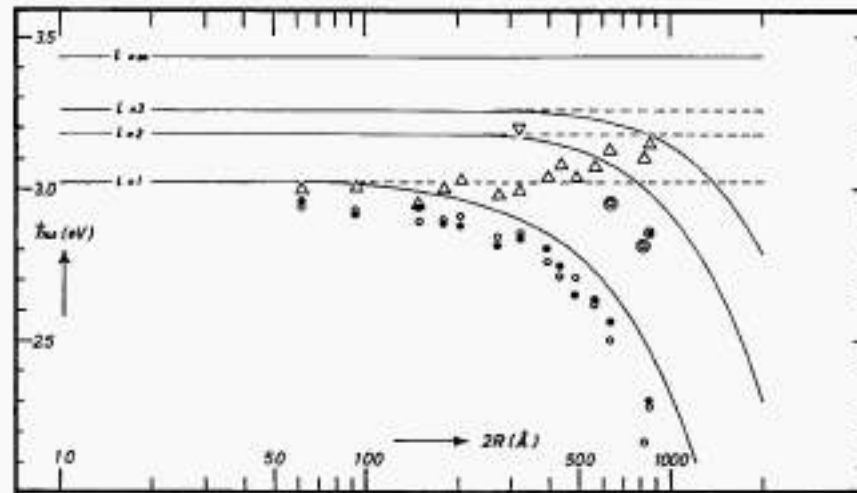


Fig. 8

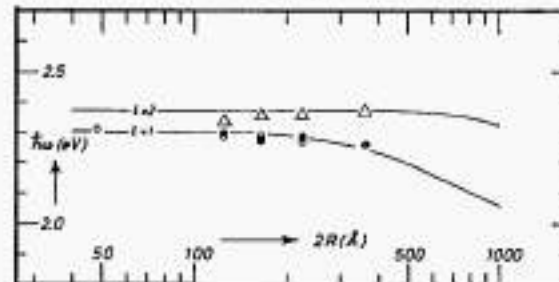


Fig. 9

Figs. 8 and 9. Size dependence of the energies of the optical extinction band maxima, and the surface plasmon modes excited by electrons, of spherical Ag particles (Fig. 8) and Au particles (Fig. 9). Continuous lines: Optical energies due to the el. partial oscillations, computed with Eqs. (5) and (6). Dashed lines: Energies of the surface plasmon modes, computed with Eq. (4). Measured energies: Δ Energy loss maxima; \bullet : extinction maximum energies of particle layers; \circ : extinction energies of aqueous colloidal solutions, converted to $n_0 = 1.54$. Δ Second mode energy, separated in loss measurement; \circ and \odot second extinction band energies, separated in optical measurements on layers and on aqueous solutions, respectively

Quantum plasmon resonances of individual metallic nanoparticles

Jonathan A. Scholl¹, Ai Leen Koh² & Jennifer A. Dionne¹

The plasmon resonances of metallic nanoparticles have received considerable attention for their applications in nanophotonics, biology, sensing, spectroscopy and solar energy harvesting. Although thoroughly characterized for spheres larger than ten nanometres in diameter, the plasmonic properties of particles in the quantum size regime have been historically difficult to describe owing to weak optical scattering, metal-ligand interactions, and inhomogeneity in ensemble measurements. Such difficulties have precluded probing and controlling the plasmonic properties of quantum-sized particles in many natural and engineered processes, notably catalysis. Here we investigate the plasmon resonances of individual ligand-free silver nanoparticles using aberration-corrected transmission electron microscope (TEM) imaging and monochromated scanning TEM electron energy-loss spectroscopy (EELS). This technique allows direct correlation between a particle's geometry and its plasmon resonance. As the nanoparticle diameter decreases from 20 nanometres to less than two nanometres, the plasmon resonance shifts to higher energy by 0.5 electronvolts, a substantial deviation from classical predictions. We present an analytical quantum mechanical model that describes this shift due to a change in particle permittivity. Our results highlight the quantum plasmonic properties of small metallic nanospheres, with direct application to understanding and exploiting catalytically active and biologically relevant nanoparticles.

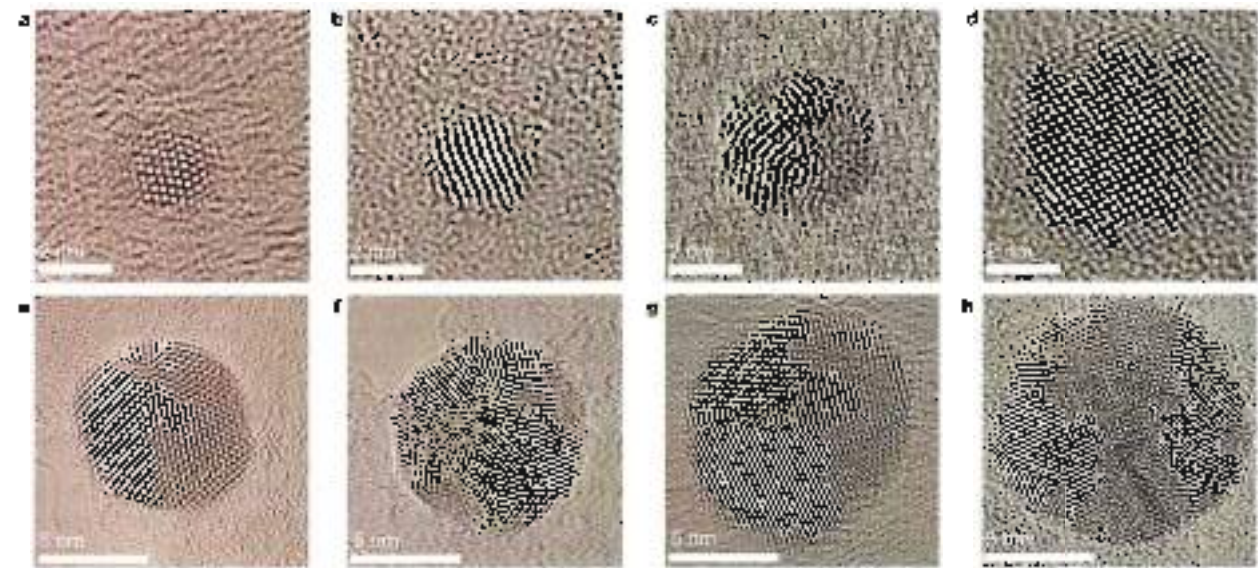


Figure 1. Alternation corrected TEM images of silver nanoparticles synthesized free of stabilizing ligands. Particles with a diameter of 2 nm (a) - 5 nm (e) and 7 nm (f) - 10 nm (g) and 12 nm (h) are shown. Scale bars: (a) - (e) 20 nm; (f) - (h) 20 nm.

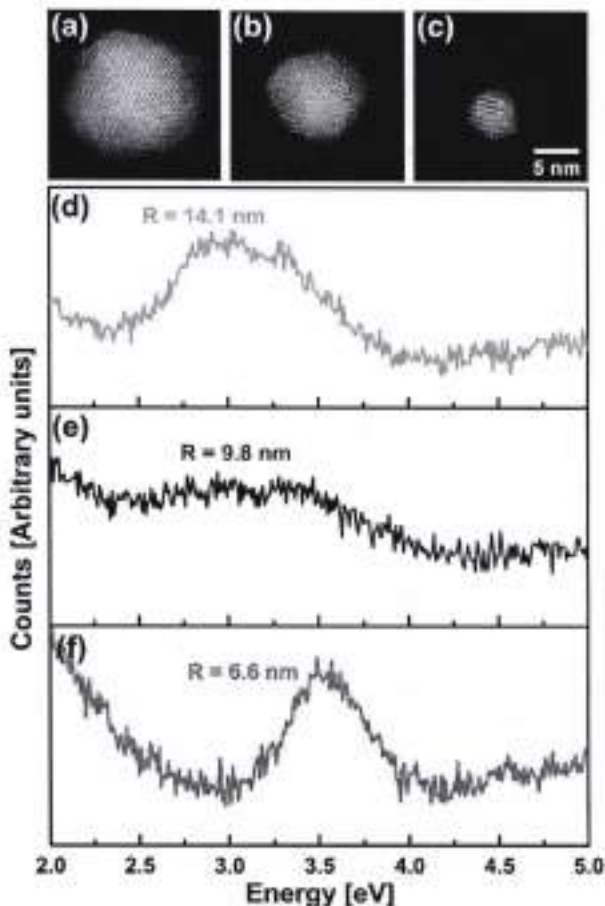


FIG. 1. Aberration-corrected STEM images of Ag nanoparticles with diameters (a) 15.5 nm, (b) 10 nm, and (c) 5.5 nm, and normalized raw EELS spectra of similar-sized Ag nanoparticles (d-f). The EELS measurements are acquired by directing the electron beam to the surface of the particle.

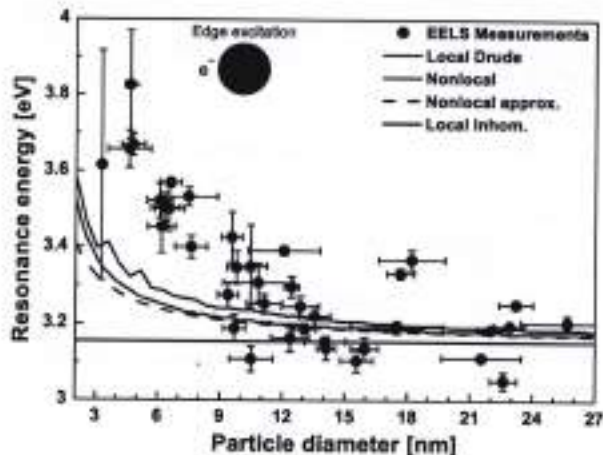


FIG. 2. Nanoparticle SP resonance energy as a function of the particle diameter. The dots are EELS measurements taken at the surface of the particle and analyzed using the RT method, and the lines are theoretical predictions. We use parameters from Ref. [41]: $\omega_p = 8.282$ eV, $\gamma = 0.048$ eV, $n_p = 5.9 \times 10^{29}$ m $^{-3}$ and $v_F = 1.39 \times 10^6$ m/s. From the average large-particle ($2R > 20$ nm) resonances we determine $\epsilon_B = 1.53$.

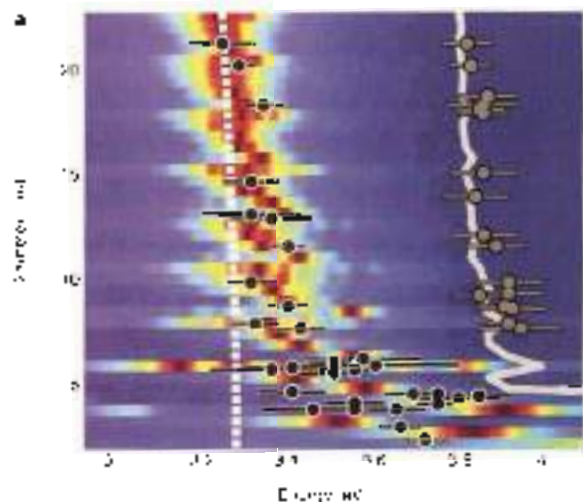


Figure 5 | Comparison of experimental data with quantum theory. Experimental data (Scanned electron spectroscopy images of silver particles Ag particles) and theory (the calculated distribution of particles) are presented. The analysis quantifies the distribution of particles and the calculated distribution is shown as a solid line. The color scale indicates the number of particles.

high-energy region, the cluster spectrum from Ag to Ag₁₀ has been identified as the main product of the reaction.

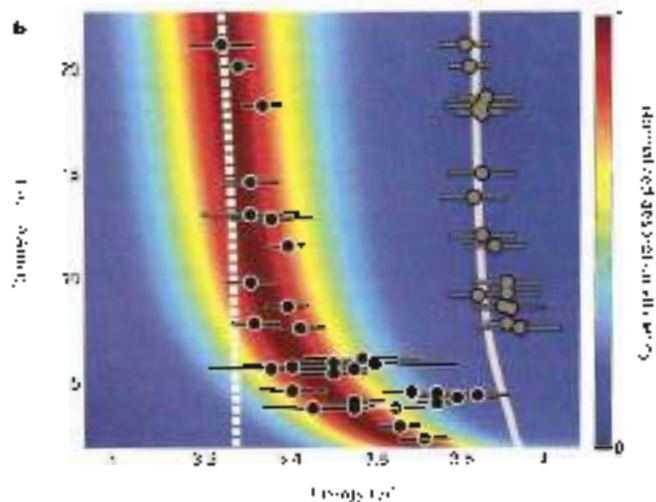
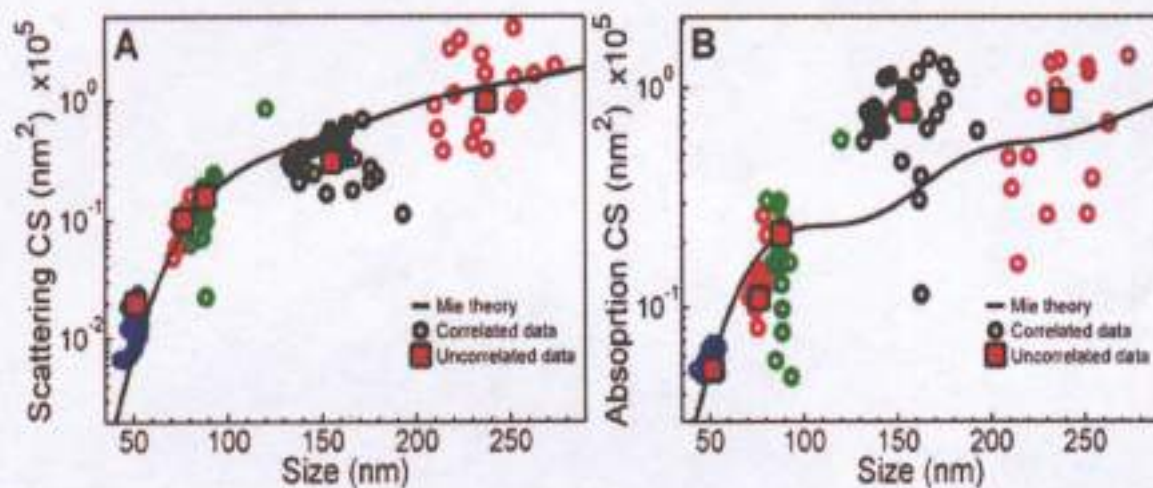


Figure 5 | Comparison of experimental data with quantum theory. Experimental data (Scanned electron spectroscopy images of silver particles Ag particles) and theory (the calculated distribution of particles) are presented. The analysis quantifies the distribution of particles and the calculated distribution is shown as a solid line. The color scale indicates the number of particles.

Discussion



LARGE COLLOIDAL GOLD NANOS:

Exp. dark field scattering (left) and photothermal absorption (right) spectra and Mie spectra (solid lines) of **SINGLE** particles at wavelength $\lambda = 532$ nm as a function of size and shape variations. Size determinations by SEM. Red squares: mean SEM size for about 250 nanos of the same sample.

A. Tcherniak, J. W. Ha, S. Dominguez-Medina, L. Slaughter, S. Link
NANO-Letters XXX (2010)

Blueshift of the surface plasmon resonance in silver nanoparticles studied with EELS

Berni Raza,^{1,2*} Nicolas Stenger,^{1,3*} Shoma Karkhachadze,⁴ Søren V. Fiebert,⁴ Natalie Kogutsha,⁴
Andriy Prishchak,^{4,5} Tobias^{4,6} Andrius Dimpas,² Marrijn Wijk,¹ and N. Agge Mortensen^{1,2,*}

¹Department of Physics, University of Copenhagen, Denmark, DK-2800 Lyngby, Denmark

²Center for Plasma Physics, Technical University of Denmark, DK-2800 Lyngby, Denmark

³Center for Nanofunctional Optics, UCLouvain, University of Leuven, Belgium, Belgium, Belgium

⁴Department of Physics and Nanotechnology, Technical University of Denmark, DK-2800 Lyngby, Denmark

*Correspondence: bernir@phys.au.dk

nstenger@phys.au.dk or agge@phys.au.dk

(Date: October 11, 2021)

We study the surface plasmon (SP) resonance of isolated spherical Ag nanoparticles in the diameter range 15–20 nm with resonant electron energy-loss spectroscopy. A significant blueshift of the SP resonance energy of 1.5 eV is measured when the nanoparticle size decreases from 20 down to 15 nm. We interpret the observed blueshift using three models for a metallic nanoparticle: a homogeneous isotropic material, a classical Drude model with a homogeneous electron density profile in the metal, a semiclassical model corrected for an inhomogeneous electron density associated with quantum confinement, and a semi-classical nonlocal hydrodynamic description of the electron density. We find that the latter two models provide a qualitative explanation for the observed blueshift, but the theoretical predictions show smaller blueshifts than observed experimentally. We attribute the larger measured blueshift to effects due to the presence of the substrate, which breaks the symmetry of a patchy cuboidal (i.e. homogeneous) metal disk.

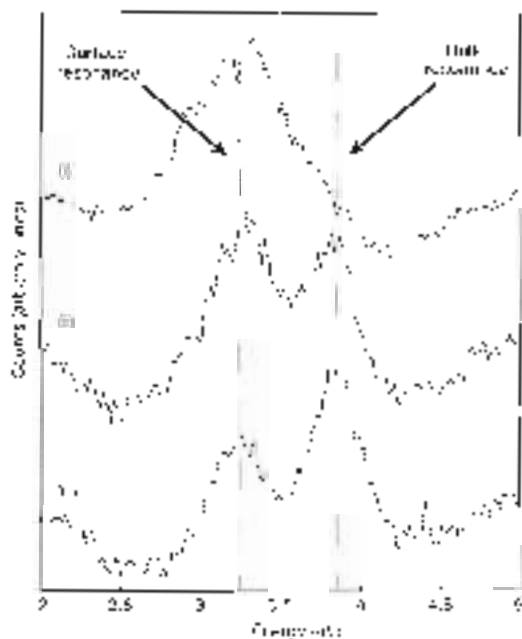
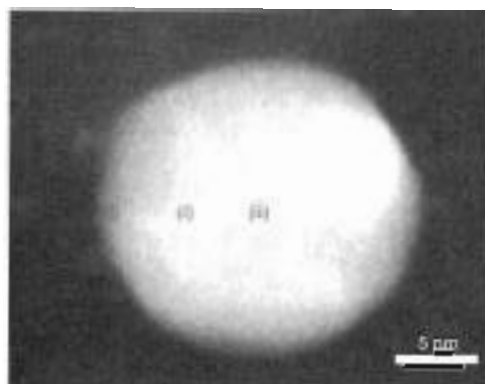


Figure 2 | STEM image of a 30 nm diameter silver particle and the associated decomposed EELS data. Spectra were collected by directing the electron beam to different locations on the surface (from the edge to the bulk) in 10 nm edge-to-edge increments located at layers of bulk resonances as indicated above.

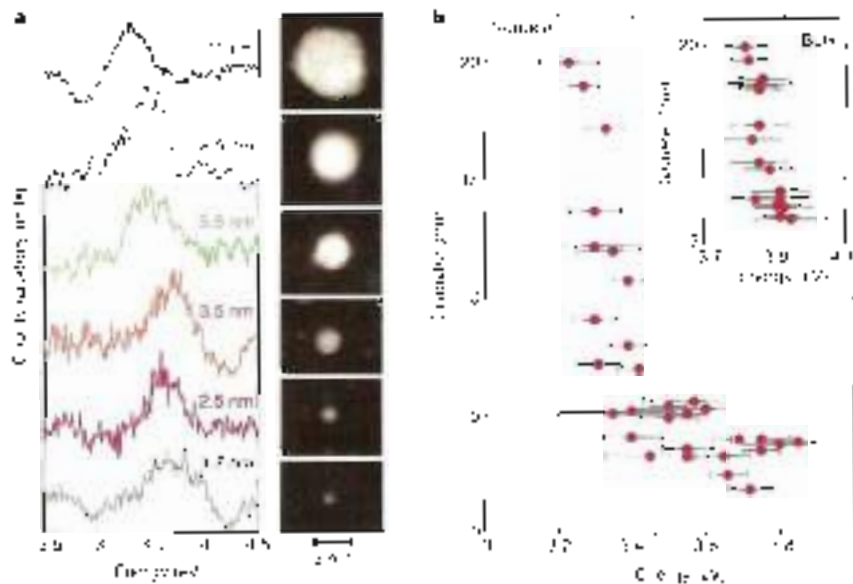


Figure 3. Correlating Ag nanoparticle geometry with plasmonic EELS data. **a.** Correlation of diameter with loss intensity for EELS data from particles ranging from 1.7 nm to 5.5 nm in diameter and their corresponding SEM images of each size. **b.** The relative loss intensity is plotted on the right of the particles without color for clarity. Resonance is highlighted in blue at the surface plasmon resonance.

average core particle diameter is 1.7 nm, and decreasing bulk plasmon frequency. The correlation between diameter and loss intensity is shown in the right plot, and the correlation between diameter and loss intensity is shown in the left plot. The correlation between diameter and loss intensity is shown in the right plot, and the correlation between diameter and loss intensity is shown in the left plot.

(6) The Nano as Optical Dipole

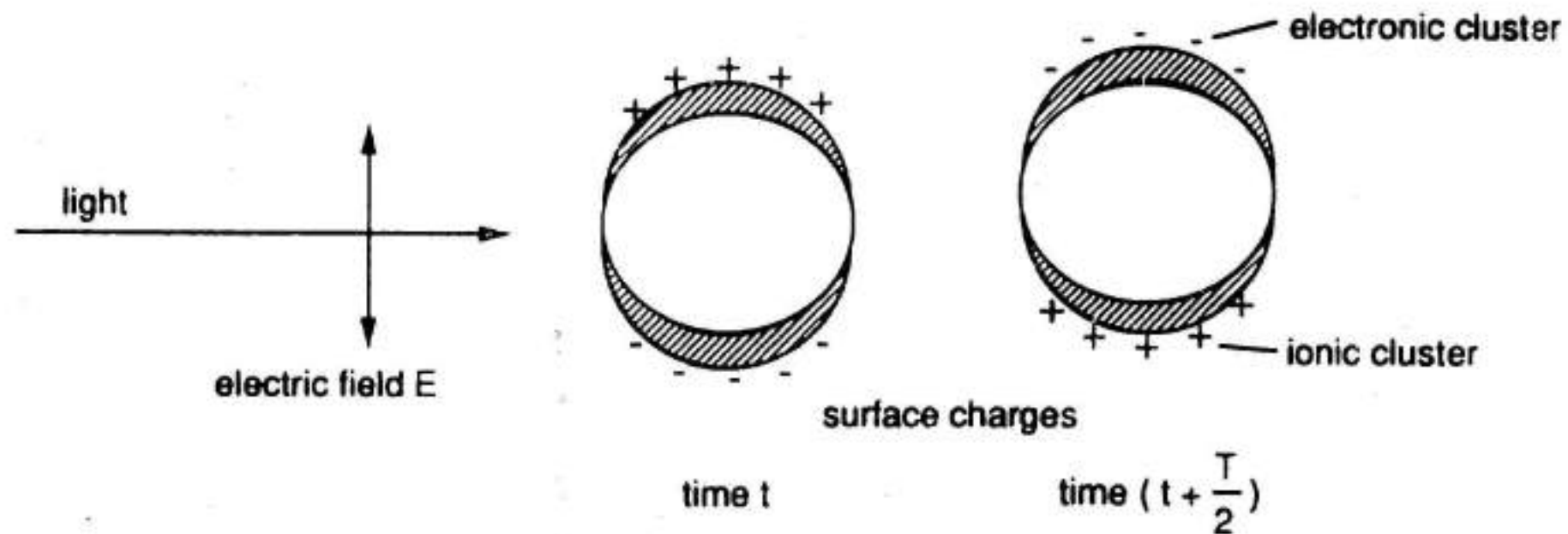
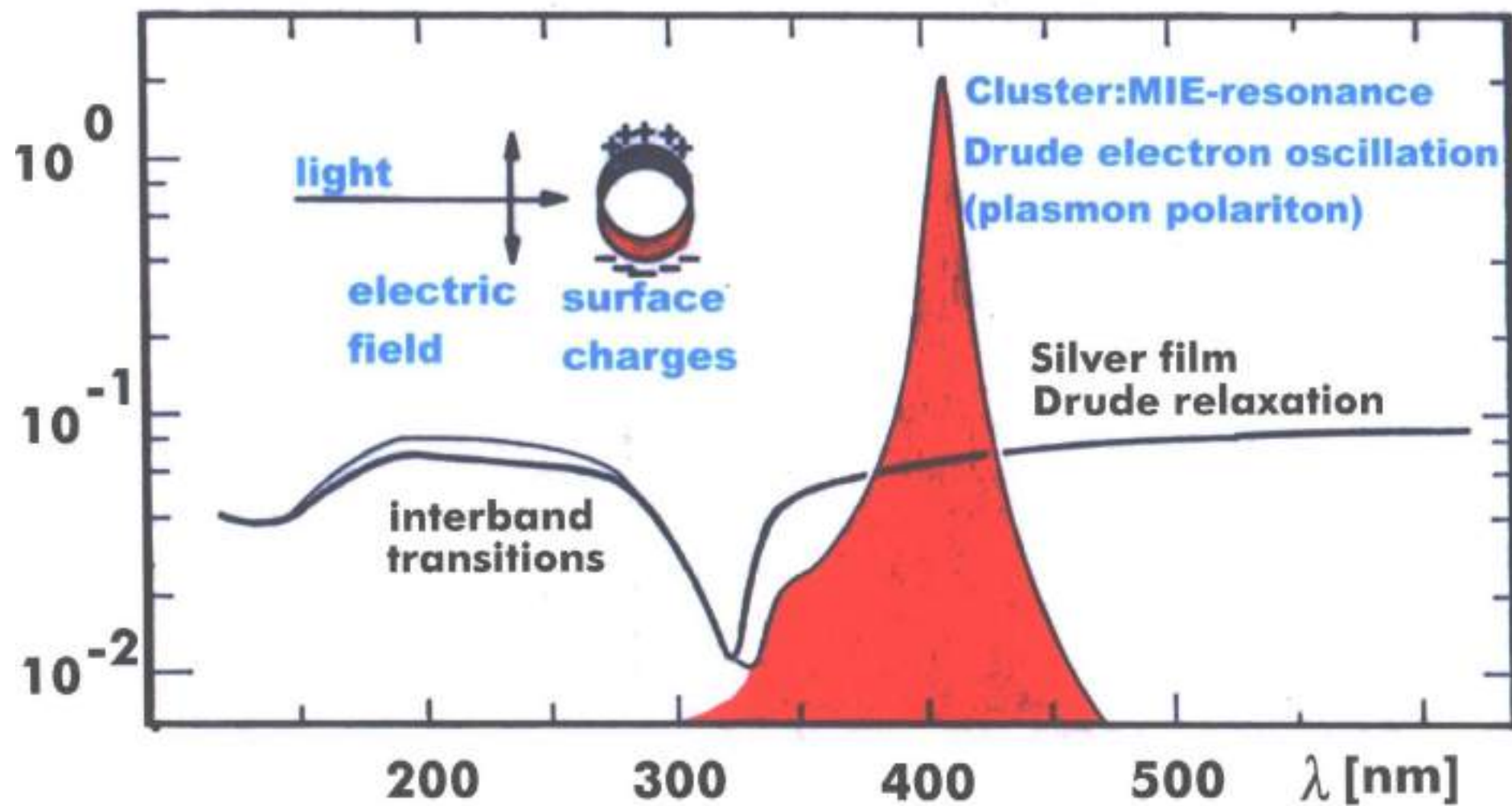


Fig. 2.4. Excitation of a dipolar surface plasmon polariton by the electric field of an incident light wave of frequency $\nu = 1/T$.



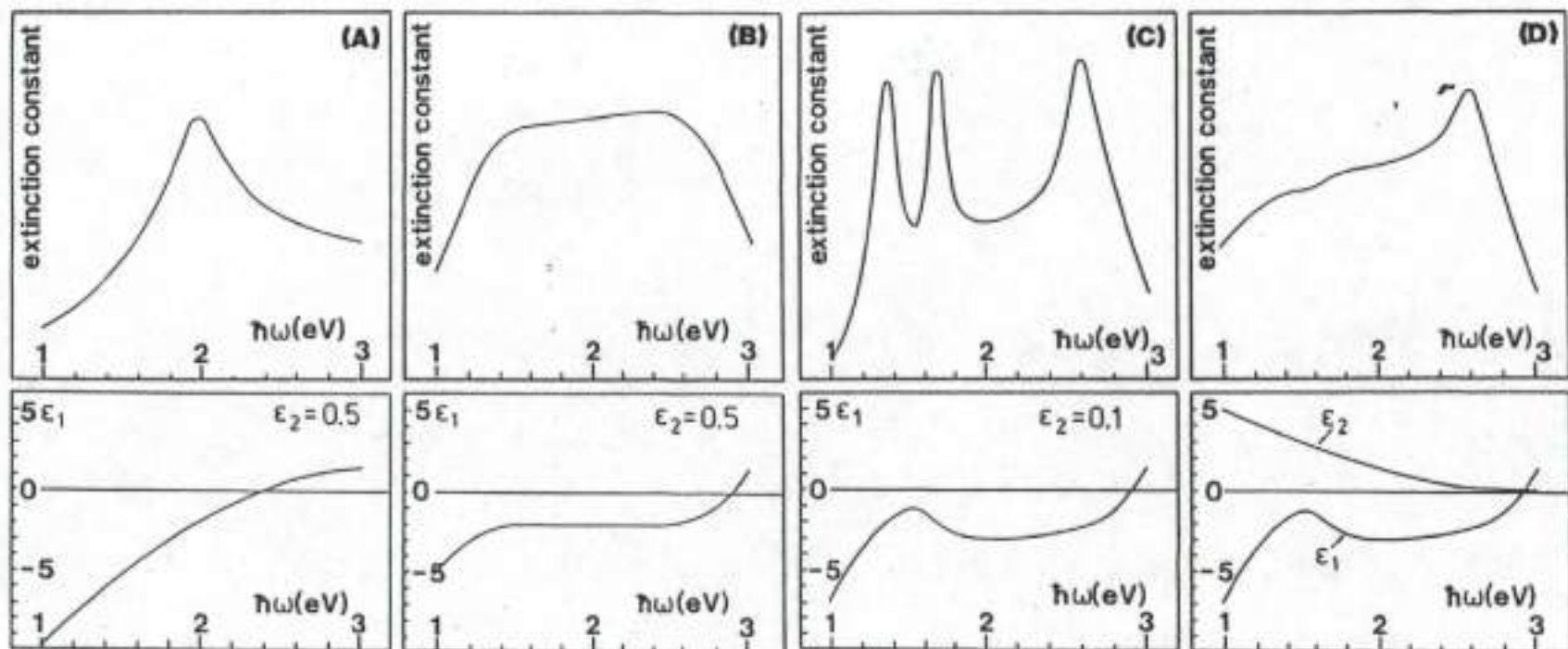
MIE-RESONANCES: DEPENDENCE ON THE DIELECTRIC FUNCTIONS

Quasistatic approximation ($\lambda \gg 2R$): dipole mode, only; no radiation damping; no retardation

Absorption cross section

$$\sigma(\omega) = \frac{9\omega}{c} V_0 \epsilon_m^{3/2} \cdot (\epsilon_2(\omega) / ((\epsilon_1(\omega) + 2\epsilon_m)^2 + \epsilon_2^2))$$

Dielectric material functions: Clusters $\epsilon_1(\omega) + i\epsilon_2(\omega)$; Matrix: ϵ_m



Band width :

$$\Gamma \approx 2 \epsilon_2(\omega_m) / [(d\epsilon_1/d\omega)^2 + (d\epsilon_2/d\omega)^2]^{1/2} \text{ with } \omega = \omega_m$$

Band position:

$$\epsilon_1(\omega_m) \approx -2 \epsilon_m$$

The average Dielectric Function used in MIE's Theory

Usually, the Dielectric function is defined macroscopically via the dielectric displacement vector

$$\text{Dielectric displacement } \mathbf{D}(\omega) = \epsilon_0 \epsilon(\omega, \mathbf{E}) \mathbf{E}(\omega)$$

$$\begin{aligned} \text{Linear response: } \epsilon(\omega) &= \epsilon_1(\omega) + i \epsilon_2(\omega) \\ &= 1 + \chi^{\text{lattice}}(\omega) + \chi^{\text{free}}(\omega) + \chi^{\text{inter}}(\omega) \end{aligned}$$

Here, the corresponding susceptibility contributions due to lattice-, conduction (free) electron-and interband transition excitations are written down separately, assuming (as usually done) that they are additive

The alternative way of a *microscopical* definition of ϵ can be used in view of application in Mie's theory, since, in fact, only the *volume averaged complex nanoparticle polarization* \mathbf{P} is required there. It is in the tradition of Maxwell's theory to use, instead, the formally related dielectric function.

The total cluster polarization is

$$\mathbf{P} = \sum \mathbf{p}_i = \sum \alpha_i \mathbf{E}_i^{\text{loc}} = \alpha \mathbf{E}^{\text{average}}$$

with α_i = local polarizabilities in the particle volume and of the particle surface/interface region.

The resulting (total) polarizability α can formally be related to ϵ by

$$\alpha(\omega \dots) = \epsilon_0 (\epsilon(\omega \dots) - 1)$$

APPROXIMATION : It is this, in general complex-valued, $\epsilon(\omega)$ that enters the theory of MIE.

BEYOND MIE'S THEORY

(A) REALISTIC ELECTRODYNAMICS :

- 1) **Incident wave** is not plane
(e.g. focused laser beam, diffuse white light source:
outgoing waves not plane)
- 2) The step-like **Maxwell boundary conditions** do not hold
(3-d particle surface/interface not included)
- 3) Additional boundary conditions (**long.** plasmons)
- 4) Inhomogeneous interface layer (traps, bonds)
- 4) **Particle shapes** are not spherical
(Polyhedra; edges; corners; surface roughness)
- 5) **Heterogeneous particle structures**
(core/shell; multigrain structures)
- 6) Atomic and molecular **adsorbates** (sensoric devices)
- 7) **Embedding** in liquid or solid matrices
(Chemical interface interactions)
- 8) **Deposition** on substrates (flattening by interface forces;
substrate interferences; interface charges;
image forces; chemical interactions)
- 9) Particles **electrically charged** (chemical potential;
charge double layers at surface)
- 10) **Many-particle systems**
(sizes, shapes, local distributions not uniform)
- 11) **Dense packing** in many-particle systems
(electrodynamical particle-particle coupling)

(B) MATERIAL PROPERTIES :

- 12) **Dielectric function of the particle material** differs from
bulk DF due to nano-size effects: $\epsilon = \epsilon(\omega, R)$
(quantum size effects; mean free path effect; band
structure effects)
- 13) **Tensorial dielectric function** (e.g. carbon particles)
- 14) **Nonlocal** electrodynamic response
- 15) **Surface** dielectric function (polarizability)
- 16) Dielectric function of the particle material is not locally
homogeneous due to **surface properties**: $\epsilon = \epsilon(\omega, r)$
- 17) Changes of ϵ due to **static and dynamic charge transfer**
- 18) D. F. of the matrix varies with **frequency** $\epsilon_{\text{matrix}}(\omega)$
- 19) D. F. of the matrix is **inhomogeneous**/ unisotropic
(e.g. close to the particle interface)
- 20) D. F. of matrix is **complex** (absorbing matrix)
- 21) D. F. of the particle material is **non-linear**
- 23) **Tunneling** among neighboring particles in densely
packed many-particle-systems
- 24) **Agglomeration** and **Coalescence** in densely packed
many particle systems (formation of particle clusters,
particle chains, larger, irregular aggregates)
- 25) etc.

Quasistatic Response of a Metallic Nanosphere to an Electromagnetic Field

Planar electromagnetic wave : $\mathbf{E}(\mathbf{r}, t) = \mathbf{E}_0 \exp(-i(\omega t + \mathbf{k} \cdot \mathbf{r}))$ (1)

$$\mathbf{H}(\mathbf{r}, t) = \mathbf{H}_0 \exp(-i(\omega t + \mathbf{k} \cdot \mathbf{r})) \quad (2)$$

Nanoparticle radius: R ; Def: quasistatic: $k \rightarrow 0$ ($R \ll \lambda$, oscillating electric field, zero magnetic field)

Dielectric function of the particle material : $\epsilon(\omega) = \epsilon_1(\omega) + \epsilon_2(\omega)$ (3)

Dielectric function of an embedding/surrounding material : ϵ_m

Metallic : positive charges locally fixed, electrons mobile

sign [$\pm i \omega t$] : $\epsilon(\omega) = \epsilon_1(\omega) \pm i \epsilon_2(\omega)$

Internal field : $E_i = E_0 \frac{3\epsilon_m}{\epsilon + 2\epsilon_m}$ (4)

Quasistatic Polarizability : $\alpha(\omega) = 4\pi\epsilon_0 R^3$ (Classic $\epsilon(0) = -\infty$) (5)

Resonance behaviour of Eq. (4) :

Max $\{E_i\}$: $|\epsilon(\omega) + 2\epsilon_m| = \text{Minimum}$ or
 $\{\epsilon_1(\omega) + 2\epsilon_m\}^2 + \{\epsilon_2(\omega)\}^2 = \text{Minimum}$ (6)

> Resonance frequency of the interior field in the nanoparticle for

$$\epsilon_1(\omega_{res}) = -2\epsilon_m \quad (7)$$

if $\epsilon_2(\omega)$ small or $\delta\epsilon_2(\omega)/\delta\omega$ small

By introducing (approximate) DRUDE dielectric function :

$$\epsilon(\omega) = \epsilon_1(\omega) + \epsilon_2(\omega) \approx 1 - \omega_p^2/\omega^2 + i\omega_p^2\Gamma/\omega^3 \quad (9)$$

with $\omega_p = \sqrt{ne^2/\epsilon_0 m}$ the "volume plasma frequency" and Γ relaxation frequency

we obtain $\omega_{res} = \omega_p/\sqrt{3}$ (10)

DRUDE being a collective, many-electron theory, the resonance follows from

- (▪) the collective displacement of the mobile Drude electrons
- (▪▪) electronic surface charging with frequency ω
- (▪▪▪) restoring linear Coulomb force against fixed positive charges
- (▪▪▪▪) finite eigenfrequency ω_{res} of the oscillating spherical system

Plasma resonances for DRUDE metal samples of various sample geometries :

Table 2.4 Book 25

wire ergänzen

Table 2.4. Plasma resonance positions for various sample geometries in vacuum. \tilde{L}_m denotes the depolarization factor (Sect. 2.1.4a), d is the film thickness and x gives the direction parallel to the film. The results for the sphere and the ellipsoid refer to the quasi-static limit.

| Geometry | Resonance condition | Resonance frequency |
|-------------------------|---|---|
| Bulk metal | $\varepsilon_1(\omega) = 0$ | $\omega_1 = \omega_p$ |
| Planar surface [2.74] | $\varepsilon_1(\omega) = -1$ | $\omega_1 = \frac{\omega_p}{\sqrt{2}}$ |
| Thin film [2.68] | $\frac{\varepsilon(\omega)+1}{\varepsilon(\omega)-1} = \pm \exp[-(\mathbf{k})_x d]$ | $\omega_1 = \frac{\omega_p}{\sqrt{2}} \sqrt{1 \pm \exp[-(\mathbf{k})_x d]}$ |
| Sphere (dipole mode) | $\varepsilon_1(\omega) = -2$ | $\omega_1 = \frac{\omega_p}{\sqrt{3}}$ |
| Ellipsoid (dipole mode) | $\varepsilon_1(\omega) = -\frac{1-\tilde{L}_m}{\tilde{L}_m}$ | $\omega_1 = \omega_p \tilde{L}_m$ |

(7) The Theory of Gustav Mie

Plasmons in Free-Electron Material (DRUDE Material) of Various Shapes in Quasistatic Approximation (Unretarded Dipole Mode)

Definition: Plasmons = Energy quantized resonance modes of collective, coherent motions of a free electron plasma. This motion is connected with a (negative) charge wave.

Depending on the sample shape and size, many different modes can be excited.

By electron relaxation processes their life-time is very short ($\approx 10^{-14}\text{s}$).

Plasmons are not included in electronic band structures (which describe single electron-hole excitations).

Localized versus propagating plasmons :

1) If the electrons are confined in a volume with dimensions smaller than the mean free path (MFP) of the single electron motion, then the plasmon is localized; the modes are oscillatory modes.

Examples are observed in nanoparticles of various shapes.

2) If the sample is large compared to the MFP the plasmon propagates as a plasma wave.

Examples are nanowires, thin films, bulk materials.

Surface versus bulk plasmons :

1) In surface plasmons, the el. excess charges are bound to the sample surface or sample/surrounding interface. Then, the wave is exponentially damped into the inner of the sample. The plasmon waves are commonly transverse.

2) In the extended bulk without surface, longitudinal volume plasmons (charge density waves) can be excited.

Free plasmons versus plasmon polaritons

1) After some pulse-like excitation (e.g. by fast-electron collisions) the electron plasma can oscillate freely with its eigenfrequency.

2) If a plasmon is excited by incident electromagnetic fields, the collective, coherent electron motions are induced via the electrical charges.

The samples act as "nano-antenna" reemitting scattering fields which, again, interact with the field outside the sample. Hence, the total excitation state is a hybrid state of the light field and the mechanical motion of the material system of the electrons, coupled by the electronic charge.

Only if the sizes of the nanostructures R are extremely small to the light wavelength, $R \ll \lambda$, then the resonance frequencies equal the eigenfrequencies of the electron system. In larger samples, the external el.mag. field changes the resonance frequency drastically. The dispersion curves $\omega(\mathbf{K})_{\text{electron}}$ of propagating plasmon waves must coincide with the light line $\omega(\mathbf{K})_{\text{light}}$.

Example: The eigenfrequencies of nanoparticles with DRUDE electrons:

The internal field in the case of a spherical nano is (see above) :

$$E_{\text{interior}}(\omega) = E_0(\omega) [3 \epsilon_{\text{medium}} / (\epsilon(\omega) + 2 \epsilon_{\text{medium}})]$$

The resonance of E_{interior} is obtained at the minimum of the denominator:

$$[\epsilon_1(\omega_{\text{resonance}}) + 2 \epsilon_{\text{medium}}]^2 + [\epsilon_2(\omega_{\text{resonance}})]^2 = \text{minimum.}$$

Since $\epsilon_2(\omega) > 0$ always, $\epsilon_1(\omega_{\text{resonance}})$ must be negative, $\epsilon_1 < 0$.

If $\epsilon_2(\omega_{\text{resonance}})$ is small or $\delta\epsilon / \delta\omega$ is small, the plasma resonance condition reads:

$$\epsilon_1(\omega_{\text{resonance}}) = -2 \epsilon_{\text{medium}}$$

Inserting simplified DRUDE equations

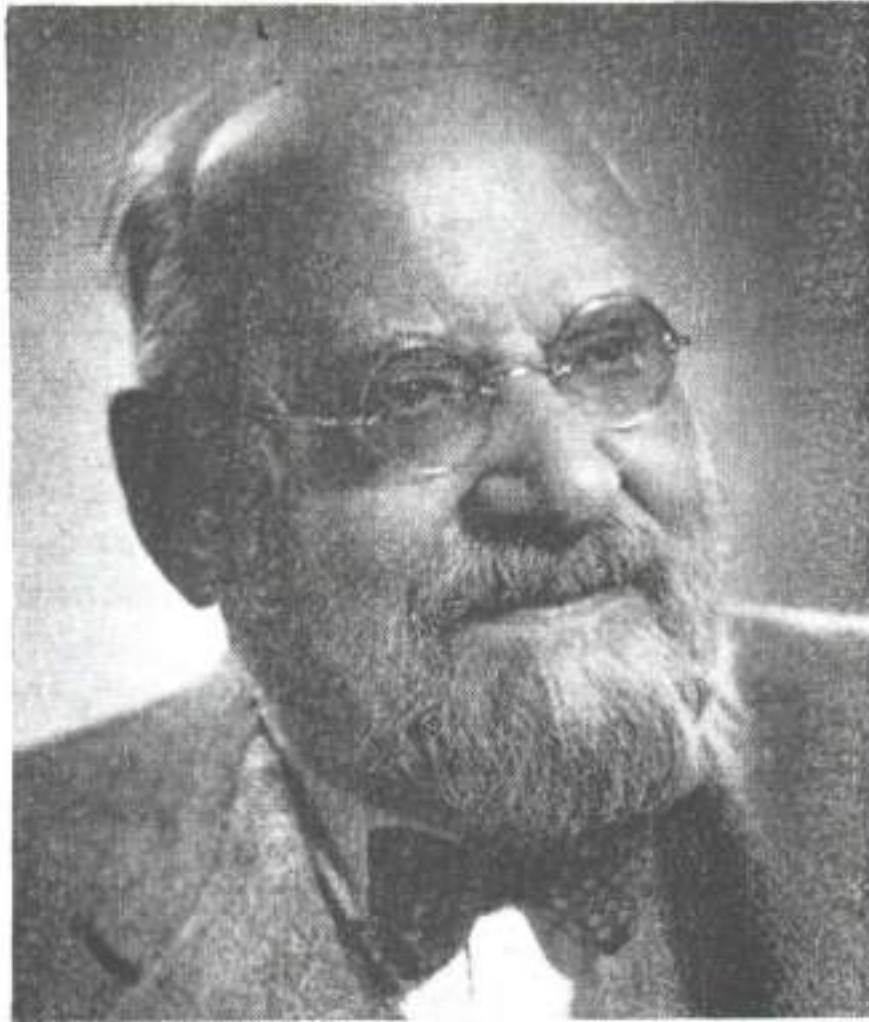
$$\epsilon_1(\omega) \approx 1 - \omega_p^2 / \omega^2, \quad \epsilon_2(\omega) \approx \omega_p^3 \Gamma / \omega^2 \quad \text{and setting } \epsilon_{\text{medium}} = 1,$$

then the resonance frequency is

$$\omega_{\text{resonance}} = \omega_p^{\text{DRUDE}} = \sqrt{(n e^2 / \epsilon_0 m_{\text{electron}})}$$

This is the classical resonance frequency; it equals the plasmon frequency after quantization.

This relation holds only for a spherical nano; similar conditions are derived for other particle symmetries.



GUSTAV MIE

* 29. September 1868 (Rostock) † 13. Februar 1957 (Freiburg i.B.)

ROSTOCK → KARLSRUHE → GREIFSWALD → HALLE → FREIBURG

„Beiträge zur Optik trüber Medien, speziell kolloidaler Metallösungen“
Ann. Physik 25 (1908)

Literatur zu Gustav Fedor Mie:

Hundert Jahre Mie-Theorie

Uwe Kreibitz

in Physik in unserer Zeit
39,Jg 2008 Nr.6, S 281 ff

und

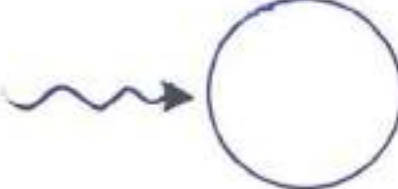
Supplement : Hundert Jahre Mie Theorie

Uwe Kreibitz

Adobe Acrobat Professional
[Hundert Jahre Supplement. pdf]

OPTICAL ABSORPTION OF CLUSTERS :

Quantum mechanical versus electrodynamic excitation:

Energy flux: $N/t \cdot h\omega$  (2R = 10nm)

Intensity $I = 1 \text{ Watt/cm}^2$; $N/t \approx 10^{19} \text{ Photons / cm}^2 \text{ sec}$

Cluster cross section σ :
geometrical $\approx 10^{-12} \text{ cm}^2$
optical (Mie resonance) $\approx 10^{-11} \text{ cm}^2$

Photon flux per cluster: $N/(t \sigma_{\text{opt}}) \approx 10^8 / \text{sec}$

Excitation life-time of Mie resonances: $\tau \approx 10 \text{ fs} = 10^{-14} \text{ s}$

\Downarrow (a) time averaging
(b) ensemble averaging
 \Downarrow

ELECTRODYNAMICS : $E = E_0 \exp(i(\omega t - kr))$; $I = E \times H$
 $H = H_0$

\Downarrow

MIE'S THEORY

MIE 's THEORY IN FEW WORDS

- 1 **Assumptions:** one spherical nanoparticle, radius R , of arbitrary material and size, embedded in a homogeneous, non-absorbing matrix.
- 2 Formulation of **Maxwell's equations** in spherical coordinates r, δ, φ .
- 3 Introduction of **Maxwell's boundary conditions**: "sharp" boundaries for the electric and magnetic fields E, M , at the particle/matrix interface, $r = R$:

$$\mathbf{E}_{\delta}^{\text{outside}} = \mathbf{E}_{\delta}^{\text{inside}} ; \mathbf{E}_{\varphi}^{\text{outside}} = \mathbf{E}_{\varphi}^{\text{inside}} ; \epsilon^{\text{outside}} \cdot \mathbf{E}_r^{\text{outside}} = \epsilon^{\text{inside}} \cdot \mathbf{E}_r^{\text{inside}}$$

- 4 Introduction of the **optical functions** $\epsilon(\omega) = \epsilon_1 + i \epsilon_2$ of the particle material and ϵ_{med} of the embedding medium from elsewhere (e.g.bulk).
- 5 Derivation of the **Helmholtz wave equation** for the three scalar potentials.
- 6 Solution by **product-ansatz** in r, δ, φ for the **potentials**.

- 7 Back-transformation into the **fields**: Introduction of electric and magnetic partial waves for the incident, interior and scattered waves.
- 8 Representation by multipole expansions (**orthogonal mode expansion**) , including infinite series of Cylinder functions (Bessel, Neumann), Spherical harmonics (Legendre polynomials) and harmonic oscillators.
- 9 Calculation of the coefficients ("**Mie coefficients**").
- 10 Application of Poyntings law to obtain **incident, absorbed and scattered intensities**.
Separate calculations of near and far field contributions, different polarization contributions and angular dependences possible.
- 11 Extrapolation to an **N-particle-system** by Lambert-Beer's law.
- 12 Results : **Spectra of absorption, elastic scattering, extinction.**

THE THEORY OF GUSTAV MIE

1. Introduction of spherical coordinates r, Θ, Φ Particle radius R .
Plane, monochromatic, harmonic incident electromagnetic wave.
Circular frequency ω , wavelength λ .

2. Solution of Maxwells equations with proper boundary conditions for one arbitrary spherical particle of complex dielectric function $\epsilon(\omega) = \epsilon_1 + i \epsilon_2$, embedded in a dielectric medium with (real) dielectric constant ϵ_m .

- Electric fields: E (divergency free) + E (curl free),
- Magnetic fields: H (divergency free).

Separation of the transverse electromagnetic fields according to their radial field components:

"electric partial waves" with $E_r = 0$

"magnetic partial waves" with $H_r = 0$.

Both are electromagnetic fields including Θ - and Φ -components, too.

Close to the particle they form complex near fields, and only at distances $r \gg \lambda$ they transform into the common far field.

- Introduction of three scalar potentials, to separate the variables:

$$\Pi_E, \Pi_M, \Gamma$$

(indices E, M : electric and magnetic partial waves; Γ stands for the longitudinal field)

They are solutions of the Helmholtz-equations:

$$\Delta \Pi_{E,M} + K_{transverse}^2 \cdot \Pi_{E,M} = 0, \quad K_{transverse}^2 = \epsilon_{trans} \omega^2 / c^2,$$

$$\Delta \Gamma + K_{longitudinal}^2 \cdot \Gamma = 0, \quad K_{longitudinal}^2 = \epsilon_{long} \omega^2 / c^2.$$

K : wave number.

3. Boundary conditions at $r = R$ ("sharp" boundary conditions)

$$E_{\Theta}^{incident} = E_{\Theta}^{interior} ; \quad E_{\Phi}^{incident} = E_{\Phi}^{interior} ;$$

$$\epsilon^{outside} \cdot E_r^{incident} = \epsilon^{inside} \cdot E_r^{interior}$$

Analog for H.

Longitudinal fields :Current density: j_{total}^{normal} continuous at $r = R$
(Sauter-Forstmann condition).

4. The linear response function of the particle material is $\hat{\epsilon}\mu$, where $\hat{\epsilon}(\omega) = \epsilon_1 + i\epsilon_2$ is averaged over the cluster volume, including the surface/interface region. The magnetic permeability μ is set 1 for the investigated high frequency regions. (This means, that genuine magnetic response of the material which may be effective at lower frequencies, is excluded throughout the following. However, the magnetic part of the electromagnetic wave contributes to the electronic excitations by creating additional eddy current modes which, unlike the electric ones, do not exhibit sharp resonances.)

6. Separation of the variables by a product-ansatz to solve the Helmholtz-equation. E.g. for Π_E holds

$$\Pi_E = F_1(r)F_2(\Theta)F_3(\phi)$$

Solution-functions are given in the following table:

| Variable | Differential equation | Solution functions |
|----------|-----------------------|---|
| r | Bessel | Cylinder-functions (Bessel, Neumann); Index L |
| Θ | Spherical harmonics | Legendre polynomials; Indices L, m . |
| Φ | Harmonic oscillation | cos/sin-functions; Index m . |

7. Back-transformation of the potentials into the fields.

The fields are divided into 3×3 groups, i.e. each of the three electromagnetic waves,

- > the incident wave,
- > the wave in the interior of the particle and
- > the scattering wave

consists of three different contributions, the "electric" partial waves,

the "magnetic" partial waves and, if present, longitudinal waves.

8. Multipole expansion : Power-series expansion of the solution functions.

First term : Dipolar symmetry,

Second term: Quadrupolar symmetry

Third term : octupolar symmetry, etc.

9. Calculations of the "Mie-coefficients" :

The Mie-coefficients a_L and b_L , following from the boundary conditions, are

$$a_L = \frac{m \psi_L(mx) \psi'_L(x) - \psi'_L(mx) \psi_L(x)}{m \psi_L(mx) \eta'_L(x) - \psi'_L(mx) \eta_L(x)}$$

$$b_L = \frac{\psi_L(mx) \psi'_L(x) - m \psi'_L(mx) \psi_L(x)}{\psi_L(mx) \eta'_L(x) - m \psi'_L(mx) \eta_L(x)}$$

$$m = \hat{n} / n_m$$

where \hat{n} denotes the complex index of refraction, $\hat{n} = \sqrt{\epsilon}$ of the particle material, and n_m the real index of refraction of surrounding medium. k is the wavevector and $x = |k|R$ the size parameter.

$\psi_L(z)$ and $\eta_L(z)$ are Riccati-Bessel cylindrical functions (see, e.g. Born "Optik"). The prime indicates differentiation with respect to the argument in parentheses.

10. Computation of the cross - sections of ONE particle for extinction, absorption and elastic (frequency conserving) scattering by applying Poynting law. The intensities I are given by the absolute value of the Poynting vector (the summations are taken over all multipoles from $L = 1$ to $L = \infty$).

- Extinction (sum of absorption and scattering losses) :

$$\sigma_{\text{abs}} = (2\pi / k^2) \sum (2L + 1) \text{Re} \{a_L + b_L\}$$

- Elastic scattering losses :

$$\sigma_{\text{scatt}} = (2\pi / k^2) \sum (2L + 1) \{ |a_L|^2 + |b_L|^2 \}$$

(In Mie's original notation, the equation contains the imaginary instead of the real part due to differing definitions of a_L and b_L .)

- Absorption losses :

$$\sigma_{\text{abs}} = \sigma_{\text{ext}} - \sigma_{\text{scatt}}$$

Separate calculations are possible of

- > near and far field contributions,
- > different polarization contributions and
- > angular dependences of scattered intensities .

11. The cross- sections hold for ONE particle. Usually, nanoparticle samples for experiments contain very many particles (e.g. colloidal systems with $Z = 10^{15}$ per cm^3), so, the

- > the extinction constant $E_{\text{ext}}(\lambda)$,
- > the scattering constant $S_{\text{scatt}}(\lambda)$ and
- > the absorption constant $A_{\text{abs}}(\lambda)$

can be calculated with Lambert-Beer's law :

$$\Delta I_j = I_0(1 - \exp(-Z \cdot \sigma_j \cdot d)) \quad , \quad d = \text{sample thickness}$$

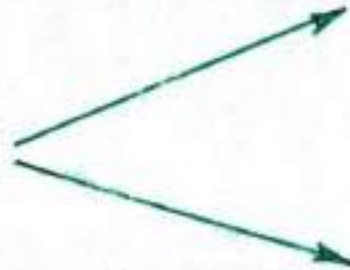
provided, the sample system consists of n identical particles, packed loosely together in a macroscopic volume with low volume concentrations $f < 10^{-4}$ to exclude electromagnetic particle-particle coupling and multiscattering events (The sample volume may be filled with some matrix material).

12. To-day, programs for Mie's theory are available in the Internet.

MIE's THEORY

LIGHT PROPAGATION:
Classical Electrodynamics

INTERACTION WITH MATERIAL:
Dielectric Functions
(Experimental data and/or Solid State theory)



LONGITUDINAL PLASMONS IN NANOPARTICLES

Additional boundary condition
of
Sauter & Forstmann :
Normal component of the current
continuous at the surface

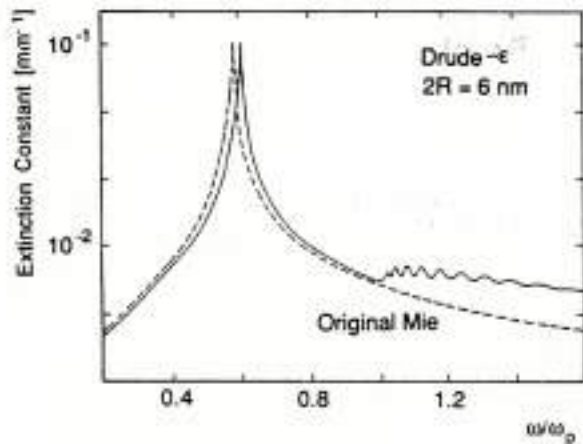
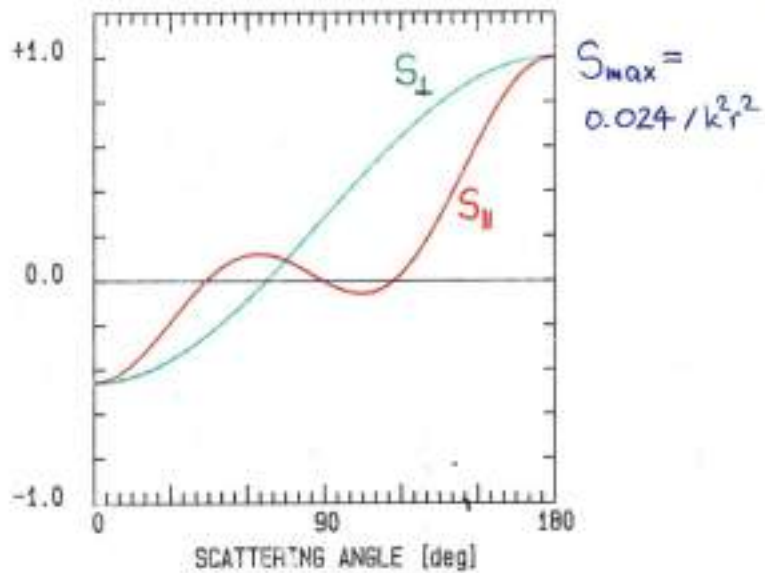
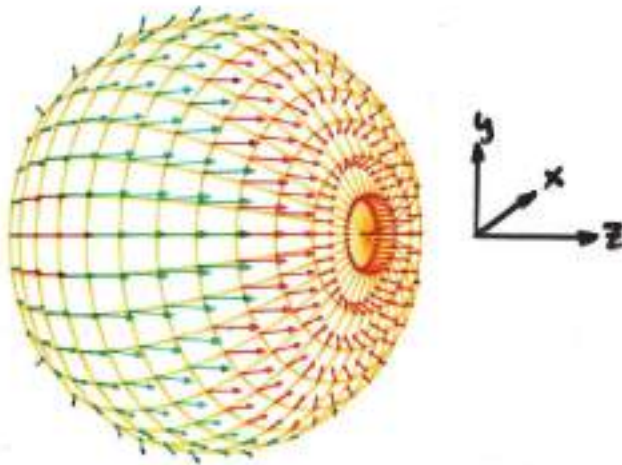


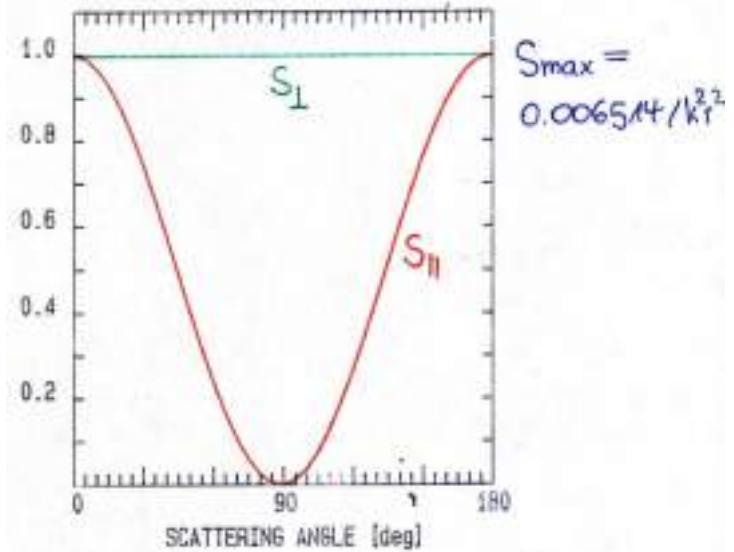
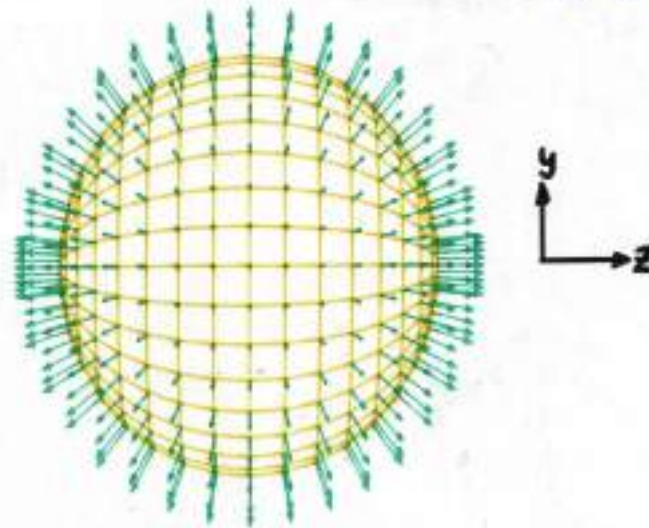
Fig. 2.38. Extinction spectrum calculated for Drude particles ($2R = 6 \text{ nm}$) with the Sauter/Forstmann boundary conditions. The possibility of excitation of longitudinal (volume) plasmons only introduces minor effects (after [2.175a]). The dashed curve corresponds to the classical Mie result.

Poynting vectors (S_R, S_θ, S_ϕ):
distance $d = 0$ nm (surface)



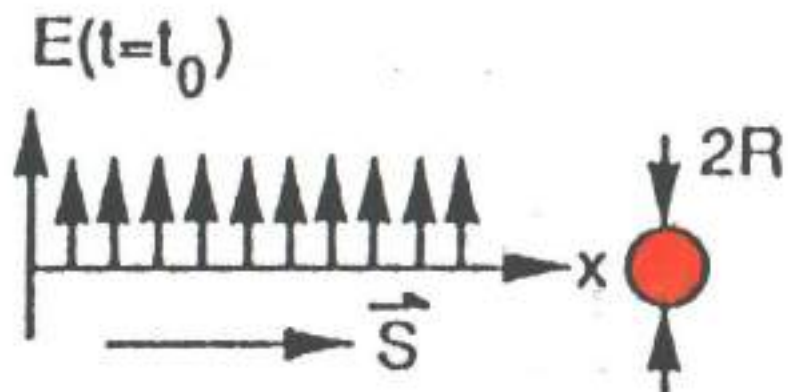
(QUINTEN 1992)

distance $d = 200$ nm Silver $2R = 40$ nm
 $\lambda = 400$ nm



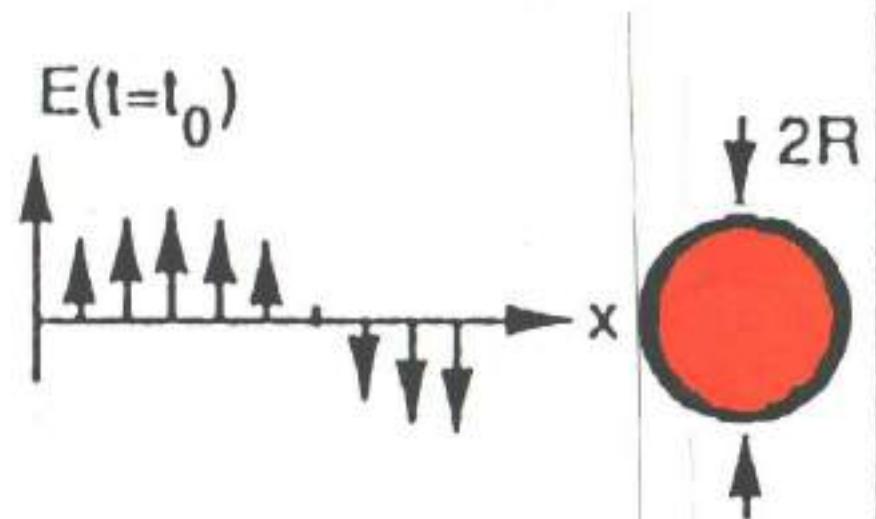
[QUINTEN 1992]

Quasi-static case: $\lambda \gg 2R$



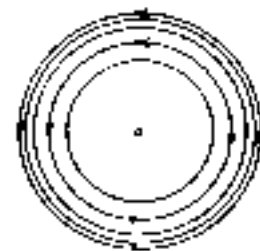
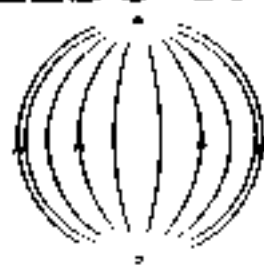
Homogeneous polarization:
dipole excitation

General case: $\lambda \gtrsim 2R$

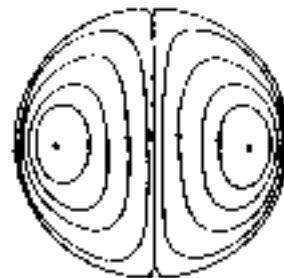
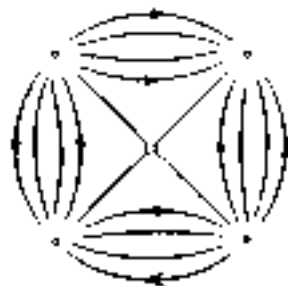


Phase shifts in the
particles: multipole excitation

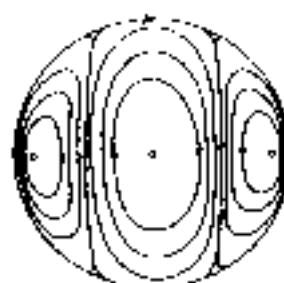
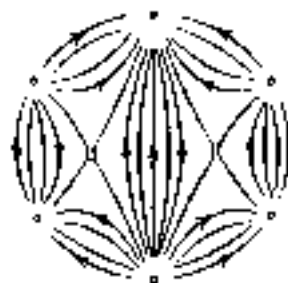
FAR FIELDS OF DIFFERENT SPHERICAL MODES



dipole
(l:1)



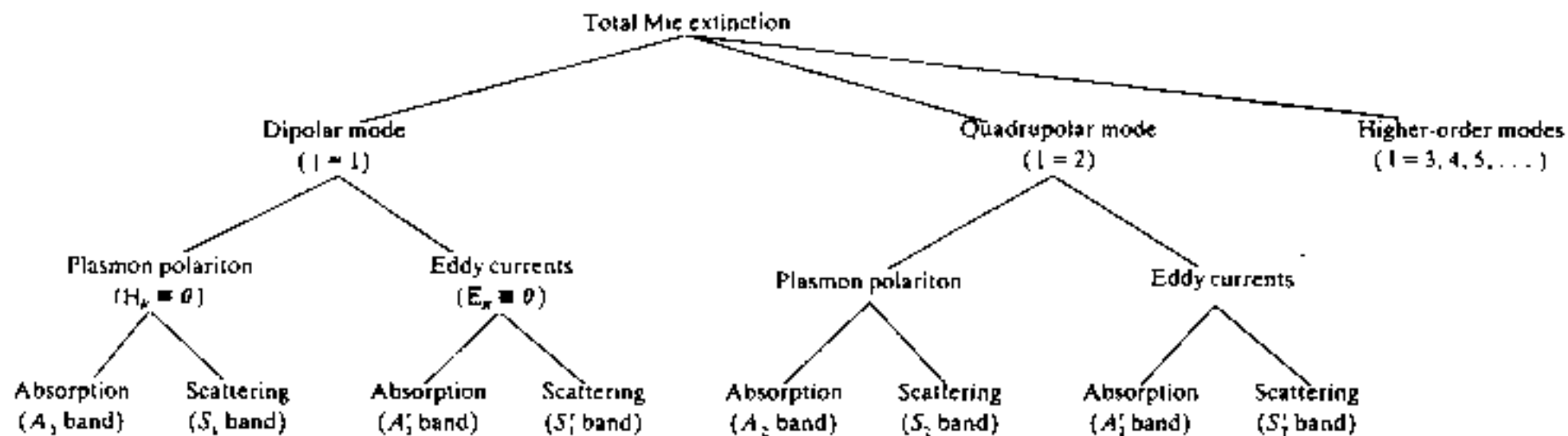
quadrupole
(l:2)



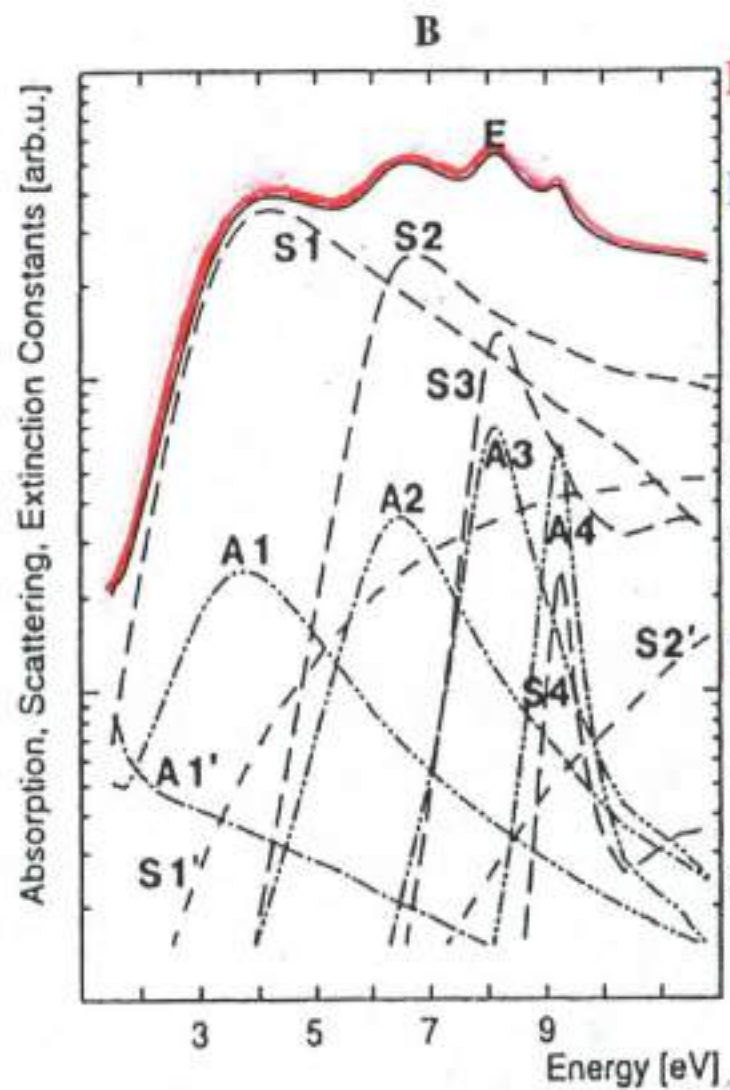
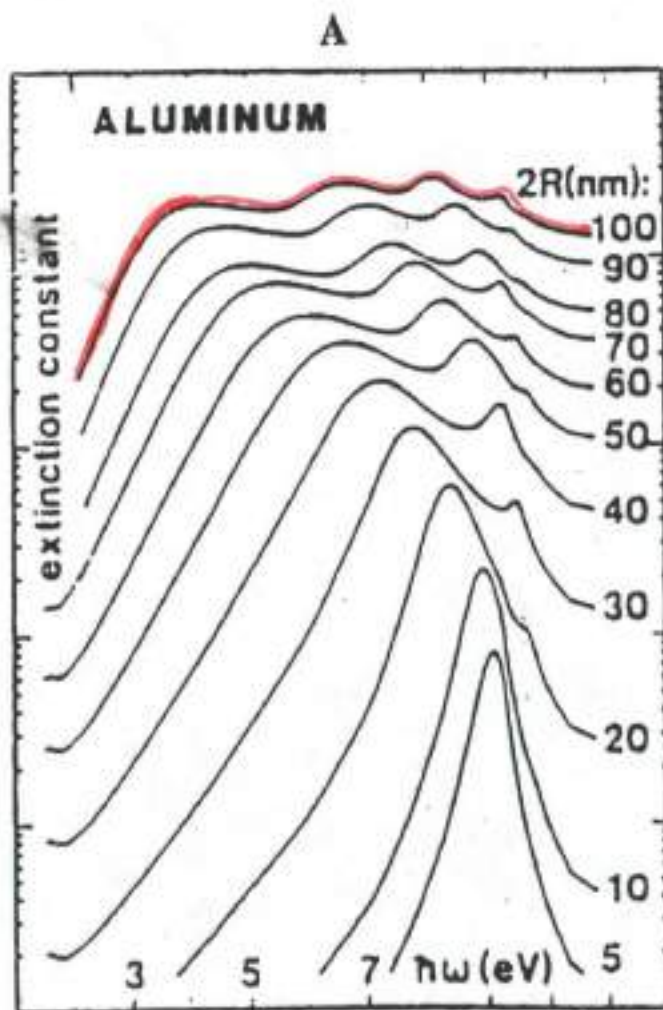
(l:3)

electric

magnetic



Ab



MIE s THEORY:

Electric modes:

A_v = Absorption of the v -th multipole

S_v = Scattering of the v -th multipole

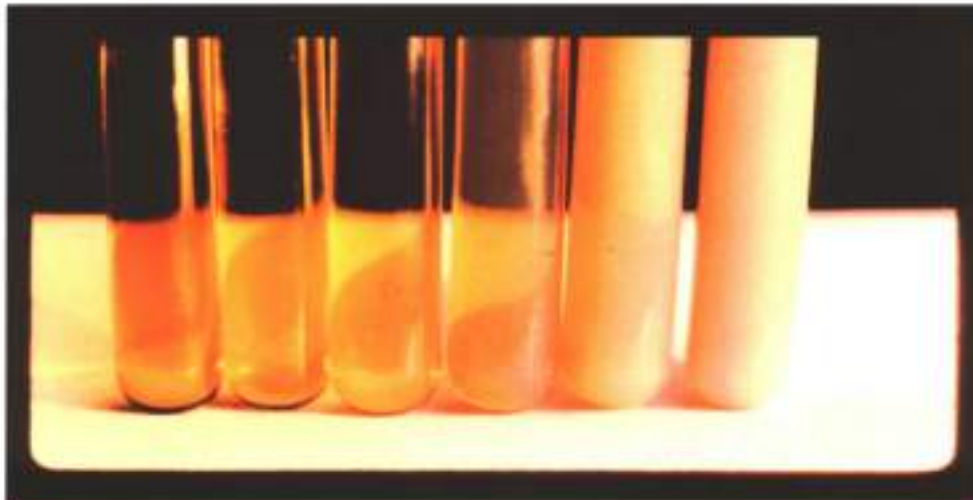
Magnetic modes:

A_v'

S_v'



ZSIGMONDY-Ag- COLLOIDS: Mean sizes increasing from 6 to 60 nm
Top: Transmitted light. Bottom: Scattered light



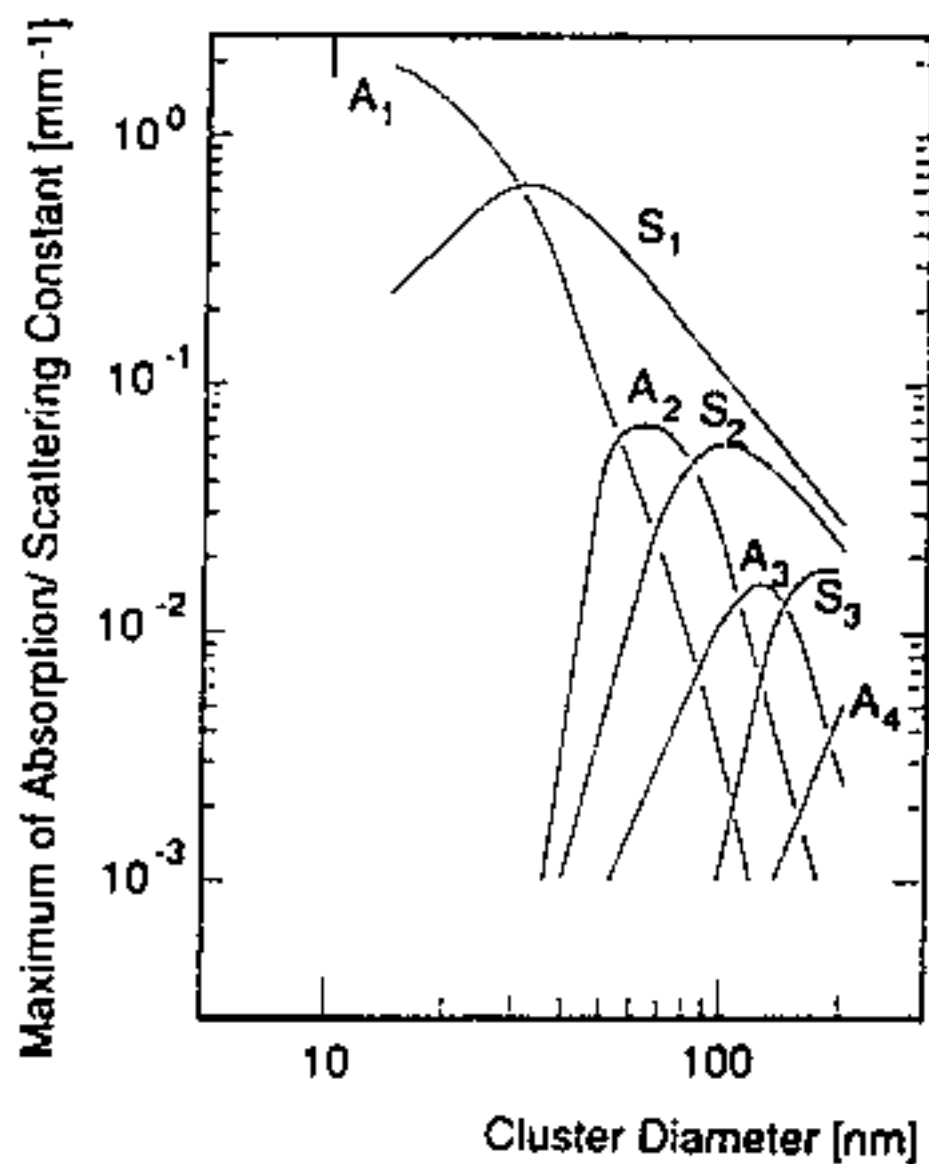


Figure 4 Mie resonances of silver nanoparticles: calculated size dependence of the maxima spectral of the modes which contribute most. A_L, S_L = absorption, scattering. L = multipolar order.

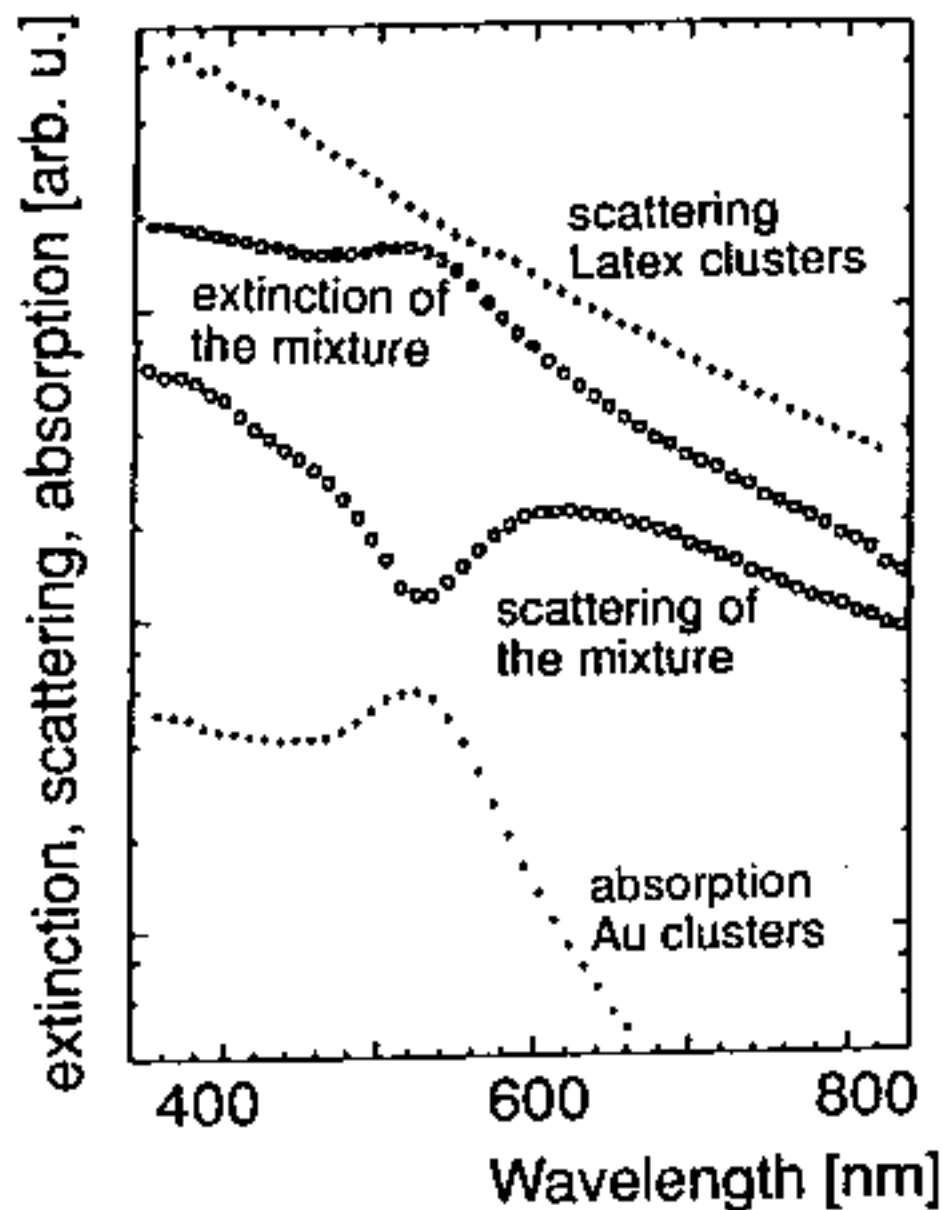
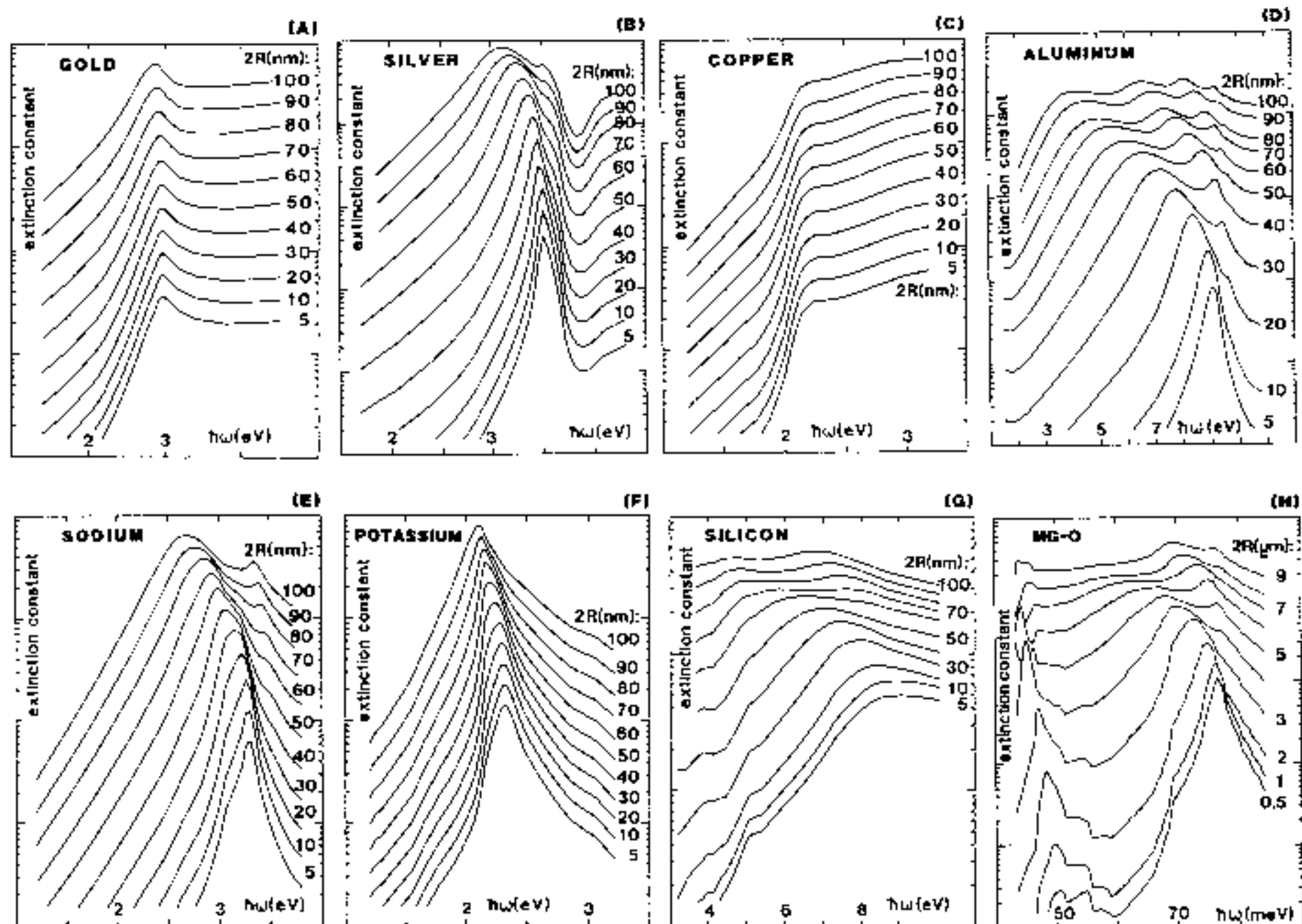


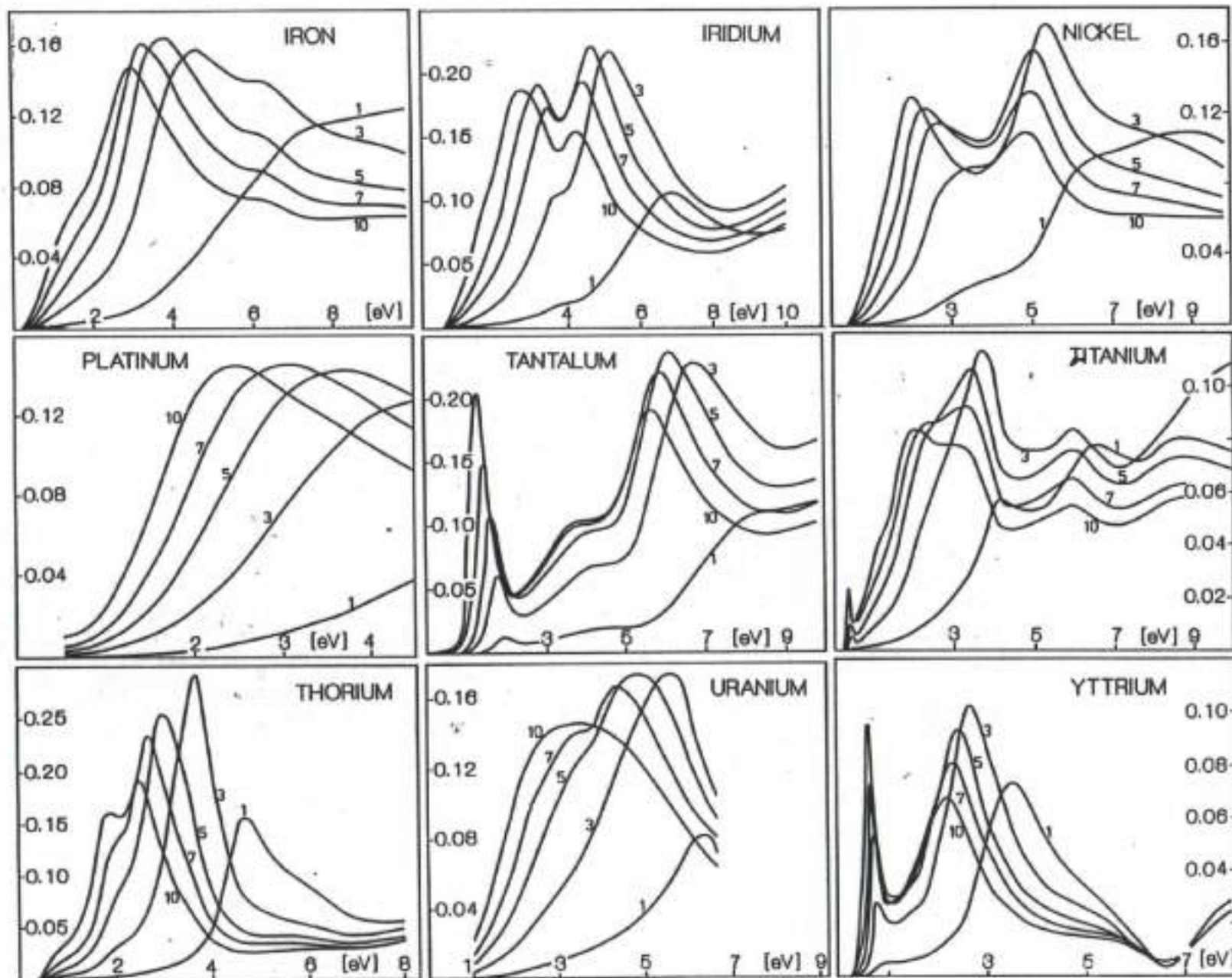
Fig. 4.11. Measured optical spectra of a hydrosol containing 6 nm Au clusters and 46 nm Latex clusters. Scattering and extinction of the mixture differ from the pure Au or Latex samples since higher order extinction processes take place (after [4.73, 75]).

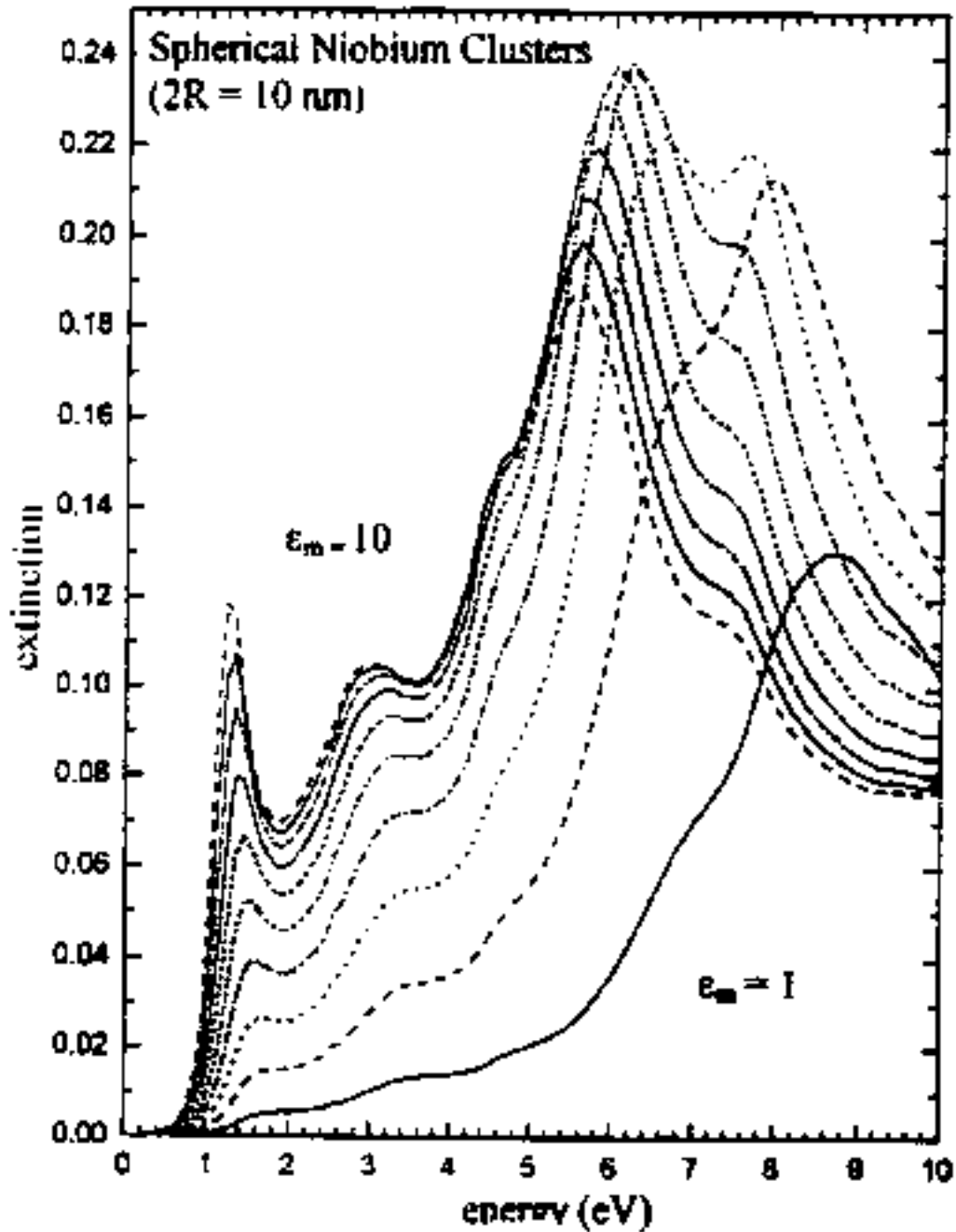


**OPTICAL
EXTINCTION
SPECTRA
(Mic-theory)**

$R = 10 \text{ nm}$
Parameter:
Dielectric function
of the embedding
material

(U.Kreibig, 1997
in
*Handbook of
Optics*
ed. R. Hummel)

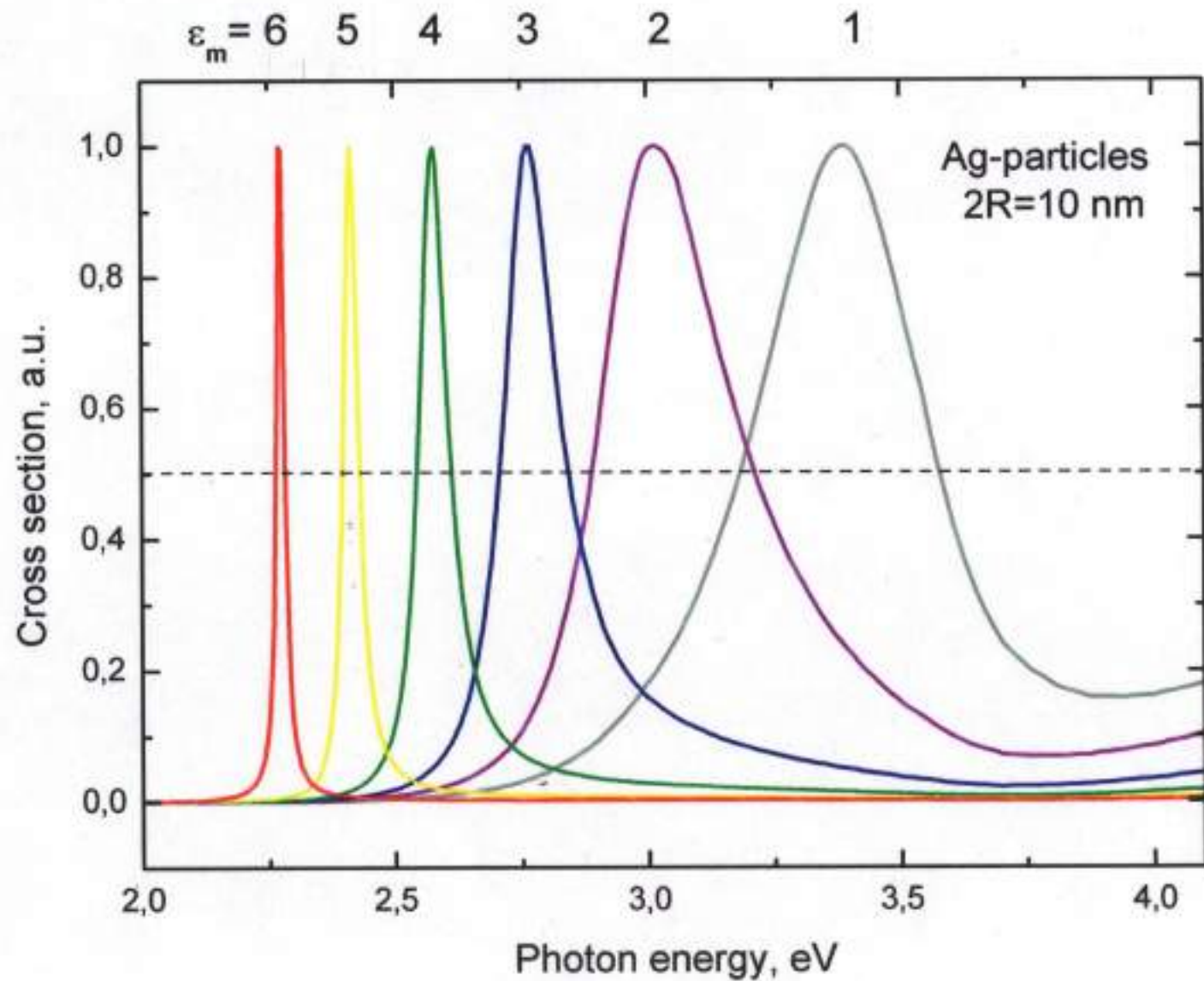




The optical extinction of well separated Niobium clusters ($2R = 10$ nm) as calculated from Mie's theory with dielectric material function of the bulk material.

The parameter is the dielectric constant of the embedding material varying in steps of 1 from 1 to 10. The differences of the spectra represent the *dielectric effect*.

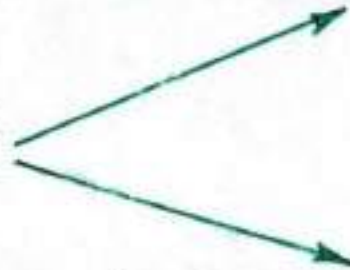
MIE - PLASMON POLARITON : DIELECTRIC SHIFT



MIE's THEORY

LIGHT PROPAGATION:
Classical Electrodynamics

INTERACTION WITH MATERIAL:
Dielectric Functions
(Experimental data and/or Solid State theory)



OPTICAL DATA - EVALUATION

Experimental Data : **Absorption spectrum**
 $K(\omega, R, \text{matrix})$



Kramers-Kronig Analysis: Relative Refractive Index of
the sample
 $S(\omega, R, \text{matrix})$



Inverted Mie theory: Optical functions of the particle
material

Dielectric function: $\epsilon(\omega, R) = \epsilon_1(\omega, R) + i \epsilon_2(\omega, R)$

Susceptibility: $\chi(\omega, R) = [\epsilon(\omega, R) - 1] =$
 $\chi_1(\omega, R) + i \chi_2(\omega, R)$



Separation of the interband transition contributions :

$\epsilon_1^{\text{interband}}(\omega, R, \text{matrix}) ; \epsilon_2^{\text{interband}}(\omega, R, \text{matrix})$

$\chi_1^{\text{interband}}(\omega, R, \text{matrix}) ; \chi_2^{\text{interband}}(\omega, R, \text{matrix})$

INVERSE MIE THEORY

Among the great many applications of Mie's Theory, the numerical simulation of measured electromagnetic spectra of nanoparticles from given DF is of great importance. More important, however, at least for comprehensive basic research on NANO-EFFECTS, is the use of "Inverse Mie Theory".

This means, to turn the functional dependences around and to start with given experimental electromagnetic spectra with the aim of evaluating the spectra of the realistic dielectric function of the nanoparticle material and explain them by proper solid state theoretical models.

This procedure is comparable with the two ways to use Fresnel's equations in the case of planar samples. (In fact, Mie's Theory together with Gans-Happel's theory (see below)) is formally the analog of Fresnel's equations for spherical symmetry.)

Of course, this DF is underlying Mie's approximative assumption of being uniform in the whole nano, including its surface.

The most straightforward way would be to vary fictitious input values of the DF by trial and error, calculate spectra and search the optimum numerical fit with the experimental spectra. Ambiguity and extreme time-consumption disqualify this route.

Two other methods are available which we will treat in the following. To make the story easier, we will restrict to very small nanos, where scattering does not play an essential role, i.e. to the "Quasi-Static Approximation".

Usually this realistic DF differs drastically from the DF of bulk material by NANO-EFFECTS (size-effects, surface-/interface-effects etc.), which, thus, can be studied in detail.

The complex DF of metals consists of the two complex conjugated parts, $\text{RE}\{\epsilon\} = \epsilon_1$ and $\text{IM}\{\epsilon\} = \epsilon_2$. So, beside Mie's absorption constant K a second experimental quantity is required to separate them. This is the "Relative Refraction Index Difference" between the many-particle

ROUTE 1 : One can measure K and L spectra directly.

As discussed before, macroscopic many-particle samples obeys Mie only for very low concentrations C of isolated particles, and this makes the direct measurement of $L(\lambda)$ pretty laborious. At $C \approx 10^{-6}$ L is also of the order of 10^{-6} , and highly sensitive interferometry (e.g. Mach-Zehnder) is required. Apparently, only one successful attempt has been made by Schoenes & v.Fragstein.

ROUTE 2: Since K and L are complex conjugated quantities, a KRAMERS-KRONIG RELATION (KKR) holds between them and can be applied to obtain L from the spectrum of K, avoiding the interferometric experiment.

For this purpose we define a Kramers-Kronig Function:

$$Z_{\text{Dipole}}(\lambda) = (2/(3 C)) L(\lambda) + i (\lambda / (6 \pi n_o C)) K(\lambda)$$

Then, the function

$$F = (Z_{\text{Dipole}}(\omega) - Z_{\text{Dipole}}(\infty)) / (\omega - \omega_o)$$

is integrated around a closed contour in the plane of complex frequencies, $\omega = \omega_1 + i \omega_2$.

By some manipulations we obtain

$$L(\omega_o) = L(\infty) + c / (\pi n_o) \mathbf{P} \int K(\omega) / (\omega^2 - \omega_o^2),$$

where the integral is over the real ω -axis from 0 to ∞ and \mathbf{P} is the principal value of the integral. The DK is obtained from $L(\omega_o)$ and the experimental value of $K(\omega_o)$ by using Mie.

The fact that experimental data of $K(\omega_o)$ are only available in limited spectral ranges makes severe but not unsolvable problems.

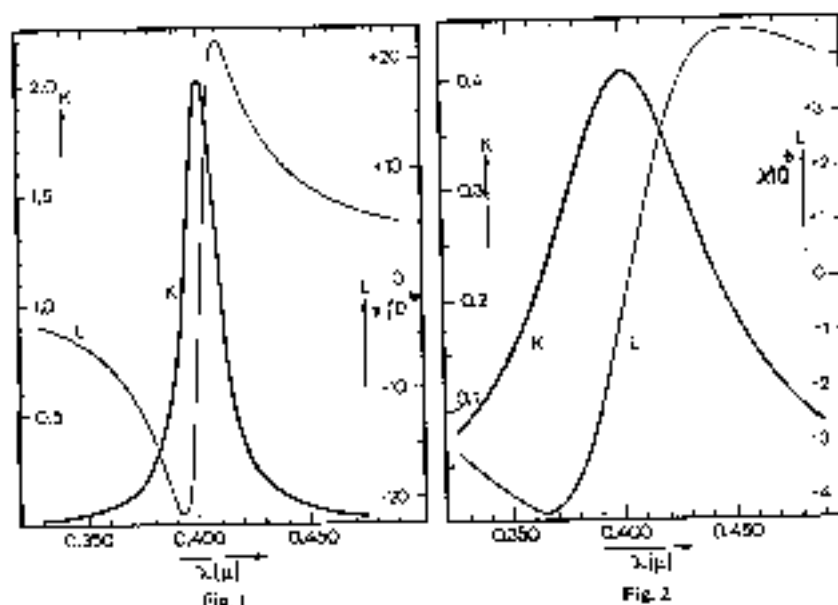
sample n_{sample} and the same sample but without particles n_0 (i.e. usually the matrix material).

$$L = (n_{\text{sample}} - n_0) / n_0$$

z

This experimentally accessible quantity has been calculated by Gans & Happel, though only in quasi-static approximation relating $L(\omega)$ with α .

As an example, the spectra of $K(\lambda)$ and $L(\lambda)$ of two samples consisting of DRUDE particles with different Drude parameters are shown :



Figs 1 and 2. Absorption K and relative dispersion L due to small particle surface plasmon resonance in particles with Drude free electrons. K was computed with Eq. (1), and L was found by Kramers Kronig analysis of the K spectrum. Particle concentration $C=10^{-4}$; $\omega_p = 1.1 \cdot 10^{16} \text{ sec}^{-1}$; $\gamma_p = 3.25$, $\omega_p = 2 \cdot 10^{14} \text{ sec}^{-1}$ in Fig. 1 and $\omega_p = 1 \cdot 10^{13} \text{ sec}^{-1}$ in Fig. 2

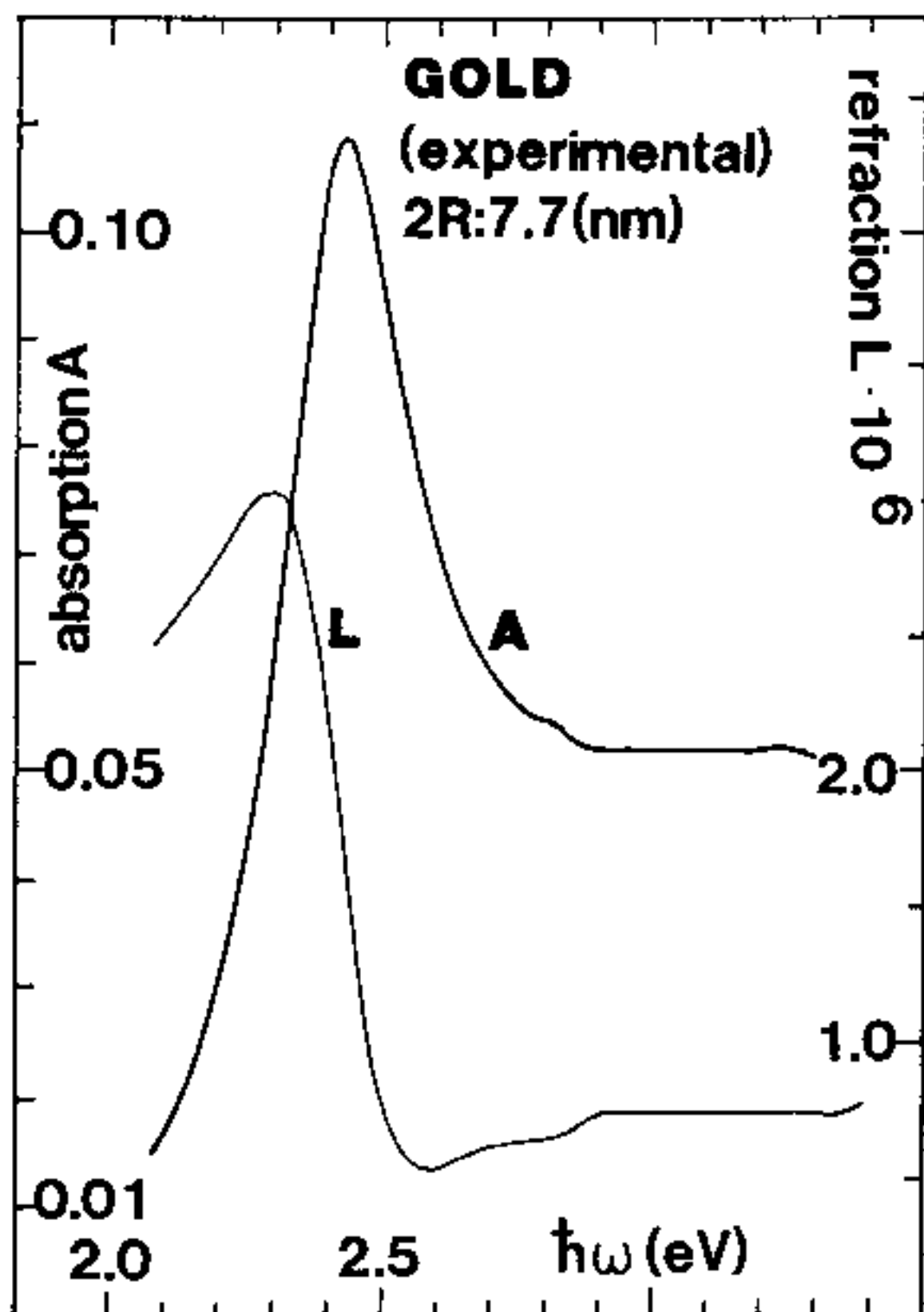


Table 3 Determination of the dielectric function from optical experiments on bulk solids, films, or clusters

| surface of bulk solid | thin solid film | spherical clusters |
|--|---|--|
| <div> <div> $R(\lambda, \varphi)$ </div> <div> $\delta(\lambda, \varphi)$ </div> <div> Kramers Kronig </div> <div> Fresnel formulae </div> <div> $\epsilon_1(\lambda), \epsilon_2(\lambda)$ </div> </div> | <div> <div> $R(\lambda, \varphi, d)$ </div> <div> $T(\lambda, \varphi, d)$ </div> <div> Kramers Kronig </div> <div> Fresnel formulae </div> <div> $\epsilon_1(\lambda, d), \epsilon_2(\lambda, d)$ </div> </div> | <div> <div> $\gamma(\lambda, R)$ </div> <div> $L_{\text{disp}}(\lambda, R)$ </div> <div> Kramers Kronig </div> <div> Mie-Gans-Happel formulae </div> <div> $\epsilon_1(\lambda, R), \epsilon_2(\lambda, R)$ </div> </div> |
| <p> R: reflectivity δ: phase difference φ: angle of incidence </p> | <p> T: transmittivity d: film thickness </p> | <p> γ: absorption / extinction constant R: cluster radius L_{disp}: relative dispersion </p> |

Dynamics of the Surface Plasmon Polariton Decay

Relaxation Processes

HIERARCHY OF RELAXATION-TIMES :

Phase Relaxation > Momentum Relaxation > Energy Relaxation

EXPERIMENTAL NUMBERS (Ag, Au Nanos):

- (1) Electron - Lattice Relaxation
(fs-spectroscopy : Perner et al (1997)) 1 - 10² ps

- (2) Electron - Electron Relaxation
(fs-spectroscopy : Perner et al (1997)) 10² fs - 1 ps

- (3) Phase relaxation, De-phasing, De-coherence 1 - 15 fs
(Lamprecht et al (1997) SHG autocorrelation)
(Kreibig et al (1997) optical, variation with surrounding media)
(Klar et al (1998) single nano in TiO₂)
(Rubahn et al (1998) optical)
(v. Plessen et al (1998) near field, hom. bandwidth)
(Lamprecht et al (1999) THG autocorrelation) 1999)
(Stietz et al (2000) "hole burning")

MIE-PLASMON-POLARITON: PHASE-DECAY RATE:

$$dN_{\text{coherent}} / N_{\text{coherent}} \rightarrow \exp\{-t / \tau_{\text{phase}}\}$$

$$1 / \tau_{\text{phase}} \approx (\text{surface collision probability}) * (\text{transition probability into adsorbate levels})$$

$$1 / \tau_{\text{phase}} \approx (v_{\text{Fermi}} / R) * A_{\text{interface}}$$

$$A_{\text{interface}} = \Phi * \rho(E_{\text{Fermi}}) * T * \tilde{N}$$

Φ = Adsorbate surface coverage

$\rho(E_{\text{Fermi}})$ = Density of the unoccupied adsorbate states close to E_{fermi}

T = interface transfer probability
= 1 (without tunnel barrier)
< 1 (with tunnel barrier)

\tilde{N} = Normalization factor

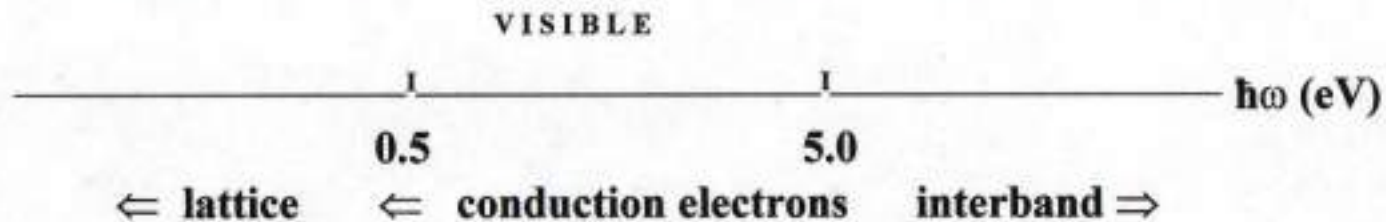
SURVEY OF NOBLE METAL NANOPARTICLE PLASMON-POLARITON DEPHASING LIFETIMES

| | |
|---|---------------------------------|
| (1) Lamprecht et al. (1997) 200 nm nonspherical Ag-particles on glass (e-beam lithography) | 10 ± 1 fs |
| (2) Klar, Perner, Grosse v. Plessen, Spirkel, Feldmann (1998) Single Au particles in TiO ₂ | 4 fs (8 fs) |
| (3) Kreibitz, Hilger et al. (1998) Free 2nm Ag-particles in UHV extrapolated to 15 nm (size dependence) embedded in Si-matrix | 7 fs 10 fs ≈ 1 fs |
| embedded in other matrices, deposited on substrates Measured: linear optical extinction line width | $5 > \tau > 1$ fs |
| (4) Klein-Wiehlke, Rubahn (1998) Ag islands; Size dependence: | $2 \leq \tau \leq 9$ fs |
| (5) v. Plessen, Feldmann (1998) ; single 40 nm Au particle Measured: Near-field homogeneous linewidth | 7(8) fs |
| (6) Lamprecht, Leitner, Aussenegg (1999) Aggregate islands, non-centrosymmetric ~ 100 nm (e-beam lithography). Measured SHG - autocorrelation | |
| Ag- particles | 7 ÷ 10 fs |
| Au- particles Homogeneous linewidth | 6 ± 1 fs |
| (5) Lamprecht, Leitner, Aussenegg (1999) Ag islands 14 nm /150 nm on glass (e-beam lithography). Measured : THG-autocorrelation. Homogeneous line width | 6 fs |
| (6) Stietz, Träger et al. (2000) Ag islands on glass; ellipsoids 5nm/15nm ; Measured by „hole burning“ | ≤ 5 fs |

(8) Linear Optical Material Functions (DF)

LINEAR OPTICAL RESPONSE OF METAL NANOPARTICLES

Susceptibility $\chi(\omega, \mathbf{R}) = (\epsilon(\omega, \mathbf{R}) - 1) = \chi^{\text{lattice}} + \chi^{\text{Drude}} + \chi^{\text{interband}}$



lattice excitations χ^{lattice} :

reduced
electron-shielding;

special atomic
structures
(molecule-solid state
transition);

surface/interface
modes.

**Collective conduction
electron excitations** χ^{Drude} :

MIE-PLASMON POLARITONS

single electron-hole
excitations $\chi^{\text{interband}}$:

quantum size effects;

band gap/edge effects;

DOS – effects;

DIELECTRIC FUNCTION OF A METAL OR SEMICONDUCTOR.

$$[\text{Dielectric displacement } \vec{D}] = \epsilon \cdot [\text{Field } \vec{E}]$$

A basic expression was given by Bassani and Parravicini

$$\hat{\epsilon}(\omega) = \epsilon_1(\omega) + i \cdot \epsilon_2(\omega) = 1 - \underbrace{\frac{(ne^2 / \epsilon_0 m_{eff})}{\omega^2 + i \gamma \omega}}_{\text{conduction electrons}} + \underbrace{\chi^{inter}}_{\text{interband transitions}}$$

with

$$\chi^{inter} = \frac{8 \hbar^3 \pi e^2}{m_{eff}^2} \sum_{f,f} \int_{B.Z} \frac{2 d\vec{K}}{(2\pi)^3} |e \cdot M_{ff}(\vec{k})|^2 \left\{ \frac{1}{[E_f(\vec{k}) - E_i(\vec{k})][(E_f(\vec{k}) - E_i(\vec{k}))^2 - \hbar^2 \omega^2]} + i \frac{\pi}{\hbar^2 \omega^2} \delta[E_f(\vec{k}) - E_i(\vec{k}) - \hbar \omega] \right\}$$

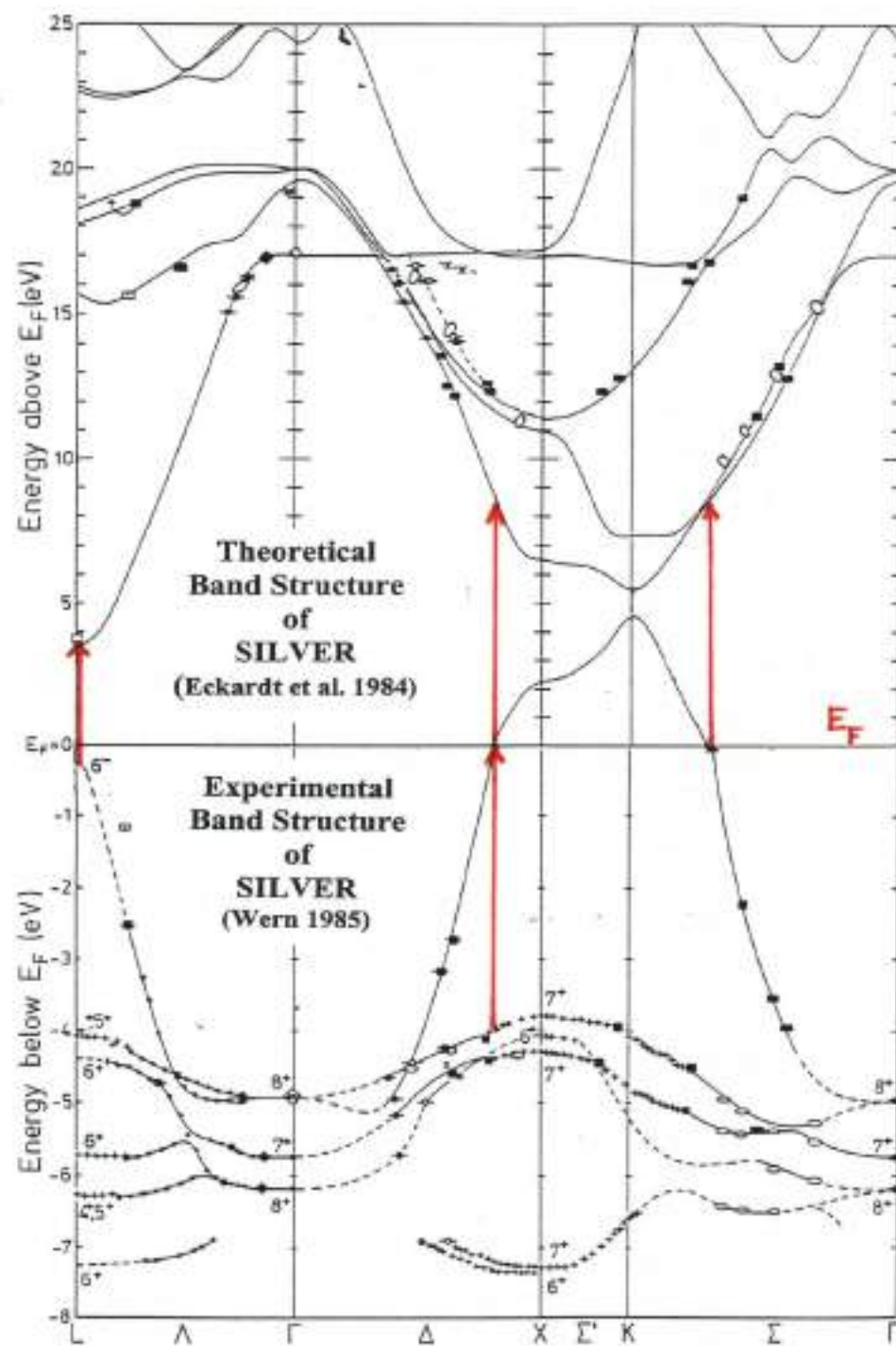
n = electron density

m_{eff} = effective mass

γ = relaxation frequency

M_{ff} = transition matrix elements

E_i, E_f = initial and final energy band state



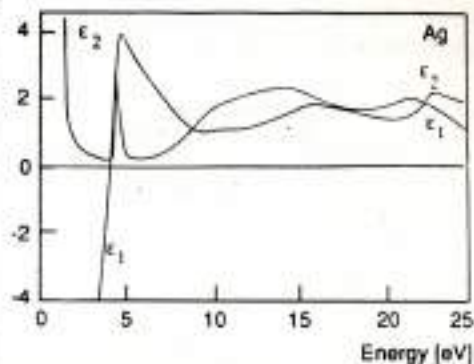
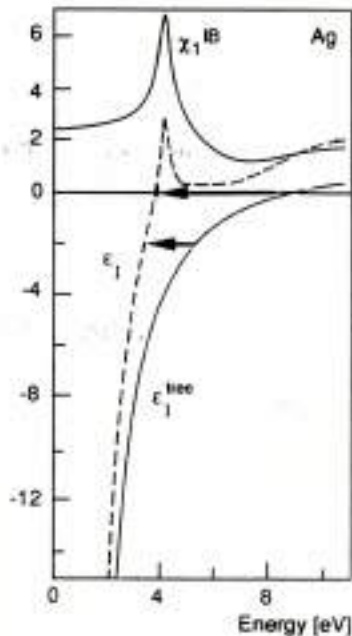


Fig. 2.1. Right: Dielectric functions $\epsilon_1(\hbar\omega)$ and $\epsilon_2(\hbar\omega)$ for bulk solid silver (after [2.26]). Below about 4 eV $\epsilon(\hbar\omega)$ is dominated by free electron behavior, above 4 eV by interband transitions. Left: Decomposition of measured $\epsilon_1(\hbar\omega)$ into the free electron contribution ϵ_1^{free} (Drude) and the interband transition contribution χ_1^{IB} . Due to χ_1^{IB} , the energy for $\epsilon_1(\hbar\omega) = 0$ is redshifted by about 5 eV from the free electron value.

Au

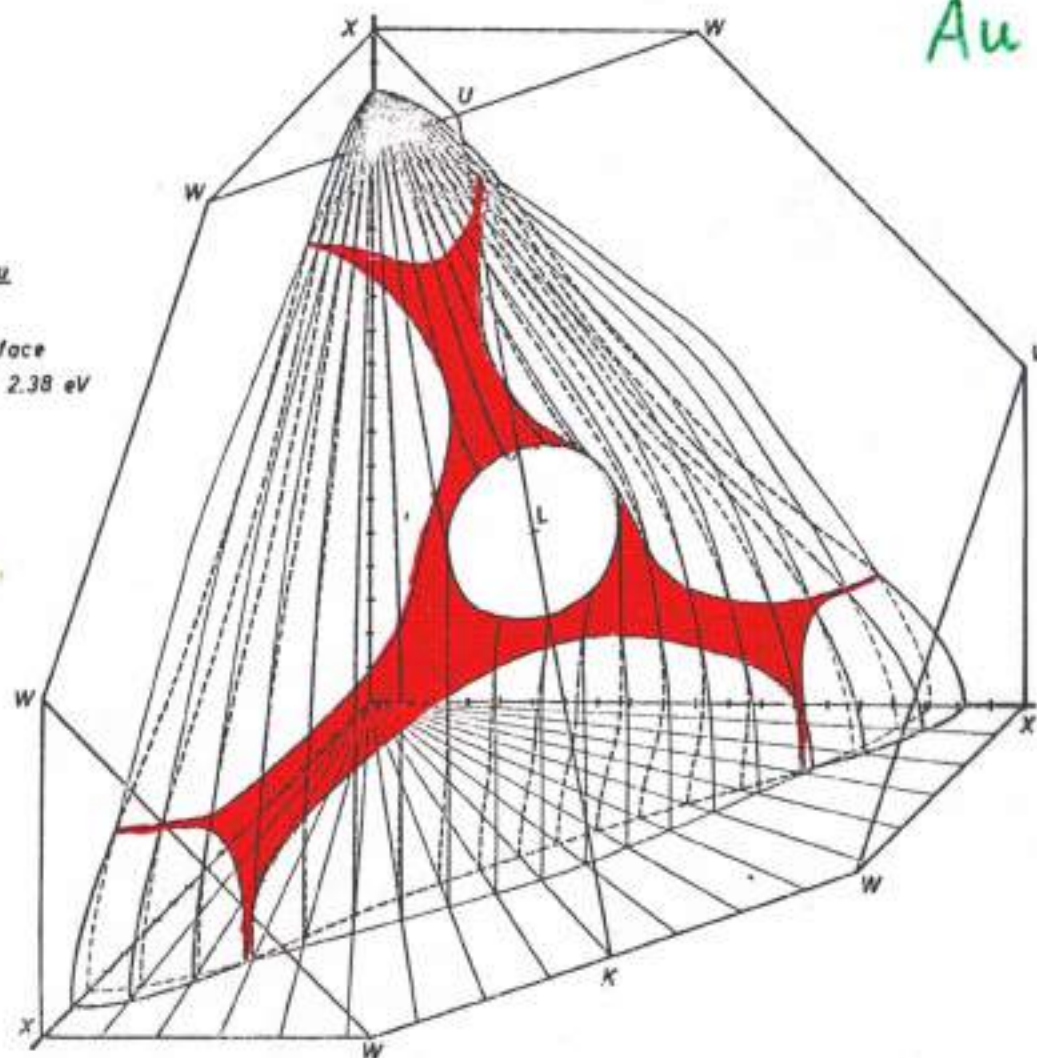
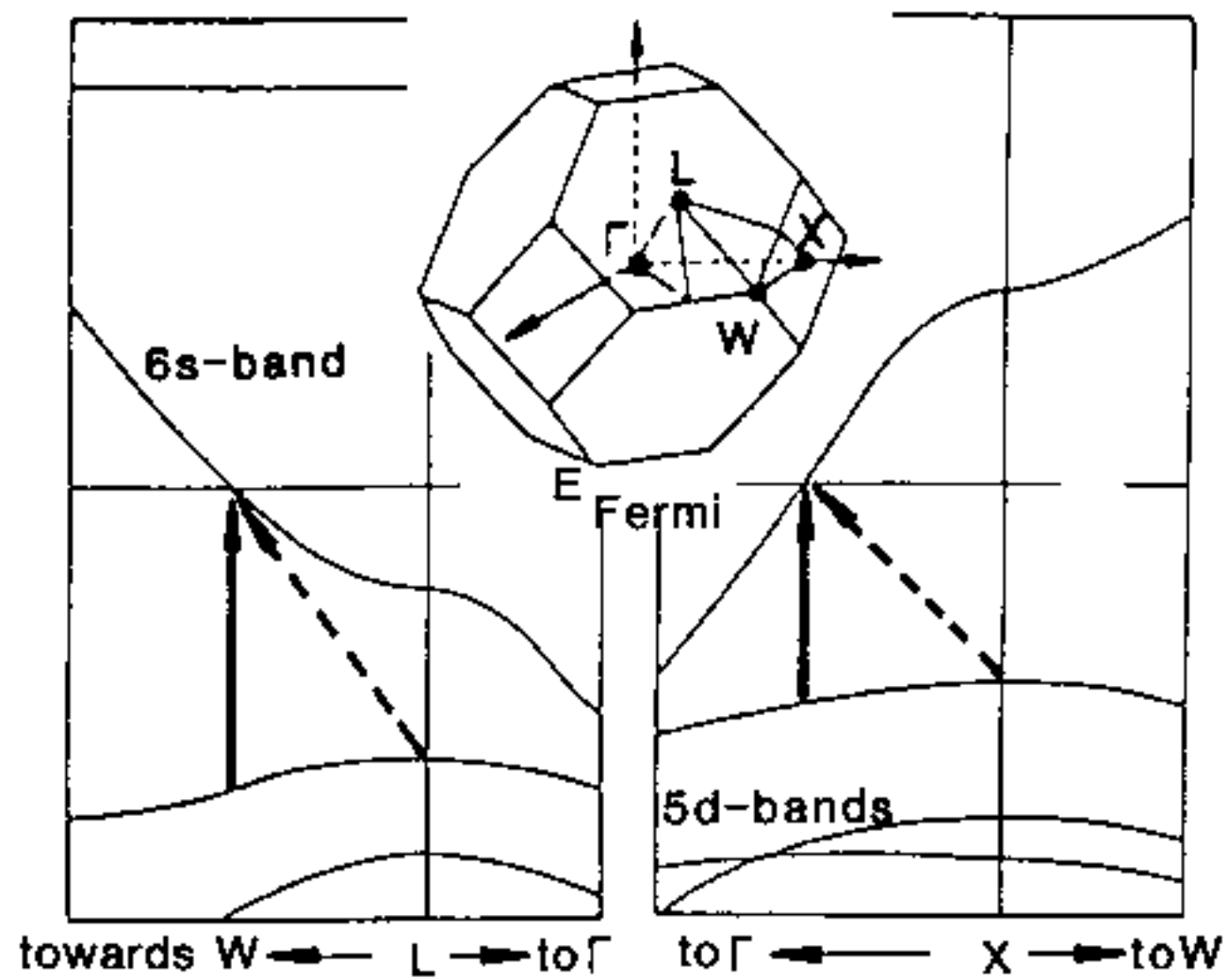
RAPW AuFermi surface
and CEDS 2.38 eV

FIG. 23. Axiometric plot of sections of the Fermi surface (fine lines) and the CEDS corresponding to $E_F - E_I = \hbar\omega_I = 2.38$ eV (heavy lines) for constant azimuthal angles. In the hatched area, the two surfaces coincide. \vec{k} vectors in this region correspond to the states giving the steep increase of the absorption at the interband edge $\hbar\omega_I = 2.38$ eV.



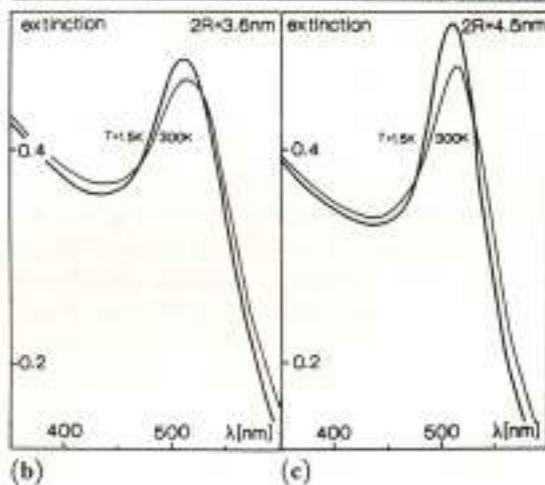
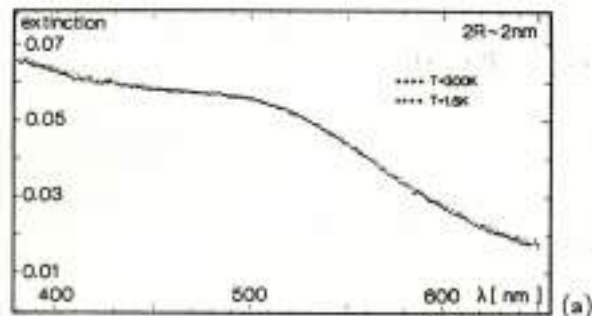


Fig. 4.27. Temperature dependence of optical properties of Au clusters. The absorption spectra in (b) and (c) correspond to sizes of 3.6 and 4.5 nm, respectively and were recorded at $T = 300 \text{ K}$ (thick lines) and $T = 1.6 \text{ K}$ (thin lines). For even lower sizes (a), the temperature dependence vanishes (after [4.117]).